PALACKÝ UNIVERSITY OLOMOUC

FACULTY OF SCIENCE

LABORATORY OF GROWTH REGULATORS

&

DEPARTMENT OF BOTANY

Aleš Pěnčík

The development and application of an analytical protocol for the isolation and quantification of indole-3-acetic acid and its derivatives in plant material

Ph.D. thesis

1501V BIOLOGY – BOTANY

Olomouc

2010

Poděkování (Acknowledgements)

BIBLIOGRAPHICAL IDENTIFICATION

Author's first name and surname: Aleš Pěnčík, Mgr.
Title: Development and application of an analytical protocol for the isolation and quantification of indole-3-acetic acid and its derivatives in plant material
Type of thesis: Ph.D. Thesis
Department: Department of Botany
Supervisor: RNDr. Jakub Rolčík, Ph.D.
The year of presentation: 2010

Abstract

Indole-3-acetic acid (IAA) is the most important member of the group of phytohormones known as auxins, which regulate many aspects of plant growth and development. The concentration of IAA in cells and tissues is controlled by various mechanisms, including *de novo* biosynthesis, synthesis and hydrolysis of IAA conjugates, conversion of IAA to indole-3-butyric acid (IBA), and oxidative degradation. This thesis deals with those conjugates of indole-3-acetic acid in which IAA is coupled through its carboxyl group to an amino acid.

The aim of this thesis was to develop an efficient, specific and sensitive analytical method suitable for the isolation and quantification of indole-3-acetic acid and its amino acid conjugates in diverse plant materials. To achieve this, a specific immunoaffinity extraction procedure was developed and implemented into an analytical protocol starting with a phosphate-buffer-based extraction followed by a Solid-Phase Extraction (SPE) and ending up with the final analysis done by High-Performance Liquid Chromatography coupled to tandem Mass Spectrometry (LC-MS/MS).

The protocol allows routine quantification of IAA and seven amino acid conjugates in samples as small as 20 mg fresh weight, with overall quantitative recovery ranging between 30 and 70 per cent. The limits of detection of the final analysis, based on the use of heavy-labeled internal standards, vary typically around 1 fmol per injection.

The developed analytical protocol was successfully used to quantify IAA and seven amino acid conjugates in immature seeds of the Christmas rose (*Helleborus niger* L.). Three of these conjugates were isolated and identified for the first time in higher plants. Currently, the method is being routinely used for the study of IAA and its derivatives in a variety of plant materials, which is documented by the enclosed articles published in scientific journals.

Keywords: Indole-3-acetic acid (IAA), immunoaffinity purification, high performance liquid chromatography (HPLC), tandem mass spectrometry (MS/MS), IAA conjugates, *Helleborus niger* L.

Number of pages: 34
Number of appendices: 4
Language: English

Contents

Abbreviations

ABP1	Auxin-Binding Protein
BSA	Bovine Serum Albumin
4-Cl-IAA	4-Chloroindole-3-acetic acid
ELISA	Enzyme-Linked ImmunoSorbent Assay
ESI	ElectroSpray Ionization
GC	Gas Chromatography
HPLC	High-Performance Liquid Chromatography
IAA	Indole-3-acetic acid
IAAla	Indole-3-acetyl-alanine
IAAsp	Indole-3-acetyl-aspartate
IAGlc	Indole-3-acetyl-glucose
IAGlu	Indole-3-acetyl-glutamate
IAGly	Indole-3-acetyl-glycine
IAInos	IAA-*myo*-inositol
IALeu	Indole-3-acetyl-leucine
IAM	Indole-3-acetamide
IAN	Indole-3-acetonitrile
IAOx	Indole-3-acetaldoxime
IAP1	IAA-modified protein 1
IAPhe	Indole-3-acetyl-phenylalanine
IAVal	Indole-3-acetyl valine
IBA	Indole-3-butyric acid
IEt	Indole-3-ethanol
IPA	Indole-3-pyruvic acid
LC	Liquid Chromatography
MS	Mass Spectrometry
MS/MS	Tandem Mass Spectrometry

NAA	Naphtylacetic acid
OxIAA	Oxindole-3-acetic acid
PAA	Phenylacetic acid
RIA	Radioimmunoassay
SCF	Skp1-Cullin-F-box protein complex
SPE	Solid-Phase Extraction
TIR1	Transport inhibitor response 1
UHPLC	Ultra-High Performance Liquid Chromatography
UPLC	Ultra Performance Liquid Chromatography

1. Introduction

The sweeping recent developments in modern analytical methods and instrumentation have made an enormous contribution to our understanding of the complexities of plant growth and development at all levels, from the subcellular to that of the whole plant. Thanks to these dramatic technological advances, phenomena and processes until recently hidden from us are now being revealed in ever-increasing detail. Our growing ability to investigate the minutiae of plant processes, however, presents us with an ever increasing array of novel questions, the answers to which require the effort and collaboration of plant biologists from many specialized disciplines including molecular biology, biochemistry, genetics, physiology and cell biology. Each of them uses his/her own specialized tools and methods to yielding appropriate information. Among the specializations of critical importance, the development of new and sophisticated techniques of chemical analysis has a crucial part to play. Nowhere are these developments more crucial than in the study of the chemical signals which regulate plant growth and development, particularly the so-called phytohormones.

All the phytohormones – the major classes of which are auxins, cytokinins, gibberellins, abscissic acid, brassinosteroids and ethylene – act at very low concentrations. The disparity between the amounts of phytohormone present and all the other components forming the plant organism is immense. Thus, the isolation, identification and quantification of phytohormones is extremely difficult and represents a highly challenging task requiring advanced instrumentation as well as deep understanding of the nature of the particular phytohormone and of the plant material in which it is found.

This doctoral thesis describes the development of a specific and sensitive analytical protocol suitable for the isolation, quantification and identification of one important group of plant hormones, namely the auxins.

2. Aims and scopes

Because of the extremely low quantities of phytohormones typically present in plants, the analytical chemistry which aims to measure these naturally occurring compounds is regarded as so-called "trace analysis". As such, it necessitates the use of sensitive up-to-date instrumentation. In this investigation, a sensitive and selective combination of (Ultra-) High Performance Liquid Chromatography (HPLC or UHPLC) and tandem mass detection (MS/MS) often comes into use.

However, even state-of-the-art instrumentation does not necessarily ensure efficient phytohormone analysis due to the enormous complexity of the plant material from which the phytohormone must be extracted. Many elaborate purification steps are necessary before the final analysis in order to successfully overcome the problems presented by the plant matrix. One way of avoiding such a time-consuming sample preparation is to use a simple, highly specific immunoaffinity purification method.

The above-mentioned problems apply with particular force to the group of phytohormones known as auxins, which are easily degradable by components of plant matrix and by light. Hence, the objectives of this doctoral thesis were:

1. *To prepare and characterize polyspecific anti-IAA antibodies and to develop and optimize an immunoaffinity extraction method for the isolation of IAA and its derivatives.*

2. *To develop and optimize an analytical protocol based on immunoaffinity extraction, combining the method with solid-phase extraction and LC-MS/MS final analysis.*

3. *To apply the developed protocol to the study of IAA and its amino acid conjugates in diverse plant species.*

3. Literature review

3.1. Indole-3-acetic acid (IAA) and auxins

Auxins are biologically active low-molecular-weight compounds with similar physiological effects on plant growth and development (see Chapter "Auxin Biology"). All auxins are weak organic acids with an aromatic skeleton. Most of the naturally occurring auxins such as indole-3-acetic acid (IAA), indole-3-butyric acid (IBA) and 4-chloroindole-3-acetic acid (4-Cl-IAA) are based on an indole ring; only one non-indolic auxin - phenylacetic acid (PAA) - has been identified in plants (Wightman & Lighty, 1982). However, a couple of synthetic non-indolic substances with auxin-like activity are used in both research and in the commercial field (Fig. 1).

A.

Indole-3-acetic acid (IAA)

4-chlorindole-3-acetic acid (4-Cl-IAA)

Indole-3-butyric acid (IBA)

Phenylacetic acid (PAA)

B.

2-Methoxy-3,6-dichlorobenzoic acid
(dicamba)

Naphtalene acetic acid (NAA)
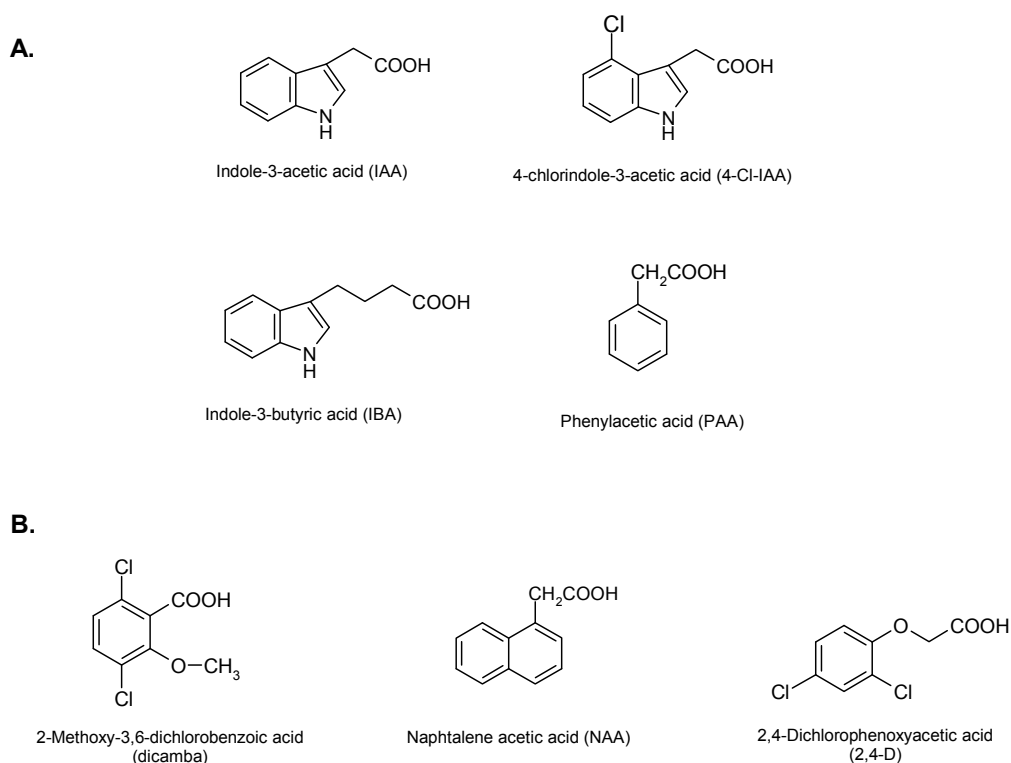
2,4-Dichlorophenoxyacetic acid
(2,4-D)

Figure 1. Naturally occurring compounds with auxin activity (A) and examples of synthetic auxins (B).

The predominant naturally-occurring auxin is indole-3-acetic acid (IAA; sometimes called simply "auxin", though the name "heteroauxin" may also be found in literature). In addition to higher plants, IAA has been found in algae (Crouch et al., 1991), bacteria (Prinsen et al., 1998) and fungi (Ek et al., 1983). The chlorinated derivative of IAA – 4-chloroindole-3-acetic acid – has been detected in several plant species and exhibits high activity in some auxin bioassays (Reinecke, 1999). Low endogenous levels, weak activity and specific spatial distribution of phenyl acetic acid within the plant suggests that it does not play a considerable role as an auxin or it has a specific, up to now unknown, function (Ludwig-Müller & Cohen, 2002). The principle of auxin-like effects of indole-3-butyric acid remains unclear. There is some evidence to indicate that IBA does not act directly, but only after biochemical conversion to IAA (Bartel et al., 2001). Reversible conversion of IBA and IAA is involved in maintenance of auxin homeostasis (Chapter 3.1.2.).

3.1.1. Auxin biology

The name given to this class of plant hormones, "auxins" (originating from the Greek "auxein", meaning "growth"), well describes the biological actions of these compounds. They are involved in the regulation of practically all aspects of plant growth and development. The concept of a mobile, growth-regulating "stimulus" was first proposed by Charles Darwin, who observed that the bending of coleoptiles toward a light source involved light perception at the coleoptiles tip and a growth response some distance from the tip (Darwin, 1880). The existence of a growth-affecting substance in coleoptile tips was demonstrated by Fritz Went. He applied agar blocks containing diffusates from coleoptile tips (auxin) on decapitated *Avena* coleoptiles, which resulted in their growth (Went, 1926). In relation to the topic of this thesis it is interesting to note that Went was the author of the first quantitative method for auxin estimation. Using asymmetrically placed agar blocks containing auxin on coleoptiles, he demonstrated that the resulting curvature of the coleoptiles was proportional to the concentration of auxin in the block (Went, 1928).

Thanks to this assay, it is known today that auxin is transported basipetally within the stem from the tip, and that it promotes coleoptile elongation and mediates response to directional

light and gravitational stimuli. Subsequent experiments involving especially exogenous application of the hormone and the study of several auxin mutants revealed the complexity of auxin action. Auxin strongly affects root development, inhibiting root elongation and inducing root branching. It mediates the asymmetric growth responses of roots to gravitational stimuli and it is involved in embryo development, vascular tissue differentiation, fruit ripening and abscission. In some species it also plays a role in flowering. At the cellular level, auxin promotes both cell elongation and division. For many physiological responses, interaction of auxin with other hormones is important. It is well known that auxins and cytokinins have inverse effects on root and shoot development. Auxins also affect the biosynthesis of other hormones, especially cytokinins and ethylene. General aspects of the biological effects of auxin were reviewed by Davies et al. (1995; 2004).

A major challenge in auxin research has been to identify an auxin receptor and other components involved downstream in auxin signal transduction. A single protein with strong affinity to auxin – auxin-binding protein (ABP1) – has been found in several plant species (Hertel et al., 1972; Palme et al., 1992). Although there is evidence that ABP1 is connected with some physiological responses such as cell elongation – and it is known that the *abp1* loss-of-function mutant is lethal (Chen et al., 2001) – the integration of ABP1 into a complete signal transduction pathway has not been established. Recent genetic investigations led to the discovery of a new auxin signaling pathway in which ABP1 is not included. Here, auxin interacts directly with TIR1 protein, a member of the multi-protein complex SCF^{TIR1}. This complex mediates ubiquitination of transcriptional repressors (AUX/IAA) with subsequent degradation of these proteins on proteasome resulting in expression of specific auxin-responsive genes (Paciorek & Friml, 2006).

Crucial for many developmental processes are local gradients of auxin within the plant (Benková et al., 2003). The asymmetric distribution results from interaction between synthesis, metabolism and directional transport of auxin. The direction of flow is determined by the distribution of PIN proteins, auxin efflux transport carriers (Morris et al., 2004). Dynamic changes in subcellular localization of PINs are caused by endosomal recycling, which is strongly regulated by auxin itself (Paciorek et al., 2005).

3.1.2. Biosynthesis and metabolism

Biochemical pathways contributing to the control of free IAA levels within plant tissues include *de novo* biosynthesis, synthesis and hydrolysis of IAA conjugates, conversion of IAA to IBA, and oxidative degradation (Fig. 3).
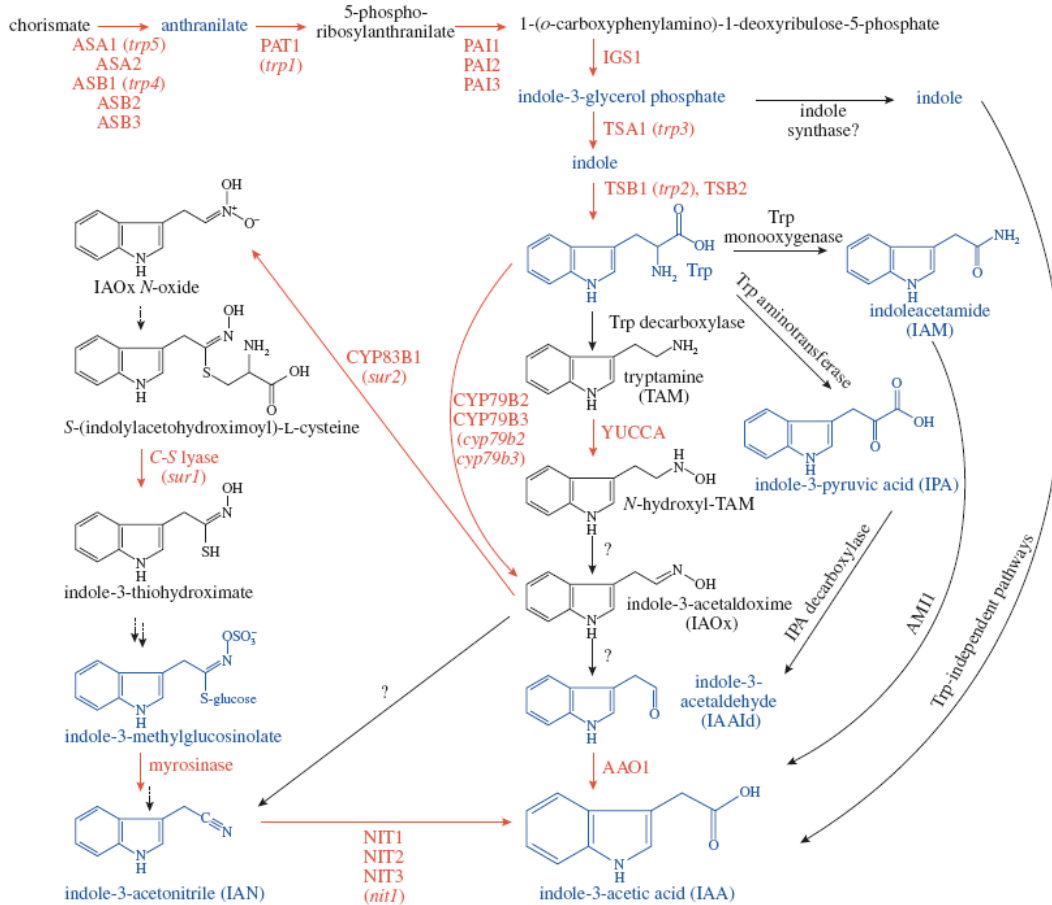
Figure 2. Putative pathways of IAA biosynthesis in plants (adopted from Woodward & Bartel, 2005).

All plant tissues, including roots, are capable of synthesizing IAA. Nevertheless, young leaves are the main source of *de novo* synthesized auxin (Ljung et al., 2001; 2005). Several pathways leading to IAA have been described, some of them involving tryptophan as an intermediate while others are tryptophan-independent. The shikimate biosynthetic pathway is a common source of the indole ring. Potential IAA biosynthetic pathways comprising identified

enzymes with appropriate genes are depicted in Figure 2. An indole-3-acetamide (IAM) pathway and an indole-3-pyruvic acid (IPA) pathway are also present in some microorganisms (Koga, 1995; Patten & Glick, 1996) and the respective intermediates have also been found in *Arabidopsis* (Pollman et al., 2002; Tam and Normanly, 1998). In other tryptophan-dependent pathways, indole-3-acetaldoxime (IAOx) is a key intermediate. Tryptophan may be converted to IAOx directly (IAOx pathway) or via tryptamine (tryptamine pathway). Subsequent steps leading from IAOx to IAA may include indole-3-acetaldehyde (IAAld) or indole-3-acetonitrile (IAN) as an IAA precursor (Cohen et al., 2003). In addition, tryptophan-independent IAA biosynthesis was revealed by Normanly et al. (1993), branching from indole-3-glycerol phosphate or indole. Thus, the biosynthetic pathways leading to IAA are very complex and the relative importance of each pathway varies depending on plant species.

Crucial for the homeostatic control of auxin levels in the plant, a requirement for precise hormone action, is IAA inactivation. This may either be irreversible by direct oxidation of IAA, or reversible by conversion of IAA to IBA or by the formation of various conjugates (see Chapter 3.1.3.) The major product of IAA oxidation – oxindole-3-acetic acid (OxIAA) – has repeatedly been detected in plants at high concentrations, indicating the importance of oxidative degradation in IAA metabolism (Kowalczyk & Sandberg, 2001; Bandurski et al., 1995). OxIAA can be further modified by its conjugation to hexose and/or by hydroxylation (Östin et al., 1998).

IAA can be converted to indole-3-butyric acid (IBA), which may contribute to IAA inactivation and affect IAA pool in the plant. For a long period, IBA was considered to be a synthetic auxin, widely employed commercially as a rooting enhancer. However, several studies have shown that IBA occurs naturally in plants (Epstein & Ludwig-Müller, 1993; Ludwig-Müller & Cohen, 2002). The activity of IBA synthase, which catalyzes the synthesis of IBA from IAA, is influenced by diverse endogenous and environmental factors, such as light and osmotic stress (Ludwig-Müller, 2000). IAA can be resynthesized from IBA by a process similar to fatty acid β-oxidation (Bartel et al., 2001). Although there have been many studies of IBA and its function in plants, the relative importance of the IBA pathway in auxin metabolism remains obscure.
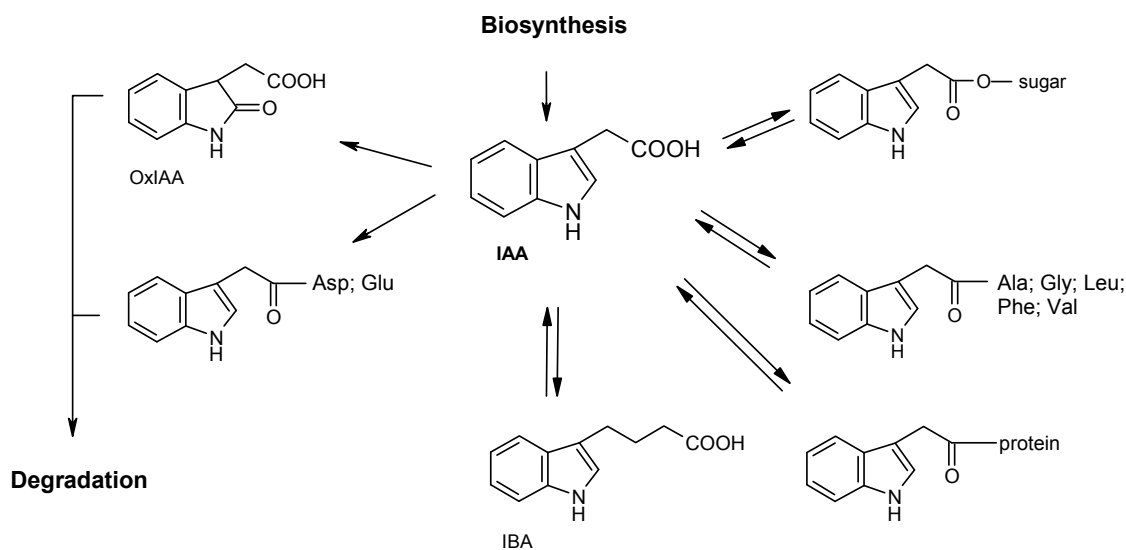
Figure 3. Potential pathways of IAA metabolism and degradation.

3.1.3. IAA conjugates

Free indole-3-acetic acid represents only approx. 1% of the total IAA in *Arabidopsis* seedlings. The bulk of the auxin is present in conjugated forms in which IAA is joined to other molecules through either ester or amide linkages (Tam et al., 2000). Such conjugates not only play an important role in IAA homeostasis but also act as non-active transport forms of auxin and are a major source of active auxin, especially during seed germination and seedling development. Although the profile of IAA conjugates may differ from species to species, conjugates are so widely distributed that it is clear that IAA conjugation is a common phenomenon across plant kingdom.

In many plant species including *Arabidopsis*, a large proportion of the conjugated IAA is represented by high-molecular-weight forms. IAA-modified macromolecules, including proteins and polysaccharides, play a role in the storage of both auxin and amino acids or sugars which can be released during seed germination and early seedling development. IAA-modified protein (IAP1) was identified in bush bean seeds (Walz et al., 2002). The gene *iap1* is expressed during seed development and the degradation of the protein increases dramatically after germination is initiated. In addition, the ester conjugates IAA-*myo*-inositol (IAInos), IAA-*myo*-inositol glycosides

and IAA-glucans are the main IAA storage conjugates in germinating maize kernels (Bandurski et al., 1995). IAInos does not undergo hydrolysis in the kernel, but is rapidly transported to the growing region of the shoot. The main precursor of sugar conjugates in maize kernels is 1-*O*-D-IAA-glucose (IAGlc), formed from IAA and UDP-glucose by the enzyme UDP-glucosyl transferase (Slovin et al., 1999). In *Arabidopsis*, low levels of IAA-glucose were found (Tam et al., 2000) as well as a homologue of maize glucosyl transferase (Jackson et al., 2001).
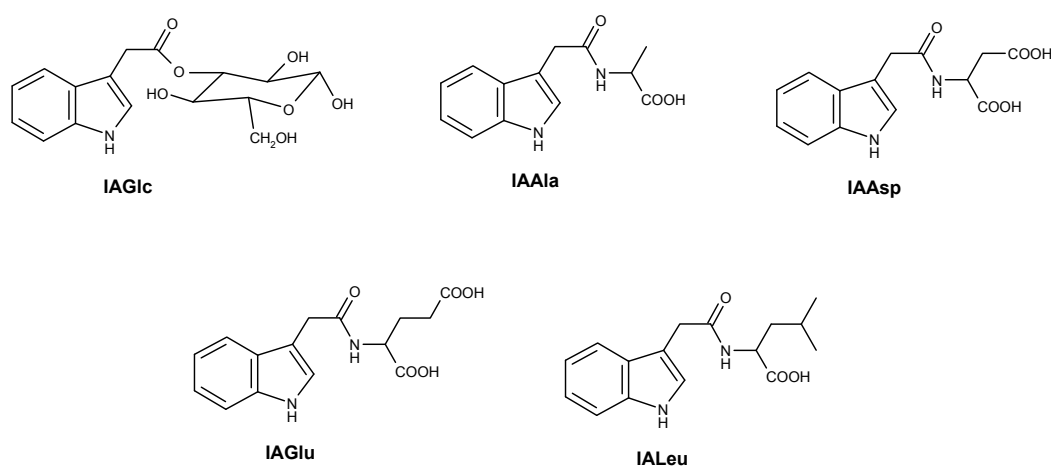
Figure 4. Low-molecular-weight conjugates of IAA.

In addition to storage proteins and sugar IAA storage conjugates, single amino acid conjugates are also present in plants. Although low-mass amide-linked conjugates represent only small part of total IAA pool (Ljung et al., 2002), their formation and hydrolysis may strongly contribute to the control of IAA homeostasis at the cellular and subcellular level. Conjugates with aspartate (IAAsp) and glutamate (IAGlu) usually occur at relatively high concentrations. Conjugates with other amino acids, such as alanine (IAAla), glycine (IAGly), leucine (IALeu), phenylalanine (IAPhe) and valine (IAVal), have also been identified but their levels in plant tissues are significantly lower (Kowalczyk and Sandberg, 2001; Matsuda et al., 2005; Pěnčík et al., 2009; Tam et al., 2000). This difference is probably caused by the specificity of IAA amidohydrolases; IAAsp and IAGlu are not favored substrates (LeClere et al., 2002). While the other conjugates may be reversibly converted to IAA, IAAsp and IAGlu serve as degradation

intermediates. Enzymes responsible for the conjugation of IAA to amino acids have been characterized in *Arabidopsis*. They are encoded by auxin-induced genes, members of the *GH3* gene family (Staswick et al., 2002). Thus the regulation of IAA release and IAA homeostasis are under feed–back control by IAA levels themselves.

3.2. Auxin analysis

The analysis of IAA and its conjugates is a difficult task which presents a number of problems. Their concentrations in plant tissues are usually quite low – typically tens of picomols per gram fresh weight for IAA and even two or more orders less for IAA conjugates. These compounds are also relatively unstable and easily undergo degradation or interconversion. Furthermore, plant material is a very complex matrix which constitutes a reactive environment containing enzymes and radicals which can easily degrade the analytes. Rapid progress in the development of analytical instrumentation during the last two decades has played an important part in helping to overcome some of problems inherent in phytohormone analysis; thus it is now possible to quantify auxins with great accuracy and reproducibility in even a few milligrams of fresh plant material.

3.2.1. Extraction and purification

A sample of plant tissue designated for auxin analysis has to be homogenized first and subsequently extracted with a suitable solvent, such as absolute (Ostin et al., 1998), 90% (Peters et al., 2000) or 80% (Sundberg, 1990) methanol. Other widely used extraction solvents are acetone (Bandurski & Schulze, 1974) or a 70% solution of acetone (Sundberg, 1990). However, anhydrous organic solvents such as acetone or diethylether are unsuitable for the extraction of IAA from lyophilized plant tissue due to their poor penetration of the dried material. Consequently, they do not extract the analyte effectively and results of analyses are biased (Sundberg, 1990). Organic solvents are primarily used because of the greater solubility of the analyte in such solvents. However, such organic solvents also readily extract interfering compounds such as pigments, lipids and other non-polar ballast substances which can strongly

contaminate the extracts. Hence, a buffer of neutral pH is alternatively employed in auxin extraction (Nordstrom & Eliasson, 1991). However, it is necessary to bear in mind that chemical degradation and/or enzyme activation leading to metabolic changes, such as conjugate hydrolysis, may occur in an aqueous environment. Buffer extraction must therefore be performed at low temperatures. Reduction of extraction time to a minimum and the use of antioxidants are also reasonable precautions (Hofinger, 1980; Ernstsen et al., 1986).

After extraction, the crude extract has to be freed of interfering compounds such as lipids, proteins and pigments, in order to obtain a sample of sufficient purity for the final analysis. Nowadays, SPE (*Solid Phase Extraction*) is the most popular purification technique in plant hormone research because of its efficiency and high-throughput. One of the sorbents widely used for IAA purification is a non-polar C18 phase (Matsuda et al., 2005; Hou et al., 2008). Purification based on ion exchange combined with reverse phase is also very effective (Dobrev et al., 2005).

3.2.2. Immunoaffinity purification

Radioimmunoassay (RIA; Weiler, 1981) and Enzyme-Linked ImmunoSorbent Assay (ELISA; Weiler et al., 1981) have been successfully used for the quantification of IAA for some time. Recently, immunoassays have been replaced by more efficient instrument-based techniques, especially High-Performance Liquid Chromatography (HPLC) coupled to Mass Spectrometry (MS). Nevertheless, it remains advantageous to use antibodies in sample preparation. Immuno-based sample purification represents a unique tool for trace analysis thanks to its great specificity and selectivity, particularly in combination with powerful instrumentation. Hence, it is frequently employed in phytohormone analysis. Immunoaffinity purification has been utilized in protocols for the quantification of various plant hormones including cytokinins (Prinsen et al., 1998; Redig et al., 1996; Novák et al., 2003; Hauserová et al., 2005), abscisic acid (Kannangara et al., 1989; Hradecká et al., 2007) and auxins, based on both polyclonal (Sundberg et al., 1986) and monoclonal antibodies (Ulvskov et al., 1992).

3.2.3. Instrumental methods

For the final analysis of indole-3-acetic acid, a range of instrumental techniques was used. Aside from HPLC coupled to UV or fluorimetric detection (Crozier et al., 1980), the most widely utilized method is a combination of gas or liquid chromatography with mass spectrometry (GC-MS; LC-MS). As an alternative to chromatographic methods, capillary electrophoresis may be used, for instance in combination with a fluorimetric detection (Bruns et al., 1997).

Gas chromatography combined with mass detection is a powerful tool allowing quantification of IAA in samples as small as 0.1 mg fresh weight (Ljung et al., 2001). Prior to separation by gas chromatography, IAA must be derivatized, which is most frequently done by methylation (Schneider et al., 1985) or trimethylsilylation (Edlund et al., 1995). However, such a derivatization step considerably extends an analytical protocol. High performance liquid chromatography coupled to mass spectrometry (HPLC-MS) is therefore more and more widely employed in IAA analysis, especially when high throughput is required. Very high sensitivity and selectivity is characteristic for HPLC coupled to tandem mass detection (MS/MS) based either on an ion trap (Prinsen et al., 1998; Ma et al., 2008) or triple quadrupole (Chiwocha et al., 2003). Such a configuration is efficient for quantification of IAA as well as less abundant IAA metabolites. IAA conjugates with some amino acids were detected by HPLC-ESI-MS/MS in rice (Matsuda et al., 2005).

If the liquid chromatography is used to separate analytes, their derivatization is not essential; nevertheless, it may substantially improve the separation and enhance ionization in the source block of a mass spectrometer, resulting in a higher sensitivity of the method and lower limits of detection. Using HPLC-MS technique with prior derivatization, IAA conjugates with alanine (IAAla) and leucine (IALeu) were quantified at femtomolar levels in *Arabidopsis* (Kowalczyk & Sandberg, 2001).

4. Materials and methods

Polyclonal anti-IAA antibodies were raised in the Laboratory of Growth Regulators, Olomouc, Czech Republic, and tested by ELISA, as described by Jirásková et al. (2009).

The developed analytical protocol for the isolation and quantification of IAA and its amino acid conjugates, as well as the materials and instrumentation used, are described in a paper by Pěnčík et al., 2009 (*Supplement I*).

The plant materials studied by the developed analytical protocol were as follows:

- Immature seeds of the Christmas rose (*Helleborus niger*); in a research performed by Pěnčík et al. (2009, see *Supplement I*).

- Seedling parts and hypocotyl subsections of Bugle Lily (*Watsonia lepida*). For further details, see *Supplement II* (Ascough et al., 2009).

- Lyophilized samples of two seaweeds: *Ulva fasciata* (Chlorophyta) and *Dictyota humifusa* (Phaeophyta). The detailed description can be found in *Supplement III* (Stirk et al., 2009).

- Root tips of 1 mm in length of three different genotypes of *Arabidopsis thaliana* (Zhang et al., 2010; enclosed as *Supplement IV*).

5. Survey of results

5.1. Analytical protocol for the isolation and quantification of indole-3-acetic acid (IAA) and its derivatives

5.1.1. Anti-IAA antibodies and immunoaffinity purification

The aim of this thesis was to develop an analytical protocol suitable for the isolation and quantification of indole-3-acetic acid (IAA) and its derivatives; among them, preferentially IAA conjugates with amino acids. To achieve this, a specific immunoaffinity extraction procedure was developed and implemented into the protocol, thus allowing very efficient single step purification prior to the final analysis which was done by liquid chromatography coupled to tandem mass spectrometry (LC-MS/MS).

The specificity of immunoaffinity purification is based on a unique interaction between antibodies coupled to a solid support (sorbent) and antigens (*i.e.* analytes) against which the antibodies were raised. This means that all the other compounds contained in a raw or pre-purified plant extract are easily removed or their content substantially reduced as they are simply washed out of the immunoaffinity sorbent. Such purification is successfully used in the analysis of both natural and synthetic compounds in biological samples (for review, see Tsikas, 2010).

To raise antibodies discriminating only the indole ring regardless of its substitution in position 3, rabbits were immunized with an IAA-BSA conjugate prepared by linking indole-3-acetic acid to the protein through its carboxyl group (IAA-C1'-BSA), as described earlier (Ulvskov et al., 1987; Weiler, 1981). The obtained antibodies were characterized by ELISA and their expected wide specificity (polyspecificity) was confirmed: Cross-reactivities of IAA and its amino acid conjugates, tested after they were transformed into their methyl esters, ranged between 85 and 140 per cent. (The values found for free acids were, however, lower by one order, which is in full accordance with previous experience which indicates that free acids have to be methylated before they are subjected to an antibody-antigen interaction.)

The antibodies were purified and an immunoaffinity gel was prepared. It was tested for capacity and recovery by applying various amounts of indole-3-acetamide which is not volatile – in contrast to the methyl ester of IAA. The capacity was found to vary around 3 nmol per column (containing approximately 150 µl of immunoaffinity gel), with recovery between 95 and 100 per cent.

5.1.2. Identification and quantification of IAA and its conjugates in seeds of the Christmas rose (*Helleborus niger* L.)

The developed immunoaffinity extraction was integrated into a complex analytical protocol starting with a phosphate-buffer-based extraction followed by a Solid-Phase Extraction and ending up with LC-MS/MS final analysis.

The SPE was adopted from a protocol for free IAA extraction kindly provided by Karin Ljung (Umeå Plant Science Center, Sweden). Its correct operation was verified for all the 3-substituted indole standards in use (IAA and its conjugates with Asp, Glu, Ala, Gly, Leu, Phe, and Val; and also IEt: indole-3-ethanol; IAM: indole-3-acetamide and IAN: indole-3-acetonitrile).

As for the final analysis by liquid chromatography, a base-line separation was achieved in a linear gradient of aqueous methanol containing formic acid (1%; v/v). All accessible parameters of MS/MS detection were optimized and are listed in an enclosed paper (*Suppl. I*).

The analytical protocol, based on a string of respective techniques (extraction – SPE – methylation with diazomethane – immunoaffinity purification – LC-MS/MS), was thoroughly optimized and tested on both standards alone and on various types of spiked plant material. It turned out to be robust enough to ensure overall quantitative recovery of between 30 and 70 per cent. Using this protocol, typical amounts of plant tissue recently used for analysis of IAA and its conjugates have been reduced to as little as between 15 and 30 mg fresh weight. All the compounds routinely analyzed are quantified by using corresponding heavy-labeled internal standards.

Using this protocol, the content of endogenous IAA and its conjugates was studied in immature seeds of *Helleborus niger* L. (the Christmas rose), where preliminary estimation indicated very high levels of free IAA. In this material, the profile of the quantified conjugates

was similar to those described before in *Arabidopsis thaliana* (Tam et al., 2000; Kowalczyk & Sandberg, 2000) and rice (Matsuda et al., 2005).

Besides successful quantification, three novel IAA conjugates with the following amino acids: Gly, Phe and Val, previously not described in higher plants, were identified in *Helleborus niger* seeds (Fig. 5). Thus the superior parameters of the developed method were confirmed.

IAGly

IAPhe

IAVal
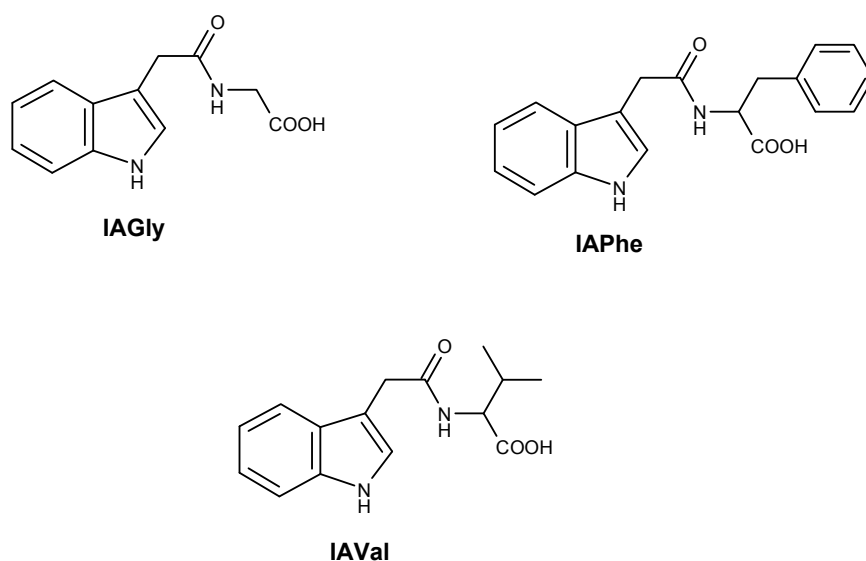
Figure 5. Novel IAA amino acid conjugates discovered in *Helleborus* seeds by Pěnčík et al. (*Supplement I*)

5.2. Quantification of IAA and its derivatives in *Watsonia lepida* seedlings (*Supplement II*)

The paper by **Ascough et al., 2009** (*Supplement II*) describes an example of successful application of the developed method in biological research. In this, auxins as well as cytokinins were studied and their level compared with cell division activity and *in vitro* regeneration of *Watsonia lepida* seedling parts and hypocotyl subsections.

To quantify auxins, samples consisting of 10 mg of lyophilized tissue were analyzed. This amount was based on a rough assessment of water content in the plant material; for 70 to 80 per cent it would correspond approximately to 30 to 50 mg fresh weight.

Of the seven IAA amino acid conjugates detected by the developed method, only those with aspartic and glutamic acids were found, and in quantities which were significantly lower than that of free IAA, which ranged between 100 and 600 pmol per gram of dry weight. In addition to free IAA and these amino-acid conjugates, indole-3-acetamide and indole-3-ethanol were also identified in the seedlings. The highest concentrations of both auxins and cytokinins were found in the hypocotyl subsection characterized by the highest cell division activity. However, the highest regeneration response *in vitro* was achieved in a different region of the hypocotyl (i.e. different hypocotyls subsection) which had fewer dividing, but more developmentally plastic, cells.

5.3. Study of annual variation of auxins in seaweeds (*Supplement III*)

Another powerful demonstration of robustness typical of a complex analytical protocol based on a highly-specific immunoaffinity purification is afforded by the work described in the paper by **Stirk et al., 2009** (*Supplement III*). In this, we monitored variations in endogenous auxins, cytokinins and abscisic acid in two seaweeds: *Ulva fasciata* (Chlorophyta) and *Dictyota humifusa* (Phaeophyta) bimonthly over a one-year period,

In this example, the biological material to be analyzed was characterized by a high content of ballast compounds, resulting in an SPE-purified extract with an atypically dark brown color. The presence of high amounts of reactive compounds was further indicated by excessive amount of diazomethane required for successful methylation of the sample. The high efficiency of the subsequent immunoaffinity purification was corroborated by the fact that the peak areas of respective internal standards corresponded to their peak areas typically measured in other types of plant material.

Of the auxins recovered from the seaweed species studied, only IAA and indole-3-acetamide were quantified, reaching their maxima in March and September (*Ulva fasciata*) and in May and November (*Dictyota humifusa*). For further details, see *Supplement III*.

5.4. Quantification of IAA in *Arabidopsis thaliana* root tips (*Supplement IV*)

Indole-3-acetic acid plays a crucial role in driving plant growth along the apical-basal axis. Based on the directional flow of IAA, axial growth and development is closely tied to the polar localization of PIN transporters on the plasma membrane.

In a paper by Zhang and coworkers published in 2010 (*Supplement IV*), the influence of PIN1 phosphorylation at Ser337/Thr340 in its central hydrophilic loop has been studied. By site-directed mutagenesis, these amino acids were both replaced either with Ala (which cannot be phosphorylated) or Asp (the carboxylate of which simulates a phosphate group). GFP-facilitated visualization revealed the predominantly basal localization of PIN1 proteins in the case of PIN1-GFP(Ala) and non-polar or basal-to-apical shift in the case of PIN1-GFP(Asp). As a result, the *DR5*-visualized auxin response was higher in *PIN1-GFP(Ala),* but lower in *PIN1-GFP(Asp)* roots, compared to the *PIN1-GFP* genotype. These findings were further confirmed by using the developed analytical method for the quantification of free IAA in corresponding root tips.

To analyze indole-3-acetic acid, approximately 20 root tips of 6-day-old seedlings of three genotypes were harvested and extracted for 24 hours with methanol at -20°C. Afterwards the extract was evaporated to dryness and processed by a simplified version of the analytical protocol: It was directly methylated, purified by immunoaffinity extraction and then analyzed by LC-MS/MS. The results are shown in Fig. 3C of the enclosed *Suppl. IV*.

The paper (*Suppl. IV*) elegantly demonstrates how valuable even a narrowly specialized method may be in providing researchers with crucial supporting evidence during studies of complex processes such as growth and development. Studies similar to the one described here, carried out with other PIN proteins, in other species, have lead to the suggestion that cell-type-specific targeted engineering of auxin fluxes might be used to effect desired changes in plant architecture and development. (Zhang et al., 2010).

6. Conclusion and perspectives

The aim of this doctoral thesis was to develop an efficient, specific and sensitive analytical protocol for the analysis of indole-3-acetic acid (IAA) and its derivatives in diverse plant materials. This objective was fulfilled by developing and optimizing the following partial methods:

Immunoaffinity purification

Rabbit polyclonal anti-IAA antibodies were prepared and their wide specificity described repeatedly in literature was confirmed by testing various cross-reactive compounds by ELISA. The antibodies were used to prepare an immunoaffinity gel and to develop a polyspecific immunoaffinity purification procedure allowing isolation from raw or pre-purified plant extract of IAA, seven its amino acid conjugates and further IAA-related compounds. The isolation required methylation of the derivatives which contain a carboxyl group prior to the immunoaffinity purification.

LC-MS/MS quantification

Conditions of chromatographic separation and tandem mass detection were optimized for IAA and twelve other IAA-related compounds. There is a requirement for each of the analyzed compounds to be evaluated by using corresponding heavy-labeled standards. This allowed IAA and ten of its derivatives to be routinely analyzed by HPLC coupled to triple-quadrupole mass detection. The limits of detection vary typically around 1 fmol per injection.

By combining the two methods mentioned above with a preceding C8-based solid-phase extraction (adopted from Karin Ljung, Sweden), a routine analytical protocol was developed. The protocol allows relatively simple and fast processing of tens to two hundred samples a week, with overall recovery ranging between 30 and 70 per cent. The amount of plant material required for the analysis is quite low, recently between 15 and 25 milligrams. Since all the steps of the protocol were thoroughly optimized, the only bottleneck of the method is the preparation of diazomethane (which is a toxic and hazardous methylating agent) and methylation itself.

The protocol and its successful applications were published in the following papers:

Pěnčík et al., 2009 (*Supplement I*)

The paper describes the whole method and quantification of IAA and seven its conjugates, three of which were identified for the first time in higher plants.

Ascough et al., 2009 (*Supplement II*)

The method was successfully used to quantify IAA and its conjugates with Asp and Glu in *Watsonia lepida* seedlings.

Stirk et al., 2009 (*Supplement III*)

Seasonal variations of IAA and related compounds were studied in two species of seaweeds.

Zhang et al., 2010 (*Supplement IV*)

In a study of PIN1-related auxin transport, free IAA in approximately twenty pieces of 1 mm long root tips was quantified in three genotypes of *Arabidopsis thaliana*.

The method was also used to quantify IAA and its conjugates with Asp and Glu in PIN5-expressing BY-2 cells (Mravec et al., 2009). Currently, it is being routinely used for the study of IAA and its derivatives in a variety of plant samples: Tomato (*Solanum lycopersicum*), maize (*Zea mays*), rock rose (*Cistus albidus*), water carnivorous plants (*Aldrovanda vesiculosa, Utricularia australis*), etc. For this purpose, the final analysis has been recently adapted to a modern combination of Acquity UPLC and Xevo TQ MS Systems.

Further development is aimed at improving of the analytical protocol in terms of isolation, quantification and identification of a wider spectrum of IAA-related compounds. Such an improved method could be a powerful tool in current research on the biosynthesis and metabolism of indole-3-acetic acid.

7. References

Bandurski RS, Cohen JD, Slovin J, Reinecke DM (1995) Auxin biosynthesis and metabolism. In: Davies PJ (Ed.): Plant hormones: Physiology, Biochemistry, and Molecular biology (2nd ed.). Kluwer Academic Publishers, 39-65.

Bandurski RS, Schulze A (1974) Concentration of indole-3-acetic acid and its esters in *Avena* and *Zea*. Plant Physiol, 54, 257-262.

Bartel B, LeClere S, Magidin M, Zolman BK (2001) Inputs to the active indole-3-acetic acid pool: de novo synthesis, conjugate hydrolysis, and indole-3-butyric acid β-oxidation. J Plant Growth Regul, 20, 198-216.

Benková E, Michniewicz M, Sauer M, Teichmann T, Seifertova D, Jurgens G, Friml J (2003) Local, efflux-dependent auxin gradients as a common module for plant organ formation. Cell, 115, 591-602.

Bruns M, Bazzanella A, Lochmann H, Bachmann K, Ullrich-Eberius C (1997) Determination of indole-3-acetic acid in plant tissues by capillary electrophoresis. J Chromatogr A, 779, 342-346.

Chen JG, Ullah H, Young JC, Sussman MR, Jones AM (2001) ABP1 is required for organized cell elongation and division in *Arabidopsis* embryogenesis. Genes Dev, 15, 902-911.

Chiwocha SDS, Abrams SR, Ambrose SJ, Cutler AJ, Loewen M, Ross ARS, Kermode AR (2003) A method for profiling classes of plant hormones and their metabolites using liquid chromatography-electrospray ionization tandem mass spectrometry: an analysis of hormone regulation of thermodormancy of lettuce (*Lactuca sativa* L.) seeds. Plant J, 35, 405-417.

Cohen JD, Slovin JP, Hendrickson AM (2003) Two genetically discrete pathways convert tryptophan to auxin: more redundancy in auxin biosynthesis. Trends Plant Sci, 8, 197-199.

Crouch IJ, Smith MT, Van Staden J, Lewis MJ, Hoald GV (1991) Identification of auxins in commercial seaweed concentrate. J Plant Physiol, 139, 590-594.

Crozier A, Loferski K, Zaerr JB, Morris RO (1980) Analysis of picogram quantities of indole-3-acetic acid by high performance liquid chromatography-fluorescence procedures. Planta, 150, 366-370.

Darwin C (1880) The power of movement in plants. Murray, London, UK.

Davies PJ (1999) Plant Hormones, Biosynthesis, Signal transduction, Action! (2nd ed.). Kluwer Academic Publisher, Dortrecht, NL.

Davies PJ (2004) Plant Hormones, Biosynthesis, Signal transduction, Action! (3rd ed.). Kluwer Academic Publisher, Dortrecht, NL.

Edlund A, Eklof S, Sundberg B, Moritz T, Sandberg G, (1995) A microscale technique for gas chromatography-mass spectrometry measurements of picogram amounts of indole-3-acetic acid in plant tissues. Plant Physiol, 108, 1043-1047.

Ek M, Ljungquist PO, Stenstrom E (1983) Indole-3-acetic acid production by mycorrhizal fungi determined by gas chromatography-mass spectrometry. New Phytol, 94, 401-407.

Epstein E, Ludwig-Müller J (1993) Indole-3-butyric acid in plants: occurrence, synthesis, metabolism, and transport. Physiol Plant, 88, 382-389.

Ernstsen A, Sandberg G, Crozier A (1986) Effects of sodium dithiocarbamate, solvent, temperature and plant extract on the stability of indoles. Physiol Plant, 68, 519-522.

Hauserová E, Swaczynová J, Doležal K, Lenobel R, Popa I, Hajdúch M, Vydra D, Fuksová K, Strnad M (2005) Batch immunoextraction method for efficient purification of aromatic cytokinins. J Chromatogr A, 1100, 116-125.

Hertel R, Thomson K, Russo VEA (1972) In vitro auxin binding to particulate cell fractions from corn coleoptiles. Planta, 107, 325-340.

Hofinger M (1980) A method for the quantitation of indole auxins in the picogram range by high performance gas chromatography of their N-heptafluorobutyryl methyl esters. Phytochem, 19, 219-221.

Hou SJ, Zhu J, Ding MY, Lv GH (2008) Simultaneous determination of gibberellic acid, indole-3-acetic acid and abscisic acid in wheat extracts by solid-phase extraction and liquid chromatography-electrospray tandem mass spectrometry. Talanta, 76, 798-802.

Hradecká V, Novák O, Havlíček L, Strnad M (2007) Immunoaffinity chromatography of abscisic acid combined with electrospray liquid chromatography-mass spectrometry. J Chromatogr B, 847, 162-173.

Jackson RG, Lim EK, Li Y, Kowalczyk M, Sandberg G, Hoggett J, Ashford DA, Bowles DJ (2001) Identification and biochemical characterization of an *Arabidopsis* indole-3-acetic acid glucosyltransferase. J Biol Chem, 276, 4350-4356.

Jirásková D, Poulíčková A, Novák O, Sedláková K, Hradecká V, Strnad M (2009) High-throughput screening technology for monitoring phytohormone production in microalgae. J Phycol, 45, 108-118.

Kannangara T, Wieczorek A, Lavender DP (1989) Immunoaffinity columns for isolation of abscisic acid in conifer seedlings. Physiol Plant, 75, 369-373.

Koga J (1995) Structure and function of indolepyruvate decarboxylase, a key enzyme in indole-3-acetic acid biosynthesis. BBA, 1249, 1-13.

Kowalczyk M, Sandberg G (2001) Quantitative analysis of indole-3-acetic acid metabolites in Arabidopsis. Plant Physiol, 127, 1845-1853.

LeClere S, Tellez R, Rampey RA, Matsuda SPT, Bartel B (2002) Characterization of a family of IAA-amino acid conjugate hydrolases from Arabidopsis. J Biol Chem, 277, 20446-20452.

Ljung K, Bhalerao RP, Sandberg G (2001) Sites and homeostatic control of auxin biosynthesis in *Arabidopsis* during vegetative growth. Plant J, 28, 465-474.

Ljung K, Hull AK, Kowalczyk M, Marchant A, Celenza J, Cohen JD, Sandberg G (2002) Biosynthesis, conjugation, catabolism and homeostasis of indole-3-acetic acid in *Arabidopsis thaliana*. Plant Mol Biol, 50, 309-332.

Ljung K, Hull AK, Celenza J, Yamada M, Estelle M, Normanly J, Sandberg G (2005) Sites and regulation of auxin biosynthesis in *Arabidopsis* roots. Plant Cell, 17, 1090-1104.

Ludwig-Müller J (2000) Indole-3-butyric acid in plant growth and development. Plant Growth Regul, 32, 219-230.

Ludwig-Müller J, Cohen JD (2002) Identification and quantification of three active auxins in different tissues of *Tropaeolum majus*. Physiol Plant, 115, 320-329.

Ma Z, Ge L, Lee ASY, Yong JWH, Tan SN, Ong ES (2008) Simultaneous analysis of different classes of phytohormones in coconut (*Cocos nucifera* L.) water using high-performance liquid chromatography and liquid chromatography-tandem mass spectrometry after solid-phase extraction. Anal Chim Acta, 610, 274-281.

Matsuda F, Miyazawa H, Wakasa K, Miyagawa H (2005) Quantification of indole-3-acetic acid and amino acid coniugates in rice by liquid chromatography-electrospray ionization-tandem mass spectrometry. Biosci Biotechnol Biochem, 69, 778-783.

Morris D, Friml J, Zažímalová E (2004) The Transport of Auxins. In: Davies P.J. (Ed.): Plant Hormones: Biosynthesis, Signal Transduction, Action! Kluwer Academic Publishers, 437-470.

Mravec J, Skůpa P, Bailly A, Hoyerová K, Křeček P, Bielach A, Petrášek J, Zhang J, Gaykova V, Stierhof YD, Dobrev PI, Schwarzerová K, Rolčík J, Seifertová D, Luschnig C, Benková E, Zažímalová E, Geisler M, Friml J (2009) Subcellular homeostasis of phytohormone auxin is mediated by the ER-localized PIN5 transporter. Nature, 459, 1136-1140.

Nordstrom AC, Eliasson L (1991) Levels of endogenous indole-3-acetic acid and indole-3-acetylaspartic acid during adventitious root formation in pea cuttings. Physiol Plant, 82, 599-605.

Normanly J, Cohen JD, Fink GR (1993) *Arabidopsis thaliana* auxotrophs reveal a tryptophan-independent biosynthetic pathway for indole-3-acetic acid. Proc Natl Acad Sci U S A, 90, 10355-10359.

Novák O, Tarkowski P, Tarkowská D, Doležal K, Lenobel R, Strnad M (2003) Quantitative analysis of cytokinins in plants by liquid chromatography-single-quadrupole mass spectrometry, Anal Chim Acta, 480, 207-218.

Őstin A, Kowalczyk M, Bhalerao RP, Sandberg G (1998) Metabolism of indole-3-acetic acid in Arabidopsis. Plant Physiol, 118, 285-296.

Paciorek T, Friml J (2006) Auxin signaling. J Cell Sci, 119, 1199-1202.

Paciorek T, Zažímalová E, Ruthardt N, Petrášek J, Stierhof YD, Kleine-Vehn J, Morris DA, Emans N, Juergens G, Geldner N, Friml J (2005) Auxin inhibits endocytosis and promotes its own efflux from cells. Nature, 435, 1251-1256.

Palme K, Hesse T, Campos N, Garbers C, Yanofsky MF, Schell J (1992) Molecular analysis of an auxin binding protein gene located on chromosome 4 of Arabidopsis. Plant Cell, 4, 93-201.

Patten CL, Glick BR (1996) Bacterial biosynthesis of indole-3-acetic acid. Can J Microbiol, 42, 207-220.

Peters W, Ritter J, Tiller H, Valdes O, Renner U, Fountain M, Beck E (2000) Growth, ageing and death of a photoautotrophic plant cell culture. Planta, 210, 478-487.

Pollmann S, Muller A, Piotrowski M, Weiler EW (2002) Occurrence and formation of indole-3-acetamide in *Arabidopsis thaliana*. Planta, 216, 155-161.

Prinsen E, Van Dongen W, Esmans EL, Van Onckelen HA (1997) HPLC linked electrospray tandem mass spectrometry: a rapid and reliable method to analyse indole-3-acetic acid metabolism in bacteria. J Mass Spectrom, 32, 12-22.

Prinsen E, Van Dongen W, Esmans EL, Van Onckelen HA (1998) Micro and capillary liquid chromatography tandem mass spectrometry: a new dimension in phytohormone research. J. Chromatogr A, 826, 25-37.

Redig P, Shaul O, Inze D, Van Montagu M, Van Onckelen H (1996) Levels of endogenous cytokinins, indole-3-acetic acid and abscisic acid during the cell cycle of synchronized tobacco BY-2 cells. FEBS Lett, 391, 175-180.

Reinecke DM (1999) 4-Chloroindole-3-acetic acid and plant growth. Plant Growth Regul, 27, 3-13.

Rolcik J, Lenobel R, Siglerova V, Strnad M (2002) Isolation of melatonin by immunoaffinity chromatography J Chromatogr B, 775, 9-15.

Schneider EA, Kazakoff CW, Wightman F (1985) Gas chromatography-mass spectrometry evidence for several endogenous auxins in pea seedling organs. Planta, 165, 232-241.

Slovin JP, Bandurski RS, Cohen JD (1999) Auxin. In: Hoykaas PJJ, Hall MA, Libbenga KR (Eds.): Biochemistry and molecular biology of plant hormones. Elsevier, 115-140.

Staswick PE, Serban B, Rowe M, Tiryaki I, Maldonado MT, Maldonado MC, Suza W (2005) Characterization of an *Arabidopsis* enzyme family that conjugates amino acids to indole-3-acetic acid. The Plant Cell, 17, 616-627.

Sundberg B, Sandberg G, Crozier A (1986) Purification of indole-3-acetic acid in plant extracts by immunoaffinity chromatography. Phytochem, 25, 295-298.

Sundberg B, (1990) Influence of extraction solvent (Buffer, methanol, acetone) and time on the quantification of Indole-3-acetic acid in plants. Physiol Plant, 78, 293-297.

Tam YY, Normanly J (1998) Determination of indole-3-pyruvic acid levels in *Arabidopsis thaliana* by gas chromatography-selected ion monitoring-mass spectrometry. J Chromatogr A, 800, 101-108.

Tam YY, Epstein E, Normanly J (2000) Characterization of auxin conjugates in Arabidopsis. Low steady-state levels of indole-3-acetylaspartate, indole-3-acetyl-glutamate, and indole-3-acetyl-glucose. Plant Physiol, 123, 589-595.

Tsikas D (2010) Quantitative analysis of biomarkers, drugs and toxins in biological samples by immunoaffinity chromatography coupled to mass spectrometry or tandem mass spectrometry: A focused review of recent applications. J Chromator B, 878, 133-148.

Ulvskov P, Marcussen J, Rajagopal R, Prinsen E, Rudelsheim P, VanOnckelen H (1987) Immunoaffinity purification of indole-3-acetamide using monoclonal antibodies. Plant Cell Physiol, 28, 937-945.

Ulvskov P, Marcussen J, Seiden P, Olsen CE (1992) Immunoaffinity purification using monoclonal antibodies for the isolation of indole auxins from elongation zones of epicotyls of red-light-grown Alaska peas. Planta, 188, 182-189.

Walz A, Park S, Slovin J P, Ludwig-Müller J, Momonoki YS, Cohen JD (2002) A gene encoding a protein modified by the phytohormone indoleacetic acid. Proc Natl Acad Sci U S A, 99, 1718-1723.

Weiler EW (1981) Radioimmunoassay for pmol-quantities of indole-3-acetic acid for use with highly stable [^{125}I]- and [^{3}H]IAA derivatives as radiotracers. Planta, 153, 319-325.

Weiler EW, Jourdan PS, Conrad W (1981) Levels of indole-3-acetic acid in intact and decapitated coleoptiles as determined by a specific and highly sensitive solid-phase enzyme immunoassay. Planta, 153, 561-571.

Went FW (1926) On growth-accelerating substances in the coleoptile of *Avena sativa*. Proceedings of the Section of Sciences, Koninklijke Akademie van Wetenschappen, 30, 10-19.

Went FW (1928) Wuchsstoff und Wachstum. Recueil des Travaux Botaniques Neerlandais, 25, 1-116.

Wightman F, Lighty DL (1982) Identification of phenylacetic acid as a natural auxin in the shoots of higher plants. Physiol Plant, 55, 17-24.

Woodward AW, Bartel B (2005) Auxin: Regulation, action, interaction. Ann Bot, 95: 707-735.

8. Supplements

Supplement I

Pěnčík A, Rolčík J, Novák O, Magnus V, Barták P, Buchtík R, Salopek-Sondi B, Strnad M (2009) Isolation of novel indole-3-acetic acid conjugates by immunoaffinity extraction. Talanta, 80, 651-655.

Supplement II

Ascough GD, Novák O, **Pěnčík A**, Rolčík J, Strnad M, Erwin JE, Van Staden J (2009) Hormonal and cell division analyses in *Watsonia lepida* seedlings. J Plant Physiol, 166, 1497-1507.

Supplement III

Stirk W, Novák O, Hradecká V, **Pěnčík A**, Rolčík J, Strnad M, Van Staden J (2009) Endogenous cytokinins, auxins and abscisic acid in *Ulva fasciata* (Chlorophyta) and *Dictyota humifusa* (Phaeophyta): towards understanding their biosynthesis and homeostasis. Eur J Phycol 44, 231-240.

Supplement IV

Zhang J, Nodzyński T, **Pěnčík A**, Rolčík J, Friml J (2010) PIN phosphorylation is sufficient to mediate PIN polarity and direct auxin transport. Proc Natl Acad Sci U S A, 107, 918-922.

Pěnčík A, Rolčík J, Novák O, Magnus V, Barták P, Buchtík R, Salopek-Sondi B, Strnad M (2009) Isolation of novel indole-3-acetic acid conjugates by immunoaffinity extraction. Talanta, 80, 651-655.

Isolation of novel indole-3-acetic acid conjugates by immunoaffinity extraction

Aleš Pěnčík[a,1], Jakub Rolčík[a,*,1], Ondřej Novák[a], Volker Magnus[b], Petr Barták[c], Roman Buchtík[a], Branka Salopek-Sondi[b], Miroslav Strnad[a]

[a] Laboratory of Growth Regulators, Faculty of Science, Palacký University and Institute of Experimental Botany ASCR, Šlechtitelů 11, CZ-78371 Olomouc, Czech Republic
[b] Ruđer Bošković Institute, Bijenička cesta 54, HR-10000 Zagreb, Croatia
[c] Department of Analytical Chemistry, Faculty of Science, Palacký University, Tř. Svobody 8, CZ-77146 Olomouc, Czech Republic

ABSTRACT

An analytical protocol for the isolation and quantification of indole-3-acetic acid (IAA) and its amino acid conjugates was developed. IAA is an important phytohormone and formation of its conjugates plays a crucial role in regulating IAA levels in plants. The developed protocol combines a highly specific immunoaffinity extraction with a sensitive and selective LC–MS/MS analysis. By using internal standards for each of the studied compounds, IAA and seven amino acid conjugates were analyzed in quantities of fresh plant material as low as 30 mg. In seeds of Helleborus niger, physiological levels of these compounds were found to range from 7.5 nmol g^{-1} fresh weight (IAA) to 0.44 pmol g^{-1} fresh weight (conjugate with Ala). To our knowledge, the identification of IAA conjugates with Gly, Phe and Val from higher plants is reported here for the first time.

1. Introduction

Indole-3-acetic acid (IAA), referred to as auxin, is an important phytohormone. It plays crucial roles in many aspects of the regulation of plant growth and development, including cell elongation [1], tropisms [2] and the establishment of apical-basal polarity in both individual cells and the whole plant [3]. Such wide-ranging regulation of developmental processes by IAA requires that its concentration in cells and tissues is rapidly and sensitively regulated in both space and time. One of the mechanisms by which IAA level in plants is regulated is by conjugation of free IAA with amino acids, giving rise to either biologically inactive, but hydrolyzable, conjugates with alanine (IAAla) and leucine (IALeu) or to unhydrolyzable conjugates with aspartic acid (IAAsp) and glutamic acid (IAGlu). These two groups of conjugates are believed to have a storage function or to precede degradation of excessive IAA, respectively [4].

Although plant materials consist of a very complex matrix containing large amounts of ballast compounds, quantification of IAA – the quantities of which per gram of fresh weight (FW) vary typically between tens and hundreds of pmol – is not too difficult to perform. In current practice, raw extract is usually purified by solid-phase extraction [5] and analyzed by GC–MS [6] following methylation [7], trimethylsilylation [6] or other kind of derivatization [8,9]. Analysis by HPLC coupled to tandem mass detection is also an option, both with [10] or without [11] prior derivatization.

Compared with free IAA analysis, the quantification of IAA amino acid conjugates is much more elaborate due to the significantly lower levels of the analytes present in plant material. Thus in Arabidopsis thaliana, a model organism often used in plant biology, Kowalczyk and Sandberg [12] have described, together with free IAA (the amounts of which ranged between 40 and 130 pmol per gram of fresh material) conjugates with the following four amino acids: Asp, Glu (both present at picomolar level), Leu (hundreds fmol g^{-1} FW) and Ala, with quantities as low as 20 fmol g^{-1} FW. The extracts from A. thaliana were subjected to solid-phase (SPE) extraction and after methylation analyzed by HPLC linked to tandem mass detection. The protocol appeared to be notably simpler than that of Tam and coworkers [13] who used preparative HPLC before quantification of IAAsp and IAGlu by GC–MS.

Recently, an analytical protocol for the quantification of IAA and its conjugates in rice (Oryza sativa) has been described [14], which consists of SPE and subsequent HPLC–MS/MS analysis without prior derivatization. The protocol allows quantification of IAA conjugates with these amino acids: Ala, Asp, Glu, Leu, Phe and Val. It was applied to rice samples of 20–100 mg in fresh weight.

---

* Corresponding author. Tel.: +420 585 634 864; fax: +420 585 634 870.
   E-mail address: jakub.rolcik@seznam.cz (J. Rolčík).
[1] These authors contributed equally to this work.

Table 1
Selected parameters of HPLC–MS/MS analysis of methyl esters of IAA and seven IAA amino acid conjugates. In parentheses, transitions of ^{15}N- and/or ^{2}H$_5$-labeled standards are described.

RT (min)	Analyte	Transition	CV (V)	CE (eV)	LOD (fmol)	Dynamic range (pmol)	Calibration curve	R^2
8.60	IAGly-Me	247.2 > 130.1 (253.2 > 134.1)	19	22	0.2	0.004–2.5	$y = 0.9744x + 0.3592$	0.9998
11.41	IAAla-Me	261.2 > 130.1 (267.2 > 134.1)	21	19	0.7	0.004–2.5	$y = 0.9853x + 0.4162$	0.9995
12.53	IAAsp-Me$_2$	319.2 > 130.1 (325.2 > 134.1)	21	25	0.7	0.2–125	$y = 0.9829x + 0.3599$	0.9993
14.19	IAGlu-Me$_2$	333.2 > 130.1 (339.2 > 134.1)	21	35	0.6	0.04–25	$y = 1.0132x + 0.2683$	0.9998
16.19	IAA-Me	190.2 > 130.1 (195.2 > 134.1)	21	13	1.2	0.2–125	$y = 0.9693x + 0.1860$	0.9996
17.42	IAVal-Me	289.2 > 130.0 (295.2 > 134.1)	23	22	0.3	0.004–2.5	$y = 0.9962x + 0.4024$	0.9998
19.86	IALeu-Me	303.2 > 130.1 (309.2 > 134.0)	25	24	1.0	0.004–2.5	$y = 0.9888x + 0.3500$	0.9992
20.36	IAPhe-Me	337.2 > 130.0 (343.1 > 134.1)	16	27	0.6	0.004–2.5	$y = 0.9680x + 0.3064$	0.9998

However, only conjugates with Ala, Asp and Glu were detected in the selected plant material.

In this paper we introduce a complex analytical protocol suitable for isolation and quantification of IAA and a broad range of its amino acid conjugates. Based on a polyspecific anti-IAA immunoaffinity purification, it may be used to study novel (previously undescribed) naturally occurring IAA conjugates. Since we used internal standards for each of the analyzed compounds, we were able to quantify four known and three novel derivatives over a wide range of concentrations in which they are present in plant material.

2. Experimental

2.1. Reagents and materials

Indole-3-acetic acid and other indole compounds were obtained from OlChemIm (Olomouc, Czech Republic). ^{15}N- and/or ^{2}H$_5$-labeled internal standards were prepared according to Ilić et al. [15]. Affi-Gel 10 was ordered from Bio-Rad (Hercules, CA, USA). Other reagents and solvents were provided by Sigma–Aldrich (St. Louis, MO, USA). Water was purified by the Simplicity 185 water purification system (Millipore, Bedford, MA, USA).

2.2. Preparation of antibodies and their use in immunoaffinity extraction

Polyspecific polyclonal antibodies against IAA and its conjugates were obtained by immunizing rabbits with an IAA–protein conjugate. To couple IAA to bovine serum albumin (BSA) through its carboxyl group, the procedure described by Weiler [16] was used, resulting in a hapten:protein molar ratio of 23. Purification of the antibodies and the preparation of immunoaffinity columns and their use were essentially as described earlier [17]. Capacity and recovery of the columns estimated by application of various amounts of indole-3-acetamide was about 3 nmol and 95–100%, respectively.

2.3. Sample processing and LC–MS/MS analysis

The extraction and subsequent SPE were similar to those used by Karin Ljung (personal communication). Approximately 30 mg (fresh weight) of plant material frozen in liquid nitrogen was ground with pestle and mortar and extracted for 5 min

with 1 ml of cold phosphate buffer (50 mM; pH 7.0) containing 0.02% sodium diethyldithiocarbamate and the following ^{15}N- and/or ^{2}H$_5$-labeled internal standards: [^{2}H$_5$]IAA, [^{15}N,^{2}H$_5$]IAAla, [^{15}N,^{2}H$_5$]IAAsp, [^{15}N,^{2}H$_5$]IAGlu, [^{15}N,^{2}H$_5$]IAGly, [^{15}N,^{2}H$_5$]IALeu, [^{15}N,^{2}H$_5$]IAPhe, and [^{15}N,^{2}H$_5$]IAVal.

After centrifugation (36,000 × g; 10 min; +4 °C), each sample was transferred into an eppendorf tube, acidified with 1 M HCl to pH 2.7 and applied on a C8 column (Bond Elut, 500 mg, 3 ml; Varian) pre-washed with 2 ml of methanol and equilibrated with 2 ml of formic acid (1%; v/v). The column was washed with 2 ml of methanol (10%; v/v) acidified with formic acid (1%; v/v) and retained analyte was eluted with 2 ml of methanol (70%; v/v) acidified with formic acid (1%; v/v). The eluate was evaporated to dryness *in vacuo*.

Samples were reconstituted in 100 μl of methanol acidified with concentrated hydrochloric acid (1 μl per ml of methanol) and methylated with 300 μl of ethereal solution of diazomethane. After 10 min the reaction mixture was evaporated under a stream of gaseous nitrogen (40 °C).
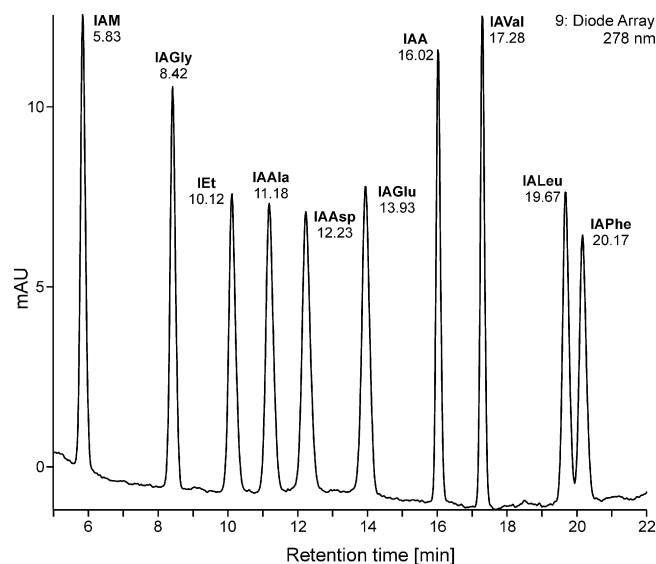

Fig. 1. HPLC–UV chromatogram (278 nm) of methyl esters of IAA, seven IAA conjugates and two other indole compounds retainable by a polyspecific anti-IAA immunoaffinity extraction: Indole-3-acetamide (IAM) and indole-3-ethanol (IEt).
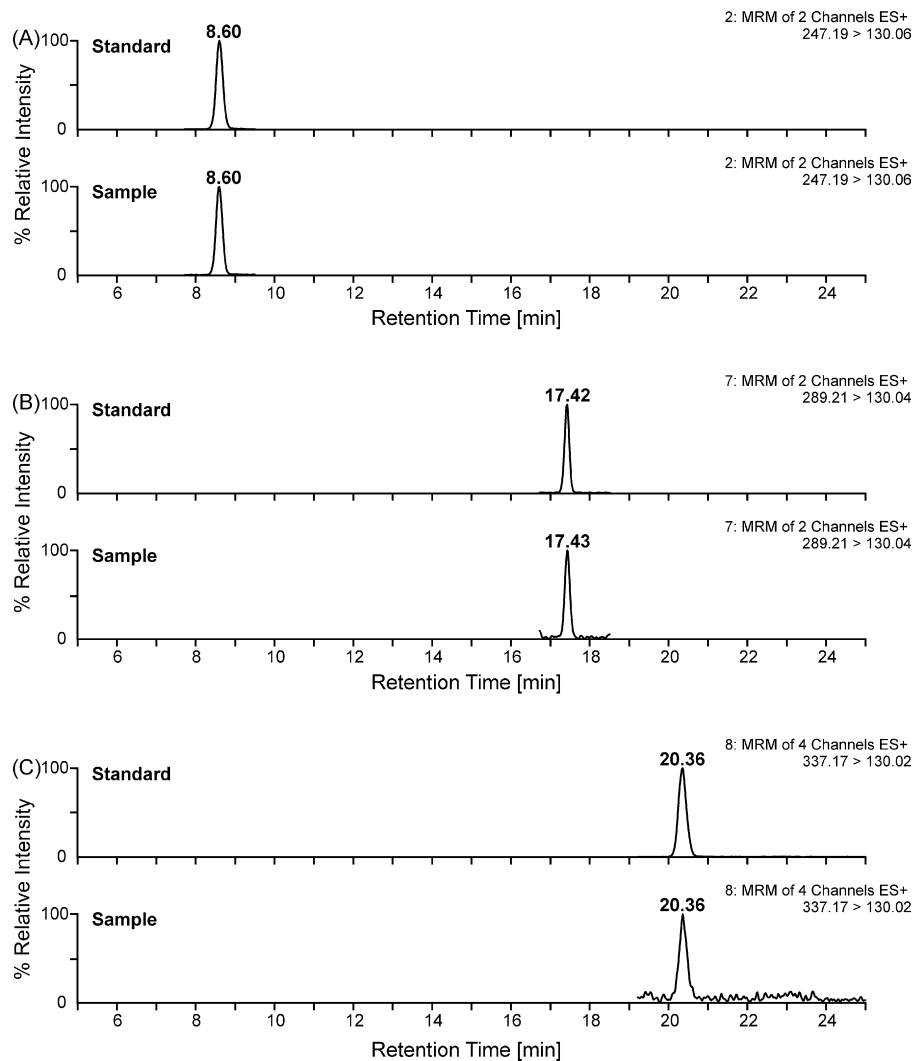
Fig. 2. Chromatograms of the newly discovered IAA amino acid conjugates compared with chromatograms of the corresponding authentic compounds: IAGly (A), IAVal (B) and IAPhe (C).

Prior to immunoaffinity purification, the sample was dissolved in 50 μl of ethanol (70%; v/v) and 450 μl of phosphate buffer (20 mM NaH$_2$PO$_4$; 15 mM NaCl; pH 7.2) and passed through a pre-column containing gel with immobilized BSA. The pre-column was then washed with 0.5 ml phosphate buffer and pooled effluent was applied on an immunoaffinity column with immobilized polyspecific rabbit polyclonal antibody against IAA. The application of the solution was repeated five-times. The immunoaffinity column was then washed three-times with 3 ml of H$_2$O and the analyte was subsequently eluted with 3 ml of methanol (−20 °C). The eluate was evaporated to dryness under nitrogen (40 °C).

Final analysis was done by HPLC coupled to tandem MS/MS detection with the use of a triple-quadrupole mass spectrometer. Separation was performed on an Acquity UPLC System (Waters) equipped with a Symmetry C18 column (5 μm, 2.1 mm × 150 mm; Waters) at 30 °C by gradient elution with a flow-rate of 250 μl min^{-1}. The mobile phase consisted of 10 mM aqueous formic acid and methanol containing 10 mM formic acid. The content of methanol kept at 25% during the first minute was then increased linearly to 38% (at 7 min), 40% (12 min), 58% (15 min), and 60% (26 min). The effluent was introduced into the ion source of a Quatro micro API tandem quadrupole mass spectrometer (Waters). The capillary voltage was set to +500 V, desolvation gas flow was 500 l h^{-1}, desolvation temperature was 350 °C and source block

temperature was 100 °C. Other settings of the instruments, together with multiple reaction monitoring (MRM) transitions of individual compounds, are listed in Table 1.

3. Results and discussion

3.1. Anti-auxin polyspecific immunoaffinity purification

Immuno-based sample preparation techniques have extraordinary potential for trace analysis [18] and have been successfully utilized in analytical protocols used for quantification of various phytohormones including IAA [19,20], cytokinins [10,21–25] and abscisic acid [20,26,27].

In our study of IAA and its conjugates, we exploited the polyspecificity of anti-IAA antibodies. These were obtained by immunizing rabbits with a BSA conjugate in which IAA was linked to the protein through its carboxyl group (IAA-C1′-BSA). Such antibodies are capable of interacting specifically not only with IAA itself but also with other indole compounds substituted in position 3, such as indole-3-acetamide and indole-3-acetonitrile [28]. Furthermore, such antibodies have been reported [16] to cross-react in radioimmunoassays with the IAA homologues indole-3-propionic and indole-3-butyric acid and with IAA conjugated with aspartic

acid. However, this relatively high cross-reactivity is contingent on the free acids being transformed into their methyl esters. Hence, it is necessary to treat samples with diazomethane prior to analysis by an immunomethod [16,29].

An extensive study of our rabbit anti-IAA antibodies, performed by ELISA, has corroborated their polyspecificity. Compared to methylated IAA, cross-reactivities of 3-substituted indoles, including indole-3-acetamide, indole-3-acetonitrile, indole-3-ethanol and methyl esters of IAA conjugates, range typically between 85% and 210%. This allows the antibodies to be used in specific immunoaffinity purification of diverse IAA derivatives. We successfully used immunoaffinity extraction based on these antibodies to isolate and subsequently quantify IAA conjugates with Ala, Asp, Glu and Leu. Furthermore, we succeeded in isolating from a vascular plant and identifying novel naturally occurring IAA conjugates with the three amino acids: Gly, Val and Phe.

3.2. HPLC–MS/MS analysis

Using a linear methanol gradient acidified with formic acid, we achieved base-line separation (see Fig. 1) of a mixture containing methyl esters of IAA and seven IAA conjugates and also two other indole derivatives retainable by the developed immunoaffinity extraction: indole-3-acetamide and indole-3-ethanol (data not shown). In Table 1 the methyl esters are listed in order of their retention time.

Positive ESI tandem mass detection was run in multiple reaction monitoring (MRM) mode. Diagnostic transitions were similar to those used by Kowalczyk and Sandberg [12]: The parent ion of the protonated molecule [M+H]+ fragments to a quinolinium ion of m/z 130.

To cover various recoveries of individual analytes, which may vary depending on the plant material being analyzed, we used internal standards corresponding to each of the studied compounds. All the standards comprised the indole skeleton labeled with five deuterium atoms; additionally, in standards of the conjugates the amino acid was ^{15}N-labeled. Thus values of m/z of internal standard parent ion differed by six units (or by five in the case of IAA) from those of the corresponding unlabeled compounds. Collision-induced dissociation yielded fragments of $m/z = 135, 134$ and 133. We used the fragment of m/z 134, the most intensive one, to perform MRM detection of labeled IAA and its conjugates. We achieved limits of detection (for signal-to-noise ratio of 3) around 1 fmol per injection. Detailed parameters together with other MS settings are listed in Table 1.

3.3. Identification of novel IAA conjugates

A recent study by Staswick et al. [30] has revealed the capability of *Arabidopsis* GH3 enzymes to catalyze synthesis of IAA conjugates with a wide range of amino acids, thus raising the question of whether IAA conjugates other than those with Ala, Asp, Glu and Leu exist. The question gains significance as Ludwig-Müller et al. [31] have very recently identified IAA conjugate with Val in non-vascular plant (moss *Physcomitrella patens*) grown on medium supplemented with IAA.

In our screening for putative IAA conjugates we concentrated on immature seeds of the Christmas rose (*Helleborus niger* L.), in which we had previously detected very high levels of free IAA (around 10 nmol g^{−1} FW). Alongside IAA and the conjugates described earlier [12] we identified novel IAA conjugates with Gly, Phe and Val.

In Fig. 2, chromatograms of newly discovered IAA conjugates are compared with chromatograms of the corresponding authentic compounds. Each pair of chromatograms is characterized by practically identical retention times of peaks for the standard and for the putative compound isolated from plant material. Each pair of chro-
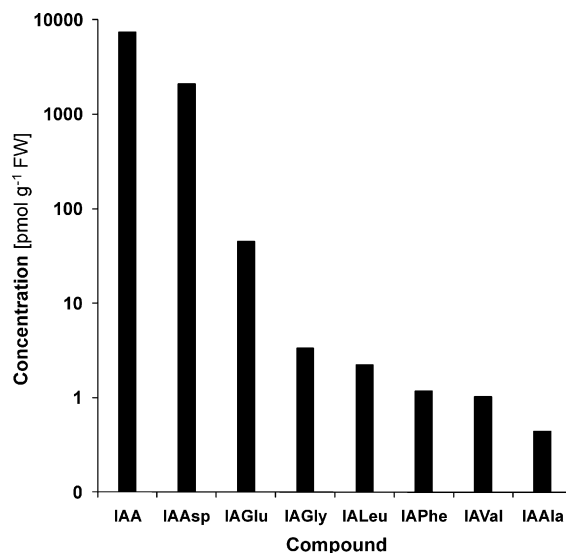

Fig. 3. Semi-logarithmic overview of IAA and seven IAA amino acid conjugates quantified in immature seeds of the Christmas rose (*Helleborus niger* L.).

matograms was obtained in MRM mode where the m/z of the parent ion corresponds to the m/z of the pseudomolecular ion [M+H]+ of the respective IAA conjugate, while an m/z equal to 130 for the daughter ion corresponds to an m/z of the quinolinium ion, which is typical of fragmentation of IAA and its conjugates.

The identity of the conjugates analyzed in *H. niger* seeds seems to be further verified by the fact that they passed through a preceding immunoaffinity purification designed to interact specifically with (3-substituted) indole skeleton. Thus, to our knowledge, for the first time naturally occurring IAA conjugates with Gly, Phe and Val have been identified in vascular plant.

3.4. Quantification of IAA and its conjugates in milligram amounts of plant material

Combination of the highly specific immunoaffinity extraction described above and a sensitive and selective LC–MS/MS – together with the application of internal standards for each of the studied compounds at the initial phase of sample processing – allowed us to reliably quantify IAA and a wide spectrum of its amino acid conjugates. Amounts of fresh plant material required for such an analysis typically lie between 25 mg and 40 mg.

On the basis of our previous experience, we supply the analyzed samples with amounts of internal standards corresponding to expected levels of respective native compounds. In a parallel manner we construct calibration curves which cover typical physiological levels of individual analytes in plant material. The curves

Table 2
Indole-3-acetic acid and its amino acid conjugates as quantified by HPLC–MS/MS in immature seeds and pericarp of *Helleborus niger*.

Analyte	Content in plant tissue (pmol g[−1] FW)[a]	
	Immature seeds	Pericarp
IAA	7378 ± 17	313 ± 16
IAAsp	2089 ± 79	62.5 ± 3.7
IAGlu	44.9 ± 1.2	2.86 ± 0.05
IAGly	3.35 ± 0.19	n.d.[b]
IALeu	2.24 ± 0.11	1.60 ± 0.14
IAPhe	1.17 ± 0.17	n.d.
IAVal	1.02 ± 0.13	n.d.
IAAla	0.44 ± 0.02	n.d.

[a] Mean value of three independent analyses ± standard deviation.

[b] n.d.: not detected.

extend to a little under three orders of magnitude, with good linearity and correlation coefficients (R^2) between 0.9992 and 0.9998 (see Table 1).

Fig. 3 shows the results of an analysis of IAA and its conjugates performed on immature seeds of *H. niger*. The semi-logarithmic plot of the results demonstrates clearly the vast difference (of about four orders of magnitude) between the contents of free IAA (7.5 nmol g^{-1} fresh weight) and IAAla, the least abundant of quantified conjugates (0.44 pmol g^{-1} fresh weight). The value found for IAA itself is comparable to that estimated by Matsuda et al. [14], who analyzed auxins in seeds of rice (*O. sativa*).

Detailed results of our quantification are listed in Table 2 together with the results obtained by analysis of *H. niger* pericarp (husk). Levels of IAA and its conjugates with Asp, Glu and Leu in the pericarp were remarkably lower than those found in seeds, while conjugates with Ala, Gly, Phe and Val were below their limits of detection.

4. Conclusion

We developed a highly specific protocol for analysis of IAA and its amino acid conjugates in small quantities (about 30 mg) of fresh plant material. The protocol is based on a combination of polyspecific anti-IAA immunoaffinity extraction and a sensitive LC–MS/MS method. We successfully used the protocol for quantification of IAA and its conjugates in immature seeds and in the pericarp of *H. niger*. Furthermore, we isolated three novel naturally occurring conjugates of IAA with Gly, Phe and Val and confirmed their identity by analysis of corresponding synthesized standards.

References

[1] A. Hager, J. Plant Res. 116 (2003) 483.
[2] C.A. Esmon, U.V. Pedmale, E. Liscum, Int. J. Dev. Biol. 49 (2005) 665.
[3] J. Friml, P. Benfey, E. Benková, M. Bennett, T. Berleth, N. Geldner, M. Grebe, M. Heisler, J. Hejátko, G. Jürgens, T. Laux, K. Lindsey, W. Lukowitz, C. Luschnig, R. Offringa, B. Scheres, R. Swarup, R. Torres-Ruiz, D. Weijers, E. Zažímalová, Trends Plant Sci. 11 (2006) 12–14.
[4] A.W. Woodward, B. Bartel, Ann. Bot. 95 (2005) 707.
[5] J. Rolčík, J. Řečinská, P. Barták, M. Strnad, E. Prinsen, J. Sep. Sci. 28 (2005) 1370.
[6] A. Edlund, S. Eklof, B. Sundberg, T. Moritz, G. Sandberg, Plant Physiol. 108 (1995) 1043.
[7] A. Müller, P. Düchting, E.W. Weiler, Planta 216 (2002) 44.
[8] C. Birkemeyer, A. Kolasa, J. Kopka, J. Chromatogr. A 993 (2003) 89.
[9] F.M. Perrine, B.G. Rolfe, M.F. Hynes, C.H. Hocart, Plant Physiol. Biochem. 42 (2004) 723.
[10] E. Prinsen, W. Van Dongen, E.L. Esmans, H.A. Van Onckelen, J. Chromatogr. A 826 (1998) 25.
[11] S.J. Hou, J. Zhu, M.Y. Ding, G.H. Lv, Talanta 76 (2008) 798.
[12] M. Kowalczyk, G. Sandberg, Plant Physiol. 127 (2001) 1845.
[13] Y.Y. Tam, E. Epstein, J. Normanly, Plant Physiol. 123 (2000) 589.
[14] F. Matsuda, H. Miyazawa, K. Wakasa, H. Miyagawa, Biosci. Biotechnol. Biochem. 69 (2005) 778.
[15] N. Ilić, V. Magnus, A. Östin, G. Sandberg, J. Labelled Compd. Radiopharm. 39 (1997) 433.
[16] E.W. Weiler, Planta 153 (1981) 319.
[17] J. Rolčík, R. Lenobel, V. Siglerová, M. Strnad, J. Chromatogr. B 775 (2002) 9.
[18] M.C. Hennion, V. Pichon, J. Chromatogr. A 1000 (2003) 29.
[19] B. Sundberg, G. Sandberg, A. Crozier, Phytochemistry 25 (1986) 295–298.
[20] P. Redig, O. Shaul, D. Inze, M. Van Montagu, H. Van Onckelen, FEBS Lett. 391 (1996) 175.
[21] P. Redig, T. Schmulling, H. Van Onckelen, Plant Physiol. 112 (1996) 141.
[22] J.A. van Rhijn, H.H. Heskamp, E. Davelaar, W. Jordi, M.S. Leloux, U.A.T. Brinkman, J. Chromatogr. A 929 (2001) 31.
[23] O. Novák, P. Tarkowski, D. Tarkowská, K. Doležal, R. Lenobel, Strnad M, Anal. Chim. Acta 480 (2003) 207.
[24] E. Hauserová, J. Swaczynová, K. Doležal, R. Lenobel, I. Popa, M. Hajdúch, D. Vydra, K. Fuksová, M. Strnad, J. Chromatogr. A 1100 (2005) 116.
[25] O. Novák, E. Hauserová, P. Amakorová, K. Doležal, M. Strnad, Phytochemistry 69 (2008) 2214.
[26] T. Kannangara, A. Wieczorek, D.P. Lavender, Physiol. Plant 75 (1989) 369.
[27] V. Hradecká, O. Novák, L. Havlíček, M.M. Strnad, J. Chromatogr. B 847 (2007) 162.
[28] P. Ulvskov, J. Marcussen, R. Rajagopal, E. Prinsen, P. Rüdelsheim, H.A. Van Onckelen, Plant Cell Physiol. 28 (1987) 937.
[29] P. Ulvskov, J. Marcussen, P. Seiden, C.E. Olsen, Planta 188 (1992) 182.
[30] P.E. Staswick, B. Serban, M. Rowe, I. Tiryaki, M.T. Maldonado, M.C. Maldonado, W. Suza, Plant Cell 17 (2005) 616.
[31] J. Ludwig-Müller, S. Jülke, N.M. Bierfreund, E.L. Decker, R. Reski, New Phytol. 181 (2009) 323.

Ascough GD, Novák O, **Pěnčík A**, Rolčík J, Strnad M, Erwin JE, Van Staden J (2009) Hormonal and cell division analyses in *Watsonia lepida* seedlings. J Plant Physiol, 166, 1497-1507.

Available online at www.sciencedirect.com

ScienceDirect

Hormonal and cell division analyses in *Watsonia lepida* seedlings

Glendon D. Ascough[a], Ondřej Novák[b], Aleš Pěnčík[b], Jakub Rolčík[b], Miroslav Strnad[b], John E. Erwin[c], Johannes Van Staden[a,*]

[a]*Research Centre for Plant Growth and Development, School of Biological and Conservation Sciences, University of KwaZulu-Natal, Pietermaritzburg, Private Bag X01, Scottsville 3209, South Africa*
[b]*Laboratory of Growth Regulators, Palacký University and Institute of Experimental Botany ASCR, Šlechtitelů 11, CZ-78371 Olomouc, Czech Republic*
[c]*Department of Horticultural Science, University of Minnesota, 1970 Folwell Ave., St Paul, MN 55108, USA*

Summary

The regeneration ability, cell division activity, auxin and cytokinin content of seedling regions and hypocotyl subsections of *Watsonia lepida* were studied. A total of 21 different cytokinins or conjugates were found in seedlings, with the highest cytokinin content in meristematic regions (root and shoot apical meristems). The greatest contribution to the cytokinin pool came from the biologically inactive *c*ZRMP, suggesting that significant *de novo* synthesis was occurring. Five different auxins or conjugates were detected, being concentrated largely in the shoot apical meristem and leaves, IAA being the most abundant. Analysis of hypocotyl subsections (C1–C4) revealed that cell division was highest in subsection C2, although regeneration *in vitro* was significantly lower than in subsection C1. Anatomically, subsection C1 contains the apical meristem, and hence has meristematic cells that are developmentally plastic. In contrast, subsection C2 has cells that have recently exited the meristem and are differentiating. Despite high rates of cell division, cells

---

Abbreviations: BA, benzyladenine; BAR, benzyladenosine; BARMP, benzyladenosine-5′-monophosphate; *c*Z, *cis*-zeatin; *c*ZOG, *cis*-zeatin-O-glucoside; *c*ZR, *cis*-zeatin riboside; *c*ZROG, *cis*-zeatin riboside-O-glucoside; *c*ZRMP, *cis*-zeatin riboside-5′-monophosphate; DHZ, dihydrozeatin; DHZOG, dihydrozeatin-O-glucoside; DHZR, dihydrozeatin riboside; DMP, 2,4,6-tri(dimethylaminoethyl)phenol; IAA, indole-3-acetic acid; IAAsp, indole-3-acetyl aspartate; IAGlu, indole-3-acetyl glutamate; IAM, indole-3-acetamide; IEt, indole-3-ethanol; iP, isopentenyladenine; iPR, isopentenyladenosine; iPRMP, isopentenyladenosine-5′-monophosphate; *m*T, *meta*-topolin; *o*T, *ortho*-topolin; *t*Z, *trans*-zeatin; *t*ZOG, *trans*-zeatin-O-glucoside; *t*ZR, *trans*-zeatin riboside; *t*ZROG, *trans*-zeatin riboside-O-glucoside; *t*ZRMP, *trans*-zeatin riboside-5′-monophosphate.
*Corresponding author. Tel.: +27 33 260 5130; fax: +27 33 260 5897.
E-mail address: rcpgd@ukzn.ac.za (J. Van Staden).

Introduction

Plant growth occurs through cell expansion and cell division, and all organs are generated either directly or indirectly through the meristems. Meristems are regions containing cells that are capable of continued division. Once cells exit the meristem, differentiation takes place, although additional cell division may occur in the areas directly behind the root and shoot apical meristems.

Totipotency, as applied to plants, is the inherent ability of a single cell to regenerate an entire plant. A pluripotent cell, however, is capable of differentiating into another cell type either directly (*trans*-differentiation or re-differentiation) or by first de-differentiating and then re-differentiating, but without necessarily re-entering the cell cycle. Should it do so, it would then progress from G_1 through the DNA synthesis phase (S-phase), through G_2 and then divide. For an intact plant to be formed, cells need to differentiate into the various tissue systems that comprise the plant organs. This requires the action of hormones such as auxin and cytokinins (Schell et al., 1993).

Cells comprising the meristem are generally thought of as undifferentiated, although it has been suggested that because they do not exhibit totipotency *in vivo*, they are differentiated (Lev-Yadun, 2003). Meristematic cells appear to be the most developmentally plastic and respond rapidly to a wide range of physiological and environmental cues. This may be related to cell age. Since cells are dividing continually and have no structural or physiological function such as photosynthesis, they remain "young". They are therefore pluripotent, and have the capability of changing fate into a number of other cell types.

Plants contain three distinct meristems: (1) the shoot apical meristem; (2) root apical meristem and (3) the vascular cambium. Stem cells are separated from their terminally differentiated progeny by an intermediate population of rapidly dividing cells known as transit amplifying cells (Singh and Bhalla, 2006). But how do stem cells remain stem cells? How is a meristem maintained? Specific genes are expressed in meristematic cells that prevent differentiation in cells directly surrounding them, thus making what is known as a "stem cell niche" (Tucker and Laux, 2007). Thus, "The balance between stem cell maintenance within the niche and differentiation of cells that exit it is regulated by local cell–cell communication, together with external cues" (Tucker and Laux, 2007). In other words, these pluripotent cells are dependent on their microenvironment (niche) for their functioning. In contrast, cells induced to enter an embryogenic pathway are truly totipotent, and exhibit a high degree of autonomy since they are not surrounded by a niche of cells (Verdeil et al., 2007).

At what point does a meristematic cell cease being meristematic? Can this be specified genetically or cytologically? The cue may be positional since daughter cells obtained from divisions in the apical meristem undergo several more divisions until they are displaced to the edge of the meristem and then differentiate (Angenent et al., 2005). Individual cells that comprise the meristem are not coordinated or synchronized with respect to the timing and commitment of cell division (de Jager et al., 2005).

What defines a de-differentiated cell? Cells undergoing de-differentiation show two phases of chromatin decondensation: The first is thought to be involved in the acquisition of pluripotentiality, while the second may be related to the new fate of the cell (Grafi, 2004; Grafi and Avivi, 2004). Whether this alteration in chromatin structure is the cause of de-differentiation, or simply a consequence, remains unknown, but it is now thought that meristem activity is at least partly regulated by chromatin remodeling (Guyomarc'h et al., 2005). Similar epigenetic changes involving chromatin organisation and histone methylation occur in animal cells undergoing a change in cell fate, suggesting similar mechanisms may be in place to regulate changes in developmental expression patterns (Costa and Shaw, 2006).

Cytokinins are key cell-cycle regulators and morphogenic agents (Sieberer et al., 2003) that can be classified according to their side-chains: (1) the isoprenoid *cis*-zeatin (*c*Z), *trans*-zeatin (*t*Z) and isopentenyladenine (iP); (2) the isoprenoid-derived

dihydrozeatin (DHZ) and (3) the aromatic benzyladenine (BA) and topolins (Zažímalova et al., 1999). Each different cytokinin type and conjugate may affect the growth and metabolism in different ways. The free bases and ribosides are regarded as the most active forms, but are readily broken down by cytokinin oxidases (Sakakibara, 2006). The ribotides are the first recognized cytokinins formed during biosynthesis, and so presence of these is considered indicative of *de novo* synthesis. The O-glucosyl conjugates are inactive stable forms of excess cytokinins that can be easily converted into free bases, and are thought to play an important role in balancing cytokinin levels, while the N-glucosides result from detoxification (Sakakibara, 2006).

Auxins are ubiquitously occurring plant hormones that are involved in many aspects of plant growth and development. They can be synthesized from tryptophan through the indole-3-pyruvic acid pathway, the indole-3-acetamide pathway, the tryptamine pathway and the indole-3-acetaldoxime pathway (Woodward and Bartel, 2005). There is also considerable evidence for a tryptophan-independent pathway. In most plants, indole-3-acetic acid (IAA) is the most active and abundant auxin. It can be sequestered by conversion to indole-3-butyric acid or reversible conjugation to sugars, amino acids and peptides. It is catabolised after ring oxidation or by conjugation to aspartate or glutamate (Woodward and Bartel, 2005).

This study was initiated following observations that only the hypocotyl region of *Watsonia* seedlings were capable of regeneration *in vitro*, with no response obtained from other parts of the seedling (Ascough et al., 2007). The aim of this study was to determine, using *Watsonia lepida*, the auxin and cytokinin distribution within intact seedlings, to test if hypocotyl subsections differ in their *in vitro* response and their cell division rate, to examine the anatomy of the hypocotyl subsections and lastly to determine the auxin and cytokinin concentrations within each hypocotyl subsection.

Materials and methods

Watsonia lepida N.E. Brown seeds were decontaminated by immersion for 15 min in a 50% (v/v) commercial bleach (Jik®, 3.5% sodium hypochlorite) solution with Tween 20 as a surfactant. Seeds were rinsed three times with sterile distilled water, placed on a 1/10 strength MS medium with 100 mgL^{-1} *myo*-inositol, 0.9% agar, but without hormones or sucrose. Culture jars were placed in

incubators at 25 °C under a 16-h photoperiod for germination. Once seedlings had reached approximately 6 cm in height, they were removed for experimentation. They were divided according to Figure 1, regions A–F (seed was removed), or the hypocotyl region C was divided into four subsections (C1–C4), and used for hormonal analysis and regeneration studies.

Cytokinin analysis

The procedure used for cytokinin purification was a modification of the method described by Faiss et al. (1997). Deuterium-labelled CK internal standards (Olchemim Ltd., Czech Republic) were added, each at 1 pmol per sample to check the recovery during purification and to validate the determination (Novák et al., 2008). The samples were purified using an immunoaffinity chromatography (IAC) based on wide-range specific monoclonal antibodies against cytokinins (Novák et al., 2003). The metabolic eluates from the IAC columns were evaporated to dryness and dissolved in 20 μL of the mobile phase used for quantitative analysis. The samples were analysed by ultra performance liquid chromatography (UPLC) (Acquity UPLC^{TM}; Waters, Milford, MA, USA) coupled to a Quatro *micro*^{TM} API (Waters, Milford, MA, USA) triple
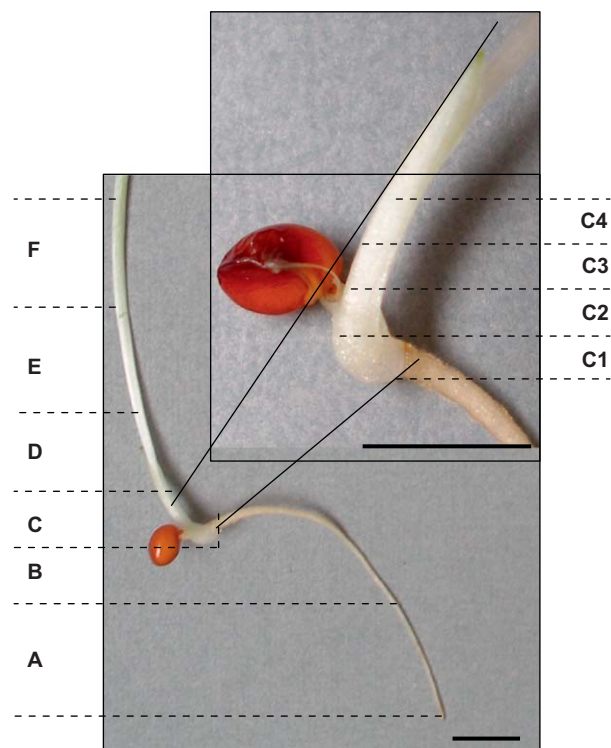

Figure 1. Diagram of *Watsonia lepida* seedling and division of regions (A–F) and hypocotyl subsections (C1–C4). Scale bar: 5 mm.

quadrupole mass spectrometer equipped with an electrospray interface. The purified samples were injected onto a C18 reversed-phase column (BEH C18; 1.7 μm; 2.1 × 50 mm; Waters). The column was eluted with a linear gradient (0 min, 10% B; 0–8 min, 50% B; flow-rate of 0.25 mL/min; column temperature of 40 °C) of 15 mM ammonium formate (pH 4.0, A) and methanol (B). Quantification was obtained by multiple reaction monitoring of $[M+H]^+$ and the appropriate product ion. For selective MRM experiments, optimal conditions, dwell time, cone voltage and collision energy in the collision cell corresponding to exact diagnostic transition were optimized for each cytokinin (Novák et al., 2008). Quantification was performed by Masslynx software using a standard isotope dilution method. The ratio of endogenous cytokinin to appropriate labeled standard was determined and further used to quantify the level of endogenous compounds in the original extract, according to the known quantity of added internal standard (Novák et al., 2003).

Auxin analysis

Plant material (approximately 10 mg DW) was extracted with 1 mL of cold phosphate buffer (50 mM; pH 7.0) containing 0.02% sodium diethyldithiocarbamate and following ^{15}N- and/or $^2H_5$-labeled internal standards: $[^{15}N,^2H_5]IAAsp$, $[^{15}N,^2H_5]IAGlu$, $[^2H_5]IEt$, $[^2H_5]IAM$ and $[^2H_5]IAA$ (Olchemim Ltd., Czech Republic). After removal of cell debris, the extracts were pre-purified by solid-phase extraction on a C8 column (Bond Elut, 500 mg, 3 mL; Varian) and then methylated with ethereal diazomethane. Methylated samples were further purified by auxin-specific immunoaffinity extraction similar to that used for melatonin analysis (Rolčík et al., 2002). Final analysis was done by high-performance liquid chromatography (Acquity, Waters) and tandem mass detection (Quattro Micro tandem mass spectrometry system, Waters). The components of interest were measured in MRM mode and quantified by Masslynx software (Waters) using the standard isotope dilution method.

Regeneration from hypocotyl subsections

The four hypocotyl subsections (C1–C4; Figure 1) from each seedling were cultured in separate tubes on MS media containing 100 mgL^{-1} *myo*-inositol, 0.9% agar, 3% sucrose and one of the following hormone combinations: control (no hormones), 0.5 mgL^{-1} NAA, 0.5 mgL^{-1} benzyladenine (BA),

0.5 mgL^{-1} NAA+0.5 mgL^{-1} BA (ratio 1:1), 0.5 mgL^{-1} NAA+0.05 mgL^{-1} BA (ratio 10:1), 0.05 mgL^{-1} NAA+0.5 mgL^{-1} BA (ratio 1:10). The four regions from one particular seedling were placed within one treatment, forming one replicate. Six replicates were conducted for each treatment, and this was repeated four times. Cultures were placed at 25 °C under fluorescent tubes providing a 16-h photoperiod and a light intensity of 12.6 μmol m^{-2} s^{-1} at culture level. After eight weeks, the response for each region was determined and number of shoots for each explant recorded. A positive response was defined as production of roots, shoots or callus. Regeneration values were arcsine transformed prior to one-way ANOVA, and means were separated using Fishers' individual error rate ($\alpha = 0.05$). The response of seedling and hypocotyl subsections to the various hormone combinations was consistent and similar both within and between treatments, thus results were combined.

Analysis of cell division in hypocotyl subsections

Each hypocotyl subsection (C1–C4) was assessed for cell division using flow cytometry by combining the same region from six seedlings of the same size. Samples were cut into very small pieces with a razor blade in 1 mL extraction buffer containing 100 mM MgCl$_2$, 40 mM trisodium citrate, 22 mM MOPS and 0.1% (v/v) Triton-X-100 with pH adjusted to 7.1. The suspension was filtered through a 50 μm mesh filter and stained with 500 μL propidium iodide. Fluorescence was measured using a Beckman Coulter Epics XL-MCL flow cytometer and DNA content for diploid and tetraploid peaks was compared with data from control regions of the leaf tip. This was repeated nine times. Data were analysed for significant differences using ANOVA and means separated using Fishers' individual error rate ($\alpha = 0.05$).

Light microscopy

In addition to investigating the hormonal and cell division aspects, light microscopy of the hypocotyl sections (C1–C4 and a leaf tip) was performed to observe cell structure characteristics. At least five tissue samples from each section were fixed overnight in 3% glutaraldehyde. The following day, after two washes for 30 min in 0.05 M cacodylate buffer, samples were stained in 2% osmium tetroxide for 2 h. Thereafter, samples were washed twice for 30 min in 0.05 M cacodylate buffer and sequentially

dehydrated by immersion in a graded ethanol series (10%, 30%, 50%, 70%, 80%, 90%, 100%) for 10 min at each concentration. Samples were then embedded in Epon resin: 2 infiltrations of 30 min in propylene oxide, followed by 2 h infiltration with 1:3 (Epon: propylene oxide) plus 1 drop 2,4,6-tri(dimethyla-minoethyl)phenol (DMP), followed by 2 h infiltration with 1:1 (Epon : propylene oxide) plus 2 drops DMP, followed by 16 h infiltration with 3:1 (Epon : propylene oxide) plus 3 drops DMP, followed by 24 h infiltration with Epon plus 4 drops DMP. Samples were placed in small aluminum dishes and incubated in an oven at 70 °C for 48 h. Thereafter, samples were sectioned using an LKB Ultratome II microtome and stained with Ladd's Multiple Stain before viewing under an Olympus AX 70 stereo light microscope.

Results and discussion

Hormonal status of seedlings

The following auxins and conjugates were found in *W. lepida* seedlings: IAA, indole-3-acetyl aspartate (IAAsp), indole-3-acetyl glutamate (IAGlu), indole-3-acetamide (IAM) and indole-3-ethanol (IEt). The sum of these compounds was lowest in regions A and B (roots), and highest in the meristem and expanding leaf (Figure 2A). Greatest contribution to the auxin pool came from IAA, followed by IEt and IAM (Figure 2C). The presence of the intermediate IAM, suggests the microbial trypto-phan-dependent biosynthetic pathway may be operating in *W. lepida*. This supports the growing body of evidence that this pathway is widespread in higher plants. Although auxin biosynthesis is thought to be genetically redundant because of the size of the gene families, the presence of multiple auxin biosynthetic pathways offers a buffered system with various control points that could be tissue- or environment-specific (Chandler, 2009). Low levels of IAAsp and IAGlu were detected, indicating that irreversible conjugation is not necessary in young seedlings, while significant quantities of IEt imply that reversible sequestration is occurring (Rayle and Purves, 1967).

A total of 21 different cytokinins were found within *W. lepida* seedlings (Table 1). The following cytokinins were not detected in any of the seedling sections: *trans*-zeatin-9-glucoside, *c*Z9G, isopentenyladenine-9-glucoside, benzylade-nine-9-glucoside, *p*T, *p*TR, *m*TR, *m*T9G, *o*T9G, dihydrozeatin-O-glucoside (dHZOG), dihydrozeatin riboside-O-glucoside, *p*TOG, *p*TROG, *m*TOG, *m*TROG, *o*TOG, *o*TROG, dihydrozeatin riboside-5′-monophosphate, *p*TRMP, *o*TRMP and *m*TRMP.

Total cytokinin content was highest in region C (hypocotyl), with the second highest concentration occurring in region A (root tip; Figure 2B). Cytokinins are predominantly synthesized in the roots, accounting for a higher level in region A than in regions B, D, E or F. Region C contains the meristematic region, as geophytic monocotyledons have a basally positioned meristem.

In meristematic and surrounding regions, lots of cell division, growth and differentiation occurs, and hence the need for large quantities of cytokinin in region C (hypocotyl). Generally, roots have been reported as the main site of cytokinin biosynthesis, but recent evidence suggests that tissues such as young leaves, meristems and immature seeds can also manufacture cytokinins (Miyawaki et al., 2004). Findings for *W. lepida* are consistent with this.

When the total cytokinin complement is separated based on structure, a more intriguing picture emerges. The distribution of isoprenoid cytokinins indicates a slight concentration gradient of iP from root to shoot (Figure 2E). Very little *t*Z or DHZ was found in seedlings. Interestingly, the distribution of *c*Z shows an identical trend with the distribution of total cytokinins within a seedling. For the most part, *c*Z is the biggest contributor by far to the cytokinin pool. This is in close agreement with Redig et al. (1996) who demonstrated that cytokinins were synthesized during cell cycle phases with a prevalence of Z cytokinins in synchronised BY-2 cells. This is of some significance, since the *c*Z isomer is generally considered less active. Recently, Kasahara et al. (2004) showed that separate pathways for the biosynthesis of *c*Z and *t*Z exist. The MEP pathway operates in plastids and produces *t*Z from DMAPP with the intermediate *t*ZRMP being the first recognized cytokinin formed.

In the cyotosol, the MVA pathway operates to produce *c*Z from DMAPP and tRNA via the intermediate *cis*-zeatin riboside-5′-monophosphate (*c*ZRMP) (Kasahara et al., 2004). Although low levels of *cis–trans* isomerisation have been observed, it appears that the majority of *c*Z is formed by tRNA prenylation with DMAPP from the MVA pathway (Kasahara et al., 2004). This could imply that high rates of tRNA turnover are occurring in all regions of *W. lepida* seedlings, and especially in regions A (root tip) and C (hypocotyl), the areas of greatest cell division, growth and morphogenesis. Alternatively, zeatin-type cytokinins may be produced through an *i*PMP-independent pathway (Åstot et al., 2000).
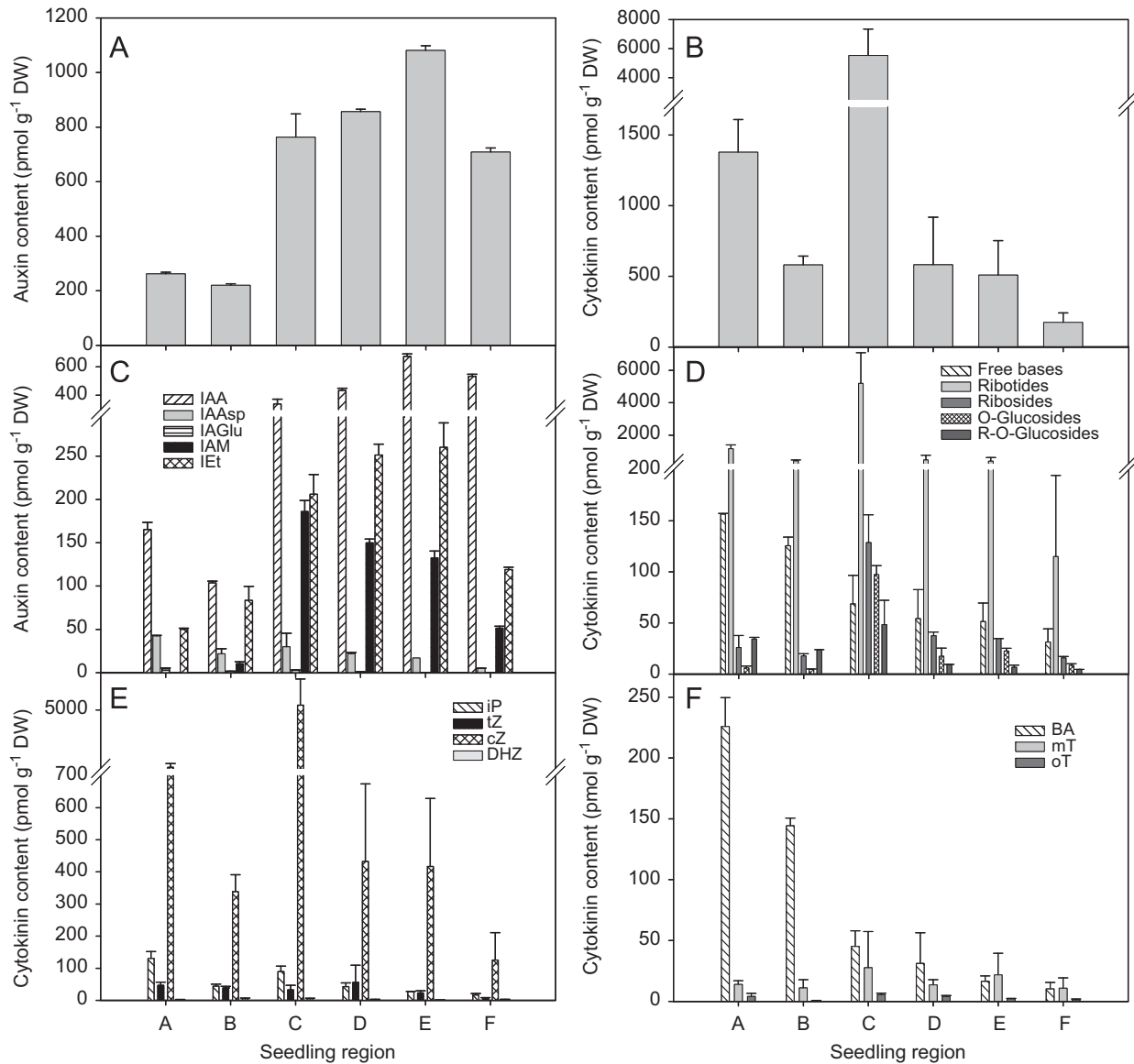
Figure 2. Auxin and cytokinin contents in seedling regions of *Watsonia lepida*. (A) Sum of quantified auxins; (B) total cytokinin content; (C) distribution of different auxins; (D) comparison of functional cytokinins; (E) distribution of isoprenoid cytokinins and (F) distribution of aromatic cytokinins.

The distribution of aromatic cytokinins is quite different from that of the isoprenoids. Both *ortho*-topolin (*o*T) and *meta*-topolin (*m*T) occur at very low concentrations and there is no clear trend in their distribution (Figure 2F). On the other hand, BA shows a distinct gradient from high levels in root sections (regions A and B) to much lower levels in the shoot and leaf. This suggests that BA is synthesized in the roots and transported acropetally to the shoot.

The cytokinin content within seedlings can also be analysed in terms of the functional types – those that are active (free bases), those that are newly synthesized (ribotides), those that are conjugated to ribose (ribosides) and those conjugated to

glucose (OG and ROG). By far, the cytokinin complement for each region is primarily constituted of ribotides (Figure 2D), especially *c*ZRMP (Table 6.1). High concentrations of *c*ZRMP were also found in pea roots after 5 h imbibition, indicating they may play an important role in radicle elongation and early seedling establishment (W.A. Stirk, personal communication). The level of free bases decreases with increasing distance from the root. A peak in the riboside content occurs in region C (hypocotyl), consistent with the observations that ribosides are biologically active and region C being young, actively dividing tissue, and hence would be using cytokinins. Low levels of OG and ROG were present in virtually all regions, with a peak

Table 1. Cytokinin content in *Watsonia lepida* seedling regions (pmol g^{-1} dry weight).

Cytokinin	Root region A	Root region B	Hypocotyl region C	Shoot region D	Shoot region E	Shoot region F
tZ	4.31±1.71	2.81±0.57	2.69±1.68	2.32±0.35	3.53±1.15	2.45±0.38
tZR	2.81±0.57	1.05±0.17	3.06±0.62	3.11±0.09	2.76±0.40	1.82±0.29
tZOG	3.00±0.09	2.79±0.79	1.04±0.06	1.77±0.02	1.94±0.32	2.93±0.72
tZROG	3.63±0.28	2.23±0.03	0.85±0.62	0.96±0.26	0.73±0.18	0.60±0.15
cZ	<LOD	<LOD	8.86±0.27	3.69±0.83	6.86±0.96	3.99±1.26
cZR	2.89±0.00	1.76±1.18	96.19±8.84	20.55±1.00	20.53±2.40	5.44±0.94
cZOG	2.89±0.00	1.76±0.00	96.19±8.84	15.55±8.07	20.53±2.40	5.44±0.94
cZROG	30.73±1.31	21.37±0.18	47.53±23.17	8.34±0.10	5.82±2.28	3.84±0.02
DHZ	<LOD	0.73±0.00	1.09±0.62	0.44±0.21	0.53±0.05	0.48±0.13
DHZR	2.92±0.13	3.34±0.00	3.46±1.19	2.16±0.50	1.33±0.03	2.39±0.23
iP	12.73±3.14	5.91±0.69	2.45±0.00	5.05±1.72	5.57±0.38	4.82±0.76
iPR	6.24±5.15	1.01±0.00	11.98±1.05	5.89±2.32	4.61±0.05	3.46±0.57
BA	130.41±4.14	110.62±9.93	33.82±10.35	31.07±25.22	16.41±4.45	10.16±5.37
BAR	3.95±2.18	4.36±3.86	0.41±0.24	<LOD	<LOD	<LOD
mT	3.99±2.5'	0.52±0.28	5.50±1.17	3.97±0.84	2.00±0.00	1.22±0.75
oT	5.07±2.56	4.91±2.44	14.15±14.47	7.68±4.36	16.42±14.87	8.11±6.75
oTR	8.86±5.50	6.14±0.00	13.49±15.29	5.80±0.14	5.44±2.79	2.63±0.00
tZRMP	34.94±12.83	29.83±5.01	25.38±16.62	47.72±52.99	14.27±8.83	<LOD
cZRMP	918.54±268.6	313.4±50.98	5082±1898	382.2±232.2	362.9±215.7	106.4±82.83
iPRMP	111.61±12.86	37.62±6.52	74.90±15.85	31.76±11.34	16.74±1.41	8.48±3.28
BARMP	91.60±25.69	29.34±7.41	10.80±2.34	<LOD	<LOD	<LOD

<LOD: below limit of detection.

occurring in the meristematic region C. However, the ability of plant tissue to respond to hormones is not only dependent on the hormonal concentration, but also tissue sensitivity. If cells comprising a tissue are not sensitive or competent to respond, hormone levels may not be significant.

Cell division and *in vitro* regeneration

From the flow cytometry results of the hypocotyl subsections (C1–C4), the proportion of nuclei undergoing cell division (4C/2C ratio) was lowest in the control (leaf tip) subsection and subsection C4 (Figure 3B). Cell division was significantly higher in subsection C2 than in subsection C1, while subsection C3 was intermediate between subsection C1 and the control (leaf tip). In terms of *in vitro* regeneration, over 95% of segments from subsection C1 responded, while a mere 23% of explants from subsection C2 responded even though cell division in this region was highest (Figure 3A). The response of seedling and hypocotyl subsections to the various hormone combinations was consistent and similar both within and between treatments, thus results were combined. Explants from subsections C3 and C4 exhibited a negligible response, even though subsection C3 had a significantly higher cell division activity than the control. It was expected that a response *in vitro*

would follow similar trends to those found in cell division, with the control region having lowest regeneration and subsection C2 having the best response. This was not the case, and it appears that cell division and an *in vitro* response are not linked.

In order for a cell to be classified as totipotent, it must undergo numerous coordinated cell divisions and regenerate into a plant. This can occur by direct or indirect organogenesis or alternatively, by embryogenesis (either somatic, gynogenic or androgenic)(Pechan and Smykal, 2001). But is the converse true – can a cell be classified as totipotent by virtue of the fact that it is undergoing cell division? Once division is complete, two cells are produced that have not yet committed to differentiation, and presumably are quite plastic in terms of their fate, which will depend on the signals they perceive from their microenvironment.

Can a cell, by virtue of the fact that it is undergoing cell division, be classified as pluripotent? This would not seem to be logical, since for example, meristemoids are only capable of limited cell division activity. It is well known that expression of genes, primarily transcription factors, is responsible for determining cell fate (Taiz and Zeiger, 2002) and this occurs because cell fate in plants is determined by position (the surrounding physiological environment and cell–cell communication) not lineage. Is it then reasonable to speculate that if actively dividing cells are removed
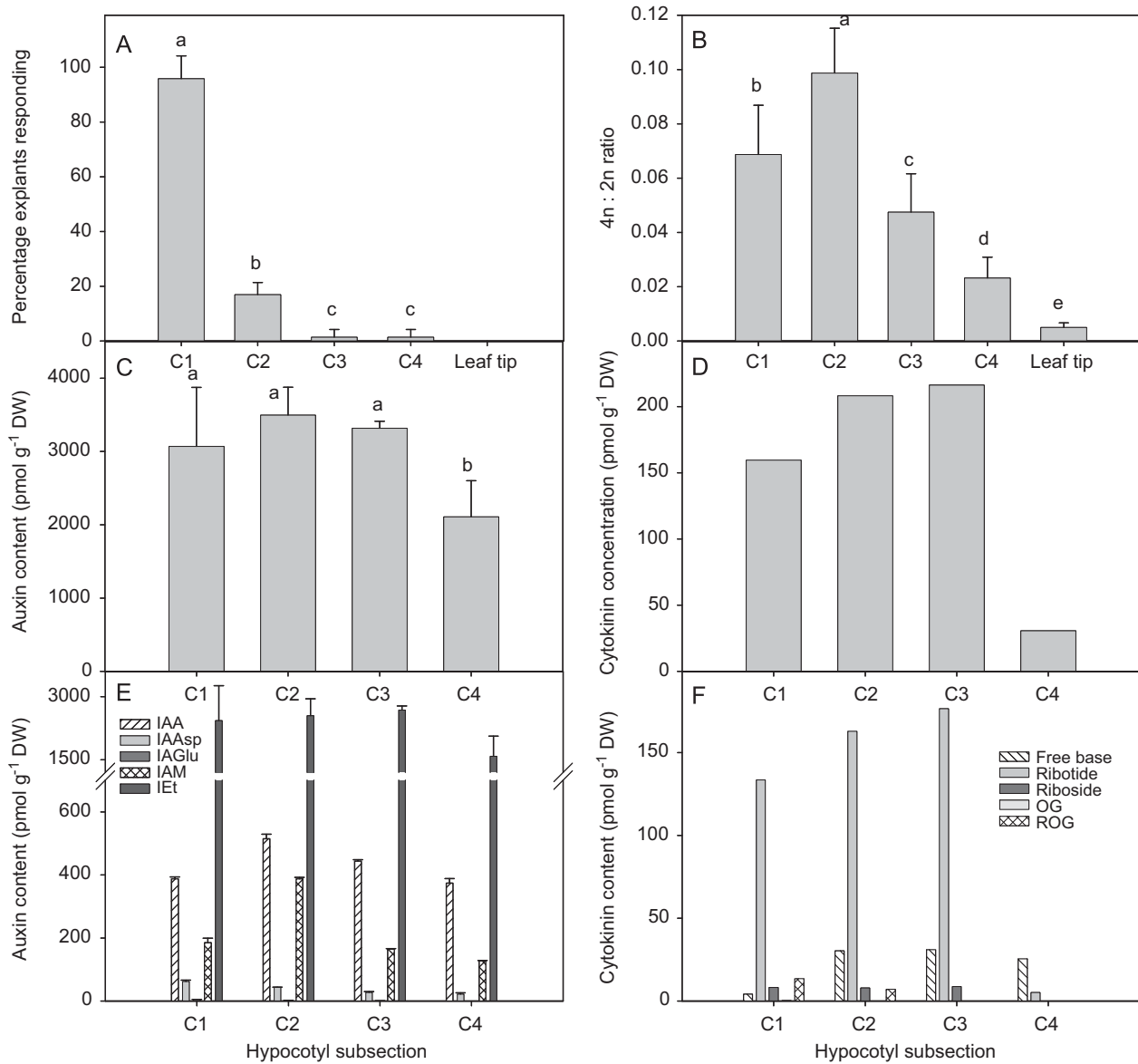
Figure 3. *In vitro* response, cell division activity and hormone content of *Watsonia lepida* hypocotyl subsections. (A) *In vitro* response; (B) cell division activity; (C) total auxin content; (D) total cytokinin content; (E) distribution of different auxins and (F) distribution of functional cytokinins. Bars with different letters are significantly different ($p < 0.05$). Insufficient plant material was available for additional replicates of (D) and (F), hence no SE bars are indicated.

from their positional cues and exposed to stimuli that promote continued cell proliferation, then differentiation would be halted and the meristematic quality maintained?

Unlike animal cells, plant cells are confined by a cell wall. A recent study by Avivi et al. (2004) suggests that protoplast formation from *Arabidopsis* leaf mesophyll cells results in de-differentiation. Apparently, this enzyme-mediated removal of the cell wall is sufficient to induce pluripotentiality (Grafi, 2004). Could isolating cells from intercellular signalling by removing them from the influence of surrounding tissues play a role? This could

well be important, since cell fate is determined not only by lineage but also by the position of the cell within the plant body (Angenent et al., 2005). Thus, the cell wall is probably not the only factor but consideration must also be given to the fact that "…multicellularity has imposed extra layers of complexity that impinge on the balance of cell proliferation and growth, differentiation and organogenesis." (Guiterrez, 2005). This may account for the low regeneration found in *W. lepida* tissues actively undergoing division.

While external conditions control the location and number of stem cells in a meristem, it is the

internal signals that regulate organ formation and initiate cell differentiation (Castellano and Sablowski, 2005). Polar auxin transport has been theorized to be involved in the development of leaf primordia that occurs in daughter cells on the periphery or just outside the meristem (Reinhardt et al., 2003). This, however, did not occur in *W. lepida* and cells in hypocotyl subsection C2 are probably not part of the meristem. Although auxin was present in the culture medium, no further development was observed.

In the case of *W. lepida* hypocotyl sections, despite the presence of both auxin and cytokinin, key cell-cycle regulators and morphogenic agents (Sieberer et al., 2003), a high level of cell division in subsection C2 was not translated into subsequent organ or plant regeneration. Could the positional cues that restrict cell proliferation be in place in such young tissues, and can they continue to operate despite being excised from the rest of the plant?

The presence of meristematic tissue and the age and physiological status of explants are important factors that contribute to successful *in vitro* response. Monocotyledonous plants that produce a dormant storage organ have basally positioned meristems. In seedlings that have not yet formed a corm, the meristem is likely to be at the very base of the shoot. Thus, subsection C1 contains the meristem, as a lower rate of cell division could signify that the cells are quiescent (in other words, stem cells). Subsection C2 may contain meristematic cells that are not necessarily stem cells, as well as cells that have just exited the meristem and beginning differentiation. Subsection C1 has markedly higher regeneration ability than C2 despite both having high rates of cell division. Because the cells in C2 are young and unspecialised, it was thought that *in vitro* response would be similar in these two regions. These cells are not terminally differentiated since they have no irreversible

modifications of their cell walls and contain their nucleus, and so should be responsive given correct induction conditions. It is also possible, however, that the conditions in the present study were not optimal.

Structure of hypocotyl subsections

Hypocotyl subsections C1–C4 were viewed under a light microscope to gain a better understanding of what was happening structurally. The micrograph of section C1 is shown in Figure 4A, and subsections C2–C4 are shown by Figure 4B, as little structural difference was found between these three sections. Section C1 contains the meristem as indicated by the small, isodiametric cells with dense cytoplasm and the presence of developing leaf primordia (Figure 4A). This accounts for the high percentage of explants from this section that were successfully regenerated *in vitro*, as this tissue is competent to divide, grow and differentiate.

Cells of subsection C1 are developmentally plastic and able to respond to external cues, such as the presence of exogenous hormones in the culture medium. In contrast, subsections C2–C4 and the leaf tip, are comprised of various cell types differentiated and grouped into tissues (Figure 4B). Four groupings of vascular bundles are separated by cortical parenchyma. In subsection C2, small meristematic-like cells were observed surrounding the vascular bundles. This presumably contributes to the high rates of cell division detected with flow cytometry analysis. Certainly, cells in C2 have exited the meristem, and therefore are in a physiological environment that promotes differentiation.

Recently, Potters et al. (2006) postulated the notion that plants exhibit common responses to a wide range of abiotic stresses. This was termed a 'stress-induced morphogenic response', and
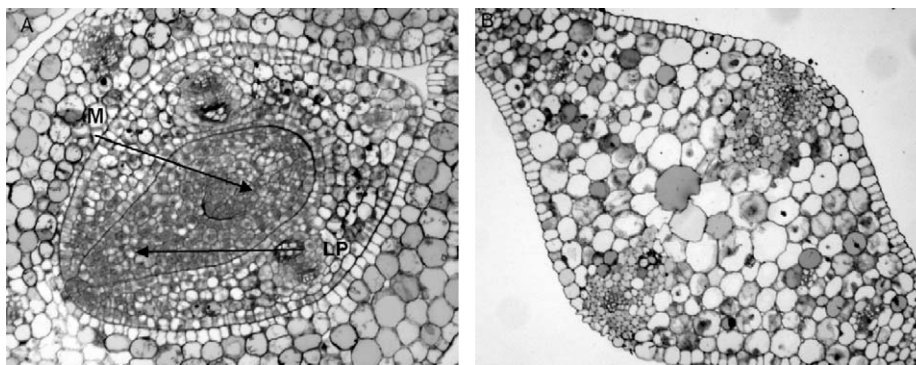

Figure 4. Micrographs illustrating transverse sections of *Watsonia lepida* hypocotyl subsections. (A) Subsection C1 (M, meristem; LP, leaf primordium) and (B) subsection C2.

comprises three components: (1) inhibition of cell elongation; (2) localised stimulation of cell division and (3) changes in morphogenesis/differentiation (Potters et al., 2006). Although these concepts are mainly drawn from reports relating to a whole-plant response, the question must be asked, whether this applies to isolated organs and tissues as in *W. lepida* hypocotyl segments? If so, then excision from the parent plant and being placed in an artificial environment with growth regulators is a significant abiotic stress. This should, therefore, promote cell division and morphogenesis, leading to a response in culture. However, this was only observed in subsection C1, and not the highly dividing cells of subsection C2.

Hormone concentrations within hypocotyl subsections

To determine if the differences observed in cell division and *in vitro* regeneration were caused by hormonal differences, level and type of auxins and cytokinins within the different hypocotyl subsections (C1–C4) were quantified. The sum of auxins quantified in subsections C1–C3 was similar, with C4 containing less auxin (Figure 3C). By far, the greatest contribution to the auxin pool came from IEt, a reversible storage form of IAA (Figure 3E). This indicates the seedlings are carefully controlling free IAA levels by reversible sequestration so that ample supply is ready when needed. Apart from a higher IAM content in C2, there are no other differences between hypocotyl subsections for auxin type and content.

Total cytokinin content was highest in subsections C3 and C2, with C1 having slightly less cytokinins (Figure 3D). Subsection C4 and the leaf tip control had very little cytokinin. This suggests that differences in cell division and regeneration are not easily explained by total cytokinin content, as subsections C1–C3 had different cell division rates and different regeneration frequencies, but similar cytokinin levels.

The majority of cytokinins present in subsections C1, C2 and C3 are the ribotides (5′-monophosphates). In subsection C4, free bases dominate, while in the leaf tip, O-glucosides and free bases dominate (Figure 3F). Compared to the other regions, the concentration of free-base cytokinins in subsection C1 is substantially lower. Interestingly, this is the region that produces the highest regeneration response *in vitro*. This could suggest that higher endogenous concentrations of free-base cytokinins inhibit or repress cells from re-differentiating and entering the cell cycle. However, this

cannot account for the high levels of cell division in C2 and low levels in C3, C4 and the leaf tip. Although embryogenic callus is characterized by a higher endogenous IAA content compared to non-embryogenic callus (Jiménez and Bangerth, 2001a, b), in both types of callus, proliferation continued, whereas in *W. lepida* very little proliferation was observed. Organogenesis is thought of as a multi-step process, requiring at least the acquisition of competence to respond to organogenic signals followed by commitment to that pathway (Moncaleán et al., 2005). Acquisition of competence requires de-differentiation and proliferation of at least some cells. This was not observed in *W. lepida* subsection C2, suggesting that cells are not competent to respond to morphogenic signals. In *Pinus* cotyledons, acquisition of competence occurred within three days of culture when endogenous BA and benzyladenosine (BAR) were detected (Moncaleán et al., 2005). Despite these compounds being present in subsection C2 of *W. lepida* hypocotyls, they were unable to respond. This suggests that additional factors may be at play to regulate cell proliferation.

Acknowledgements

References

Angenent GC, Stuurman J, Snowden KC, Koes R. Use of *Petunia* to unravel plant meristem functioning. Trends Plant Sci 2005;10:243–50.

Ascough GD, Erwin JE, Van Staden J. *In vitro* propagation of four *Watsonia* species. Plant Cell Tiss Org Cult 2007;88:135–45.

Åstot C, Dolezal K, Nordström A, Wang Q, Kunkel T, Moritz T, et al. An alternative cytokinin biosynthesis pathway. Proc Natl Acad Sci USA 2000;97:14778–83.

Avivi Y, Morad V, Ben-Meir H, Zhao J, Kashkush K, Tzfira T, et al. Reorganisation of specific chromosomal domains and activation of silent genes in plant cells acquiring pluripotentiality. Dev Dynam 2004;230:12–22.

Castellano MM, Sablowski R. Intercellular signaling in the transition from stem cells to organogenesis in meristems. Curr Opin Plant Biol 2005;8:26–31.

Chandler JW. Local auxin production: a small contribution to a big field. BioEssays 2009;31:60–70.

Costa S, Shaw P. 'Open minded' cells: how cells can change fate. Trends Cell Biol 2006;17:101–6.

de Jager SM, Maughan S, Dewitte W, Scofield S, Murray JAH. The developmental context of cell-cycle control in plants. Semin Cell Dev Biol 2005;16:385–96.

Faiss M, Zalubilová J, Strnad M, Schmülling T. Conditional expression of the *ipt* gene indicates a function of cytokinins in paracrine signalling in whole tobacco plants. Plant J 1997;12:401–15.

Grafi G. How cells differentiate: a lesson from plants. Dev Biol 2004;268:1–6.

Grafi G, Avivi Y. Stem cells: a lesson from dedifferentiation. Trends Biotechnol 2004;22:388–9.

Guiterrez C. Coupling cell proliferation and development in plants. Nat Cell Biol 2005;7:535–41.

Guyomarc'h S, Bertrand C, Delarue M, Zhou DX. Regulation of meristem activity by chromatin remodeling. Trends Plant Sci 2005;10:332–8.

Jiménez VM, Bangerth F. Hormonal status of maize initial explants and of the embryogenic and non-embryogenic callus cultures derived from them as related to morphogenesis in vitro. Plant Sci 2001a;160:247–57.

Jiménez VM, Bangerth F. Endogenous hormone levels in explants and embryogenic and non-embryogenic cultures of carrot. Physiol Plant 2001b;111:389–95.

Kasahara H, Takei K, Ueda N, Hishiyama S, Yamaya T, Kamiya Y, et al. Distinct isoprenoid origins of *cis*- and *trans*-zeatin biosyntheses in *Arabidopsis*. J Biol Chem 2004;279:14049–54.

Lev-Yadun S. Stem cells in plants are differentiated too. Curr Top Plant Biol 2003;4:93–102.

Miyawaki K, Matsumoto-Kitano M, Kakimoto T. Expression of cytokinin biosynthetic isopentenyltransferase genes in *Arabidopsis*: tissue specificity and regulation by auxin, cytokinin, and nitrate. Plant J 2004;37:128–38.

Moncaleán P, Alonso P, Centeno ML, Cortizo M, Rodríquez A, Fernández B, et al. Organogenic responses of *Pinus pinea* cotyledons to hormonal treatments: BA metabolism and cytokinin content. Tree Physiol 2005;25:1–9.

Novák O, Tarkowski P, Tarkowska D, Doležal K, Lenobel R, Strnad M. Quantitative analysis of cytokinins in plants by liquid chromatography-single-quadrupole mass-spectrometry. Anal Chim Acta 2003;480:207–18.

Novák O, Hauserová E, Amakorová P, Doležal K, Strnad M. Cytokinin profiling in plant tissues using ultra-performance liquid chromatography–electrospray tandem mass spectrometry. Phytochemistry 2008;69:2214–24.

Pechan PM, Smykal P. Androgenesis: affecting the fate of the male gamete. Physiol Plant 2001;111:1–8.

Potters G, Pasternak TP, Guisez Y, Palme KJ, Jansen MAK. Stress-induced morphogenic responses: growing out of trouble? Trends Plant Sci 2006;12:98–105.

Rayle DL, Purves WK. Conversion of indole-3-ethanol to indole-3-acetic acid in cucumber seedling shoots. Plant Physiol 1967;42:1091–5.

Redig P, Shaul O, Inzé D, Van Montagu M, Van Onckelen H. Levels of endogenous cytokinins, indole-3-acetic acid and abscisic acid during the cell cycle of of synchronised tobacco BY-2 cells. FEBS Lett 1996;391:175–80.

Reinhardt D, Pesce E, Stieger P, Mandel T, Baltensperger K, Bennett M, et al. Regulation of phyllotaxis by polar auxin transport. Nature 2003;426:255–60.

Rolčík J, Lenobel R, Sieglerová V, Strnad M. Isolation of melatonin by immunoaffinity chromatography. J Chromatogr B 2002;775:9–15.

Sakakibara H. Cytokinins: activity, biosynthesis and translocation. Annu Rev Plant Biol 2006;57:431–49.

Schell J, Koncz C, Spena A, Palme K, Walden R. Genes involved in the control of growth and differentiation in plants. Gene 1993;135:245–9.

Sieberer T, Hauser MT, Seifert GJ, Luschnig C. PROPORZ1, a putative *Arabidopsis* transcriptional adaptor protein, mediates auxin and cytokinin signals in the control of cell proliferation. Curr Biol 2003;13:837–42.

Singh MB, Bhalla BL. Plant stem cells carve out their own niche. Trends Plant Sci 2006;11:241–6.

Taiz L, Zeiger E. Plant Physiology, 3rd ed. Sunderland: Sinauer Associates, Inc.; 2002.

Tucker MR, Laux T. Connecting the paths in plant stem cell regulation. Trends Cell Biol 2007;17:403–10.

Verdeil JL, Alemanno L, Niemenak N, Tranbarger TJ. Pluripotent versus totipotent plant stem cells: dependence versus autonomy? Trends Plant Sci 2007;12:245–52.

Woodward AW, Bartel B. Auxin: regulation, action, and interaction. Ann Bot 2005;95:707–35.

Zažímalova E, Kamínek M, Březinová A, Motyka V. Control of cytokinin biosynthesis and metabolism. In: Hooykaas PJJ, Hall MA, Libbenga KR, editors. Biochemistry and Molecular Biology of Plant Hormones. Amsterdam: Elsevier Science; 1999. p. 141–60.

Stirk W, Novák O, Hradecká V, **Pěnčík A**, Rolčík J, Strnad M, Van Staden J (2009) Endogenous cytokinins, auxins and abscisic acid in *Ulva fasciata* (Chlorophyta) and *Dictyota humifusa* (Phaeophyta): towards understanding their biosynthesis and homeostasis. Eur J Phycol 44, 231-240.

Taylor & Francis
Taylor & Francis Group

Endogenous cytokinins, auxins and abscisic acid in *Ulva fasciata* (Chlorophyta) and *Dictyota humifusa* (Phaeophyta): towards understanding their biosynthesis and homoeostasis

WENDY A. STIRK[1], ONDŘEJ NOVÁK[2], VERONIKA HRADECKÁ[2], ALEŠ PĚNČÍK[2], JAKUB ROLČÍK[2], MIROSLAV STRNAD[2] AND JOHANNES VAN STADEN[1]

[1]*Research Centre for Plant Growth and Development, University of KwaZulu-Natal Pietermaritzburg, P/Bag X01, Scottsville 3209, South Africa*

[2]*Laboratory of Growth Regulators, Palacký University & Institute of Experimental Botany ASCR, Šlechtitelů 11, 783 71 Olomouc, Czech Republic*

Hormones are present in seaweeds, but little is known about their biosynthesis and regulation. The aim of this study was to investigate variation in concentration and composition of endogenous cytokinins, auxins and abscisic acid in two seaweeds collected over a 1 year period to gain a more complete picture of the types of hormones present during a range of environmental and developmental conditions. *Ulva fasciata* (Ulvales, Chlorophyta) and *Dictyota humifusa* (Dictyotales, Phaeophyta) were collected bimonthly from the inter-tidal zone at Rocky Bay, South Africa. Ethanol extracts of the samples containing a mixture of internal standards were purified using a combined DEAE-Sephadex-octadecylsilica column, followed by immuno-affinity chromatography and analysed by high-performance liquid chromatography – mass spectrometry to quantify different cytokinins, auxins and abscisic acid. *cis*-Zeatin, isopentenyladenine and their ribotide and riboside conjugates were the main cytokinins present in both *U. fasciata* and *D. humifusa* with low concentrations of *trans*-zeatin, dihydrozeatin and aromatic cytokinins. Very low concentrations of O-glucosides and riboside-O-glucosides and no N-glucosides were detected in any of the samples. Based on the cytokinins detected, we propose that as in higher plants, the ribotides are also the first intermediates formed during *de novo* biosynthesis in seaweeds and are subsequently converted to free-bases and ribosides. The only indole compounds detected in both species were free indole-3-acetic acid and indole-3-acetamide (IAM), suggesting that IAM is the intermediate in auxin biosynthesis. Endogenous abscisic acid was detected in most samples with levels in *U. fasciata* generally being higher than those measured in *D. humifusa*.

Key words: abscisic acid, auxins, cytokinins, *Dictyota humifusa*, endogenous plant hormones, *Ulva fasciata*

Introduction

Endogenous hormones play a central role in plant cell proliferation in vascular plants, regulating specific plant cell-cycle genes including those involved in DNA synthesis (Francis & Inzé, 2001). They also play a critical role in stimulating or inhibiting many physiological processes. Seaweeds also contain plant hormones, and cytokinins have been identified in *Sargassum muticum* (isopentenyladenosine - iPR and *cis*-Zeatin - cZ), *Porphyra perforata* (iPR; Zhang *et al.*, 1991) as well as *Laminaria japonica* (iPR and cZ; Duan *et al.*, 1995). More recently, nineteen cytokinin types including both isoprenoid and aromatic forms were identified in 5 Chlorophyta, 7 Phaeophyta and 19 Rhodophyta (Stirk *et al.*, 2003). Despite their diverse

evolutionary lineages, all 31 species had very similar cytokinin profiles in regard to cytokinin types, conjugation forms and their concentrations (Stirk *et al.*, 2003). Indole-3-acetic acid (IAA) has been identified in *Caulerpa paspaloides* (Jacobs *et al.*, 1985) and abscisic acid (ABA) in *Ulva lactuca* (Tietz *et al.*, 1989), *Ascophyllum nodosum* (Boyer & Dougherty, 1988) and three *Laminaria* species (Schaffelke, 1995*a*).

Very little is known about the biosynthesis and regulation of these hormones in seaweeds. Like vascular plants, seaweeds have many different growth and reproductive events during their life history that correlate to seasonal environmental fluctuations. These require some means of physiological control. It may be expected that if plant hormones are important in regulating growth and developmental processes in seaweeds, they will show some seasonal fluctuations in their

Correspondence to: Wendy A. Stirk. E-mail: stirk@ukzn.ac.za

composition and concentrations. Studies in the 1980s demonstrated there was a seasonal variation in cytokinin-like activity in some brown seaweeds, with an increase in cytokinin-like activity (cytokinin free bases and riboside-like activity) in samples collected during periods of active growth, while there was an increase in cytokinin-O-glucoside-like activity in samples collected during periods of slower growth in *Ecklonia maxima* (Featonby-Smith & van Staden, 1984), *Sargassum heterophyllum* (Mooney & van Staden, 1984) and *Macrocystis pyrifera* (de Nys *et al.*, 1990). Cytokinin-like activity also increased in the vegetative laterals of *Sargassum heterophyllum* to coincide with gamete release and the onset of regenerative growth, while activity in the reproductive laterals increased to coincide with gamete release and receptacle initiation (Mooney & van Staden, 1984). The highest cytokinin-activity (free base and riboside-like activity) was detected near the intercalary meristem in the youngest blades of *Macrocystis pyrifera*, whereas the older portions of the blade had higher levels of cytokinin-O-glucoside-like activity (de Nys *et al.*, 1990).

By monitoring the change in the hormone composition over a period of time, where different growth conditions are experienced, it should be possible to gain a more complete picture of the endogenous hormones present in seaweeds. The aim of this study was to investigate changes in the concentration and composition of endogenous cytokinins, auxins and ABA in two seaweed species collected over a 1-year period and, based on these results, to provide a framework to understand their hormone biosynthesis and homeostasis. *Ulva fasciata* Delile (Ulvales, Chlorophyta) was selected as it grew furthest up the intertidal zone and so would be exposed to the most extreme environmental fluctuations. It is also of the same evolutionary lineage as vascular plants. *Dictyota humifusa* Hörnig, Schnetter & Coppejans (Dictyotales, Phaeophyta) was selected for comparative purposes, being of a different eukaryotic lineage to *U. fasciatia*.

Materials and methods

Ulva fasciata and *D. humifusa* were collected within a 50 m² area at Rocky Bay (30°23'S; 30°43'E) situated on the east coast of South Africa. *Ulva fasciata* was always collected from the same small rock pool situated in the upper intertidal region while *D. humifusa* was collected from a gully in the mid intertidal region. It was necessary to harvest a number of individual thalli and pool them into a single sample to obtain sufficient biomass for the hormone analysis. Six bimonthly collections were made within a few days of the new moon to correspond with spring tide during 2004 (23 Jan, 22 Mar, 23 May, 17 Jul, 12 Sep and 14 Nov). KwaZulu-Natal is

a 'summer rainfall area' with average seawater temperatures fluctuating between 18°C and 24°C depending on the time of year (De Clerck *et al.*, 2005). The samples were transported to the laboratory in a cool-box. Epiphytes were removed, the samples freeze-dried and then stored at −70°C until analysed.

Identification and quantification of cytokinins

Duplicate samples (200 mg DW) were analysed for endogenous cytokinins using a modified protocol as described by Novák *et al.* (2003). During extraction in 70% ice-cold ethanol, a cocktail of 16 isoprenoid and 7 aromatic deuterium and ^{15}N-labelled standards (Olchemim Ltd., Czech Republic) was added (see supplementary material available from http://www.informaworld.com/mpp/uploads/stirk_et_al._supplementary_material.pdf), each at 5 pmol per sample to check recovery during purification.

After 3 h of extraction, the homogenate was centrifuged (15 000 × g, 4°C) and the pellets re-extracted using the same procedure. The combined supernatants were concentrated to approximately 1.0 ml under vacuum at 35°C, diluted to 20 ml with ammonium acetate buffer (40 mM, pH 6.5) and purified using a combined DEAE-Sephadex (1.0 × 5.0 cm)-octadecylsilica (0.5 × 1.5 cm) column, splitting the samples into two fractions. The first fraction included cytokinin free bases, ribosides, 9-glucosides and O-glucosides, the second fraction contained ribonucleotides. The first fraction was purified by immunoaffinity chromatography (IAC) based on generic monoclonal cytokinin antibody (Faiss *et al.*, 1997). The samples were dissolved in 50 μl 70% ethanol and 450 μl phosphate buffer solution (PBS: 50 mM NaH$_2$PO$_4$, 15 mM NaCl, pH 7.2) and subsequently applied onto immunoaffinity columns. The immunoaffinity column was equilibrated with 10 ml PBS before sample loading. The sample was repeatedly (five times) applied onto the immunoaffinity column. The column was then rinsed with 10 ml PBS and 10 ml water. The bound cytokinins were eluted by 3 ml 100% methanol.

O-glucoside derivatives not retained on the immunocolumns were treated with β-glucosidase and immunopurified again, giving a second so called 'OG-fraction'. Cytokinin ribonucleotides were treated with alkaline phosphatase and subsequently purified using the same IAC, as described above. All samples were evaporated *in vacuo* and stored in a freezer (−20°C) until further analysis was performed.

The samples were analysed by high performance liquid chromatography (HPLC) (Waters Alliance 2690) linked to a Micromass ZMD 2000 single quadrupole mass spectrometer (HPLC-MS) equipped with an electrospray interface [LC(+)ES-MS] and photodiode array detector (Waters PDA 996). Samples dissolved in 75 μl of the mobile phase for HPLC, were injected on a C18 reverse phase column (Waters; Symmetry; 3.5 μm; 150 mm × 2.1 mm) and elution performed with a methanolic gradient composed of 100% methanol (A) and 15 mM formic acid (B) adjusted to pH 4.0 with ammonium. At a flow rate of 250 μl min^{-1},

the following protocol was used: 0 min 10% A + 90% B – 25 min linear gradient; 50% A + 50% B – 30 min isocratic elution; 50% A + 50% B then column equilibration. Using a post-column split of 1:1, the effluent was introduced into an electrospray source (source block temperature 100°C, desolvation temperature 250°C, capillary voltage + 3.0 V, cone voltage 20 V) and PDA (scanning range 210–300 nm; with 1.2 nm resolution) and quantitative analysis of the different cytokinins performed in selective ion recording mode. Quantification was performed by Masslynx software using a standard isotope dilution method. The ratio of endogenous cytokinin to appropriate labeled standard was determined and further used to quantify the level of endogenous compounds in the original extract, according to the known quantity of added internal standard (Novák *et al.*, 2003).

Identification and quantification of auxins

To the duplicate samples of 50 mg DW, 1 ml of cold phosphate buffer (50 mM PBS; pH 7.0) containing 0.02% sodium diethyldithiocarbamate and a cocktail of twelve ^{15}N- and/or ^{2}H$_5$-labelled internal standards (Olchemim Ltd., Czech Republic) was added (see online supplementary data at http://www.informaworld.com/mpp/uploads/stirk_et_al._supplementary_material.pdf). Except for [^{2}H$_5$]IAA (100 fmol mg^{-1} of sample), all internal standards were added at 20 fmol mg^{-1} of sample. A tungsten-carbide bead (3 mm diameter) was inserted into each sample. Samples were homogenised with a Mixer Mill Retsch MM 301 (2 min; 30 Hz) and subsequently gently shaken in the dark at 4°C for 5 min.

After centrifugation (26000 × g; 15 min; 4°C) the supernatants were transferred into Eppendorf tubes, acidified with 1M HCl (pH 2.7), stirred and applied on C8 columns (Bond Elut, 500 mg, 3 ml; Varian), pre-washed with 2 ml of methanol and equilibrated with 2 ml 1% HCOOH. The columns were then washed twice with 1 ml 10% methanol acidified with 1% HCOOH and the metabolites eluted with 2 ml 70% acidified methanol. The eluates were evaporated to dryness *in vacuo*. After methylation with diazomethane, the samples were dried under a nitrogen stream, dissolved in a mixture of 50 μl 70% ethanol and 450 μl 20 mM PBS (pH 7.2) and subjected to auxin-specific immunoaffinity extraction almost identical, in terms of its execution, to that for melatonin (Rolčík *et al.*, 2002). The immuno-columns were preconditioned before sample purification with 9 ml PBS, 9 ml H$_2$O, 3 ml MeOH, 6 ml H$_2$O and 9 ml PBS. The following procedure was developed for using the IAA immuno-columns for the sample purification: a five times repeated application of the auxin-containing sample in PBS (1 ml); washing with distilled H$_2$O (9 ml); elution of the retained auxins with 100% MeOH (3 ml, −20°C) into a silanised glass tube; washing with distilled H$_2$O (6 ml); and washing with PBS (9 ml). After evaporation of the MeOH sample, the residue was reconstituted in 30 μl of 25% MeOH (10 mM HCOOH). A 15 μl aliquot of the mixture was injected for HPLC-MS quantification of auxins. Analysis was performed by tandem mass spectrometry

(MS/MS) after HPLC separation (Acquity, Waters). The accurate separation of the 15 indole metabolites was obtained on a Symmetry C18 column (150 × 2.1 mm; 5 μm; Waters) at 30°C by linear gradient elution from 25% to 60% (v/v) acidified methanol (1M HCOOH, pH 3.5) at a flow-rate of 250 μl min^{-1}. The effluent was introduced into an electrospray source (source block temperature 100°C, desolvation temperature 300°C, capillary voltage 500 V, cone voltage 21 V). The metabolites were measured in MRM mode with the collision energy set at 13 V. Quantification based on a standard isotope dilution method was performed by Masslynx software (Rolčík *et al.*, 2002).

Purification and quantification of ABA

Duplicate samples of the lyophilised tissues (30–500 mg DW) were powdered using a MM 301 vibration mill (Retsch GmbH & Co. KG, Haan, Germany) at a frequency of 30 Hz for 3 min after adding 3 mm tungsten carbide beads (Retsch GmbH & Co. KG, Haan, Germany) to each tube and extracted with 750 μl ice-cold methanol/water/acetic acid (80/19.5/0.5, v/v) containing sodium diethyldithiocarbamate (400 μg g^{-1} DW) as an antioxidant. To check recovery during purification and to validate quantification, deuterium-labeled ABA (50 pmol [^{2}H$_6$](+)ABA) was added to the samples as an internal standard. After 1 h extraction, the homogenate was centrifuged (15000 rpm; 10 min; 4°C) and the pellets re-extracted the same way. The combined extracts were transferred by pipette onto a 1 ml C18 column (100 mg, Varian, USA), which was conditioned with 1 ml methanol. The samples were eluted with 1 ml methanol/water/acetic acid mixture (80/19.5/0.5, v/v/v) and dried under vacuum. The dried extracts were methylated by an excess of ethereal diazomethane, and after 10 min incubation at room temperature, were evaporated under a nitrogen stream. The final purification step was based on (+)ABA specific immunoaffinity chromatography (IAC). The high affinity polyclonal antibodies used in the IAC were raised against C1-conjugated (+)ABA with bovine serum albumin (BSA) and thus were specific for the free acids and their respective C1-derivatives (Weiler, 1982). The purified samples from the C18 columns were dissolved in 100 μl of 70% EtOH and 400 μl PBS and passed through the IAC columns five times. After washing with 9 ml H$_2$O, the IAC columns were eluted with 3 ml 80% methanol/water/acetic acid (80/19.5/0.5, v/v; −20°C) into silanised glass tubes. After evaporation of the samples under a nitrogen stream, the residues were reconstituted in 100% MeOH and 10 mM HCOOH (30:70). Endogenous ABA levels in the seaweed samples were analysed in duplicate by LC(+)ES-MS as previously described (Hradecká *et al.*, 2007).

Results

Endogenous cytokinins

Despite their different evolutionary origins, both species had very similar cytokinin profiles. Eleven

isoprenoid and four aromatic cytokinins were identified in *U. fasciata* and ten isoprenoid and two aromatic cytokinins in *D. humifusa* with isoprenoid cytokinins occurring at much higher levels compared to the aromatic cytokinins (Fig. 1). The majority of the cytokinins detected in the two seaweed species were of isopentenyladenine (iP) and *c*Z origin. Among the others, only *trans*-zeatin (*t*Z), two dihydrozeatin-types (DHZ) and four aromatic cytokinins were identified. The latter occurred at very low concentrations (Table 1). The cytokinin ribotide concentrations of isopentenyladenosine-5'-monophosphate (iPRMP) and *cis*-zeatin riboside-5'-monophosphate (*c*ZRMP) and the free base iP were the main cytokinin forms present in both *U. fasciata* and *D. humifusa*. Cytokinin ribosides generally occurred in lower concentrations compared to the ribotides and very low concentrations of the cytokinin-O-glucosides and cytokinin riboside-O-glucosides were measured with less than $2.1\ pmol\ g^{-1}$ DW being detected (Table 1; Fig. 2). No N-glucosides were detected in any of the samples.

There was a gradual decrease in the cytokinin concentration in *U. fasciata* corresponding with lower water temperatures and the lowest cytokinin concentration was detected in May. With the onset of spring, there was an increase in the cytokinin content with the highest cytokinin concentration being recorded in September (Fig. 1*a*). This trend was mainly due to fluctuations in the ribotide
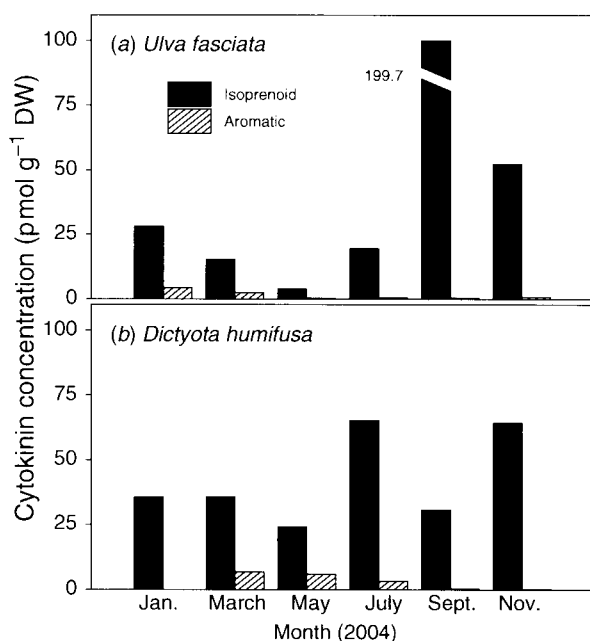
concentrations (Fig. 2*a*). There was less variation in cytokinin concentrations in the *D. humifusa* samples (Fig. 1*b*).

Endogenous auxins

Although the method used in this study is able to detect most indole forms at very low detection limits (see online supplementary data at http://www.informaworld.com/mpp/uploads/stirk_et_al._supplementary_material.pdf), the only indole compounds detected in the two seaweed species were free IAA and indole-3-acetamide (IAM). IAM generally occurred in lower concentrations than IAA except in the *U. fasciata* sample collected in September where the IAM concentration was approximately three times higher than IAA (Fig. 3). Auxin concentrations followed a similar trend to the cytokinins in *U. fasciata*, with lower concentrations detected in the samples collected during the cooler months and an increase in concentration in the warmer months (Fig. 3*a*). This trend was not apparent in *D. humifusa* with the lowest amounts detected in the January, July and September (Fig. 3*b*).

Endogenous ABA

ABA was detected in both *U. fasciata* and *D. humifusa*. ABA concentrations did not vary greatly in *U. fasciata* except for the sample collected in September where the ABA levels doubled (Fig. 4). Concentrations were always lower in *D. humifusa* compared to those measured in *U. fasciata* (Fig. 4).

Discussion

Cytokinins are classified according to the nature of their N^6-side chain. Isoprenoid cytokinins are divided into four groups, iP, *t*Z, *c*Z and DHZ, with aromatic cytokinins falling into two groups, benzyladenine (BA) and topolins. Conjugates of these free-bases include ribosides, ribotides (riboside-5'-phosphates), O-glycosides, N-glycoside and amino-acid conjugates. In vascular plants, *t*Z and its metabolites, including DHZ, are the most prevalent cytokinins, while iP-type cytokinins are generally minor components; however, in non-vascular plants such as mosses or algae, iP is generally the principle free cytokinin (Auer, 1997). The results from this study concur with this report, with iP- and *c*Z-type cytokinins being the prevalent cytokinin types in the two species analysed, with very few *t*Z and DHZ-type cytokinins being detected (Table 1). The concentrations of cytokinins detected in these two seaweed species is comparable to that found in the water fern

Fig. 1. Changes in the total endogenous cytokinin content in (*a*) *Ulva fasciata* and (*b*) *Dictyota humifusa* collected from Rocky Bay, South Africa over a 1 year period. Isoprenoid cytokinins are shown as the sum total of the iP-, *c*Z-, *t*Z- and DHZ-type cytokinins and aromatic cytokinins as the sum total of the BA- and topolin-type cytokinins detected in each sample. Abbreviations as in Table 1.

Table 1. Cytokinin concentrations (pmol g^{-1} DW) detected in *Ulva fasciata* and *Dictyota humifusa* collected from Rocky Bay, South Africa over a 1 year period (2004).

Cytokinin	Collection date					
	23 Jan	22 Mar	23 May	17 Jul	12 Sep	14 Nov
U. fasciata						
iP	–	2.44 ± 0.21	0.66 ± 0.12	5.50 ± 0.83	3.19 ± 0.49	3.76 ± 1.06
iPR	1.41 ± 0.16	1.39 ± 0.24	1.45 ± 0.31	1.44 ± 0.36	1.73 ± 0.52	2.23 ± 0.18
iPRMP	3.08 ± 0.52	2.69 ± 0.16	1.48 ± 0.43	1.32 ± 0.28	2.14 ± 0.24	2.94 ± 0.43
cZ	–	0.31 ± 0.02	–	2.74 ± 0.43	2.80 ± 0.67	2.18 ± 0.28
cZR	0.81 ± 0.02	0.83 ± 0.05	0.27 ± 0.02	0.97 ± 0.19	4.77 ± 0.82	2.30 ± 0.31
cZOG	–	0.26 ± 0.01	–	0.22 ± 0.14	0.37 ± 0.05	0.69 ± 0.05
cZROG	–	0.32 ± 0.01	–	0.14 ± 0.02	0.40 ± 0.13	0.26 ± 0.01
cZRMP	20.33 ± 1.14	5.32 ± 0.47	–	7.02 ± 0.26	184.2 ± 5.4	37.92 ± 2.14
tZ	–	–	–	0.20 ± 0.01	0.13 ± 0.00	0.09 ± 0.00
DHZ	0.30 ± 0.03	0.73 ± 0.14	–	–	–	–
DHZOG	2.17 ± 0.26	0.92 ± 0.08	0.97 ± 0.13	–	–	–
BA	0.57 ± 0.11	0.30 ± 0.02	0.36 ± 0.05	0.35 ± 0.02	0.33 ± 0.01	0.29 ± 0.01
BAR	3.43 ± 0.08	1.78 ± 0.23	–	–	–	–
oT	0.34 ± 0.04	0.37 ± 0.04	–	–	0.02 ± 0.00	0.23 ± 0.01
oTR	–	–	–	0.15 ± 0.00	0.11 ± 0.00	0.16 ± 0.00
D. humifusa						
iP	1.11 ± 0.15	15.15 ± 2.16	10.53 ± 1.56	49.58 ± 6.31	19.69 ± 1.09	22.47 ± 2.36
iPR	0.68 ± 0.23	3.48 ± 0.38	3.38 ± 0.53	5.63 ± 0.65	1.93 ± 0.04	14.07 ± 2.11
iPRMP	3.21 ± 0.46	3.87 ± 0.46	4.80 ± 1.14	2.50 ± 0.43	4.13 ± 1.18	5.28 ± 1.06
cZ	0.13 ± 0.03	1.36 ± 0.24	0.30 ± 0.01	2.28 ± 0.15	0.50 ± 0.06	1.06 ± 0.15
cZR	0.29 ± .006	1.26 ± 0.23	0.33 ± 0.02	0.87 ± 0.20	0.27 ± 0.01	2.80 ± 0.59
cZOG	0.30 ± 0.02	0.60 ± 0.18	0.26 ± 0.01	1.40 ± 0.29	0.56 ± 0.04	1.26 ± 0.43
cZROG	0.38 ± 0.07	0.64 ± 0.12	0.47 ± 0.01	0.73 ± 0.15	0.38 ± 0.07	2.46 ± 0.58
cZRMP	28.42 ± 2.15	8.82 ± 0.49	4.05 ± 0.23	1.96 ± 0.26	3.16 ± 0.33	14.66 ± 1.13
tZ	–	–	–	0.33 ± 0.02	–	–
DHZOG	–	0.45 ± 0.11		–	–	0.28 ± 0.01
BAR	–	6.64 ± 0.32	3.69 ± 0.41	3.00 ± 0.16	–	–
oT	–	–	2.26 ± 0.24	0.28 ± 0.01	0.25 ± 0.01	0.19 ± 0.01

Results are presented as mean ± SE (*n* = 2). – indicates that cytokinins were below the limit of detection.
Abbreviations: BA: 6-benzylaminopurine; BAR: 6-benzyladenosine; cZ: *cis*-zeatin; cZOG: *cis*-zeatin-O-glucoside; cZR: *cis*-zeatin riboside; cZROG: *cis*-zeatin ribosides-O-glucoside; cZRMP: *cis*-zeatin riboside-5'-monophosphate; DHZ: dihydrozeatin; DHZOG: dihydrozeatin-O-glucoside; iP: isopentenyladenine; iPR: isopentenyladenosine; iPRMP: isopentenyladenosine-5'-monophosphate; oT: *ortho*-topolin; oTR: *ortho*-topolin riboside; tZ: *trans*-zeatin.

Salvinia molesta D.S. Mitchell (82 pmol g^{-1} DW) using the same method (Arthur *et al.*, 2007). However, these concentrations were between 2 and 10-fold lower than cytokinin concentrations found in germinating *Tagetes minuta* L. achenes (Stirk *et al.*, 2005) and germinating *Pisum sativum* L. seeds (Stirk *et al.*, 2008).

Many cytokinin forms are inter-convertible in plant tissues, with these conversions mediated by specific enzymes. Furthermore, even a small substitution to the side chain has a large effect on biological activity, metabolic stability and resistance to degradation (Sakakibara, 2006). As little is known about cytokinin biosynthesis and homoeostasis in seaweeds, our knowledge of cytokinins in vascular plants provide a starting point in this regard.

As in the previous study where 31 seaweed species were analysed for their endogenous cytokinin content using the same method as in this study (Stirk *et al.*, 2003), cZ and its conjugates occurred in much higher amounts than tZ-type cytokinins in both *U. fasciata* and *D. humifusa*. *cis*-Zeatin is generally much less active in bioassays than tZ (Sakakibara, 2006). In vascular plants, cZ derivatives are produced by an alternative pathway where tRNA degradation leads to the formation of cZ. Recent studies with *Arabidopsis* suggest the involvement of the mevalonate pathway in the biosynthesis of cZ derivatives, with the first step catalysed by tRNA-isopentenyl-transferases (Kasahara *et al.*, 2004). This alternative pathway allows for the independent regulation of cZ derivatives from other isoprenoid cytokinins (Kasahara *et al.*, 2004; Sakakibara, 2006). The possibility of such an alternative pathway for the production of cZ derivatives existing in the various seaweed phyla needs to be established in view of the consistently high cZ derivative concentrations detected in the seaweed samples analysed in this study (Table 1) and previously (Stirk *et al.*, 2003).

In vascular plants, the ribotides (5-mono-, di-, triphospates of iRP and ZR) are the first metabolites formed in both the iP-dependent and iP-independent biosynthetic pathways (Åstot *et al.*, 2000; Sakakibara & Takei, 2002) and thus play
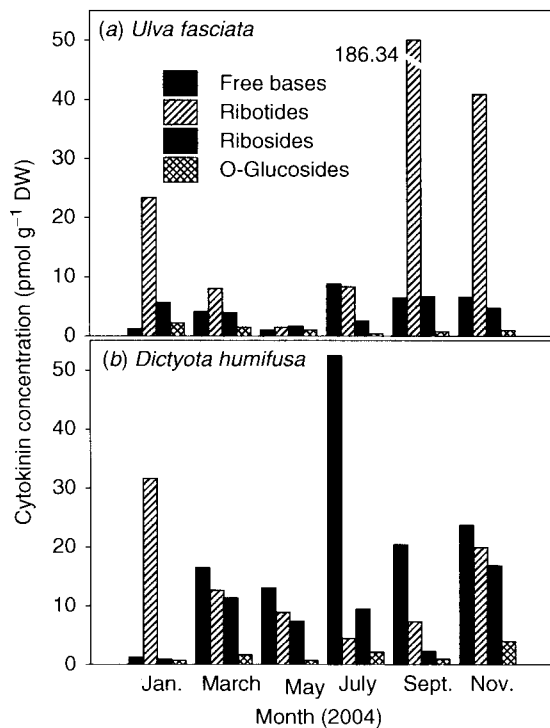
Fig. 2. Changes in the endogenous cytokinin composition of free bases (iP, cZ, tZ, DHZ, BA and oT), ribotides (iPRMP and cZRMP), ribosides (iPR, cZR, BAR and oTR) and O-glucosides (cZOG, cZROG and DHZOG) in (a) *Ulva fasciata* and (b) *Dictyota humifusa* collected from Rocky Bay, South Africa over a 1 year period. Abbreviations as in Table 1.
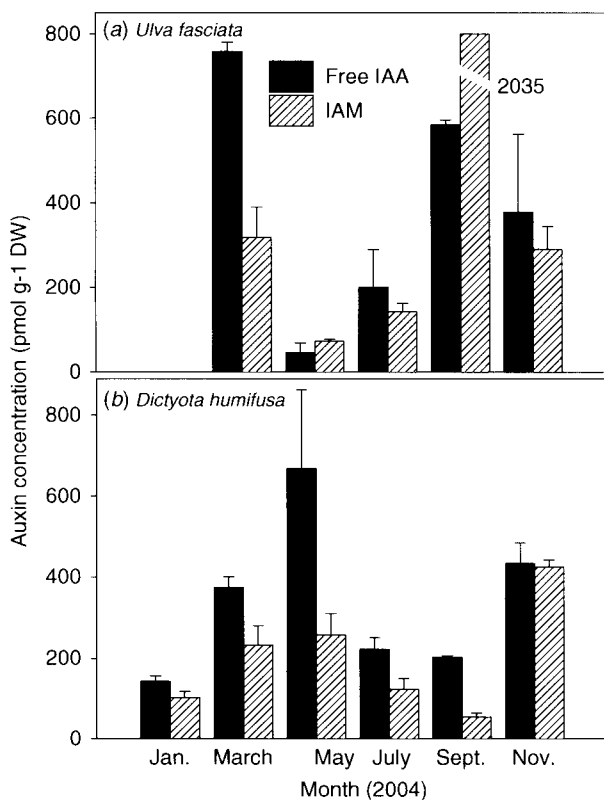

Fig. 3. Changes in the endogenous auxin content in (a) *Ulva fasciata* and (b) *Dictyota humifusa* collected from Rocky Bay, South Africa over a 1 year period. Results are presented as mean ± SE.
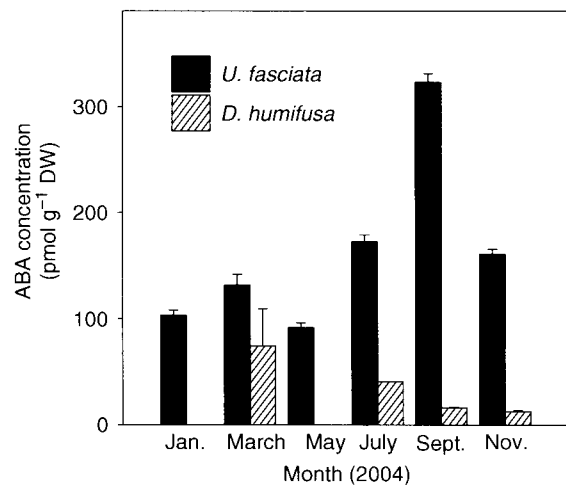

Fig. 4. Changes in the endogenous abscisic acid (ABA) concentration in *Ulva fasciata* and *Dictyota humifusa* collected from Rocky Bay, South Africa over a 1 year period. Results are presented as mean ± SE.

a key role in cytokinin biosynthesis. They are also more resistant to degradation by cytokinin oxidases compared to free-bases and ribosides (Armstrong, 1994; Galuzska, personal communication). In the two seaweeds analysed in this study and previously (Stirk *et al.*, 2003), the ribotide iPRMP generally occurred in the highest concentrations. Both iPRMP and cZRMP concentrations followed a seasonal trend with lower concentrations recorded during the winter months and increasing sharply in spring and early summer in both *U. fasciata* and *D. humifusa* (Fig. 2). This suggests that the ribotides play a key role in *de novo* cytokinin biosynthesis in seaweeds, as they do in vascular plants, and that they are an important source for conversion to other cytokinin conjugate forms.

Free-bases and ribosides are the most active cytokinin forms in vascular plants, binding with high affinity to different receptors to elicit a physiological response (Spichal *et al.*, 2004; Yonekura-Sakakibara *et al.*, 2004). However, both forms are susceptible to degradation by cytokinin oxidase (Armstrong, 1994). Assuming that the cytokinin free-bases and ribosides are the physiologically active forms in seaweeds, as they are in vascular plants, it would appear that they are derived from the ribotides and their levels are generally lower due to them being actively utilised in various growth processes, especially during the warmer summer months.

In vascular plants, free-bases and ribosides can be converted to O-glucosides by O-glycosyltransferases. When required, they are easily hydrolysed by β-glucosidase to their free-bases and ribosides. Thus, they are considered storage forms (Sakakibara, 2006). Glucosylation of the adenine ring at the 3-, 7- or 9-position forms N-glycosides.

These cytokinins have no or low activity in bioassays, are not readily converted to other cytokinin forms and are extremely resistant to enzymatic degradation (Sakakibara, 2006). Thus they are considered as deactivation products. Only low concentrations of O-glucosides and no N-glucosides were detected in the two seaweeds analysed in this study. This is consistent with the results reported for the 31 seaweed species previously analysed (Stirk *et al.*, 2003). If the glucosides have the same storage and deactivation functions as in vascular plants, this implies that unlike vascular plants, glucosylation is not a mechanism extensively used in the regulation of the concentration of the active cytokinin forms. Also, it is not known if cytokinin oxidase is found in any seaweeds and if it would be necessary to structurally modify the side chain to enhance stability against cytokinin oxidase.

Based on these results, we suggest that in seaweeds the levels of active isoprenoid cytokinins are regulated directly by biosynthesis of iPRMP, followed by the conversion of ribotides to ribosides and free-bases rather than N-glucosides. Further experiments using radio-labelled cytokinins to follow the inter-conversion pathways are needed to either confirm or disprove this theory on cytokinin homoeostasis in seaweeds. Glucosylation and the presence of cytokinin oxidase enzymes in seaweeds also need to be investigated to further understand the mechanisms for controlling cytokinin levels in seaweeds.

Endogenous aromatic cytokinins are now routinely found in vascular plants (Taylor *et al.*, 2003). Their occurrence has also previously been reported in microalgae (Ördög *et al.*, 2004) and seaweeds (Stirk *et al.*, 2003). Although aromatic and isoprenoid cytokinins have overlapping spectra of biological activity, evidence suggests that they are not merely alternative forms of the same signal and that they have separate biosynthetic pathways (Strnad, 1997). Their physiological function is not well understood but they do show a short-term increase in response to light and stress in vascular plants (Strnad, 1997). There is also clear discrimination of aromatic and isoprenoid cytokinins at the receptor level (Spichal *et al.*, 2004). The interaction of aromatic cytokinins with cellular signaling systems also appears to be different to that of isoprenoid cytokinins (Doležal *et al.*, 2006, 2007). Only four aromatic cytokinins were detected in the two seaweed species analysed in this study with benzyladenosine (BAR) occurring at relatively high concentrations in both species (Table 1). The physiological function of this group of cytokinins in seaweeds needs to be further investigated, perhaps in response to environmental stress.

In bioassays, IAA is generally the most biologically active indole compound (Woodward &

Bartel, 2005). IAA levels are regulated by a balance between biosynthesis, conjugation and degradation (Sztein *et al.*, 1999). In vascular plants, there are several tryptophan-dependent biosynthetic pathways where tryptophan is converted to IAA via various intermediates such as indole-3-pyruvic acid, indole-3-acetaldehyde, or indole-3-acetonitrile. A tryptophan-independent pathway has also been elucidated (Woodward & Bartel, 2005). IAA conjugation facilitates storage, transport and protection from peroxidation and catabolism and free IAA is formed by the hydrolysis of these conjugates (Woodward & Bartel, 2005). IAA links either with sugars to form ester conjugates, or with amino acids and small peptides to form amide conjugates (Sztein *et al.*, 1999).

Sztein *et al.* (1995, 1999) showed that while vascular plants were able to conjugate exogenous ^{14}C-IAA within 22 h to many indole conjugates, mosses and hornworts were only able to synthesise a few conjugates, while liverworts required longer incubation periods before the exogenous IAA was metabolised to moderate amounts of conjugates. This slower rate of conjugation suggests that free IAA in liverworts is regulated primarily via the balance between biosynthesis and degradation. In the liverworts, mosses, lycophytes and ferns, IAA metabolites were almost exclusively amide conjugates rather than ester conjugates.

Very little is known about IAA metabolism in seaweeds as most methods used have not been able to identify conjugate forms. The method used in the current study is able to detect most of the indole forms at very low detection limits. The results of the two seaweed species analysed in the present study concur with the evolutionary framework suggested by Sztein *et al.* (1999). While free IAA was detected in the samples, the only other indole-compound detected in these samples was IAM.

Many pathogenic bacteria are able to produce IAA by a tryptophan-dependent pathway where IAM is the intermediate (Lambrecht *et al.*, 2000). Tryptophan is converted by the enzyme tryptophan monooxygenase to IAM which is then hydrolysed by IAM hydrolase to IAA (Kawaguchi *et al.*, 1993). This IAM pathway was originally thought only to occur in pathogenic bacteria, but IAM has since been identified in a few vascular plants such as sterile *Arabidopsis* seedlings (Pollmann *et al.*, 2002), Japanese Cherry Trees (Saotome *et al.*, 1993) and transiently in young fruit of Trifoliate oranges (Kawaguchi *et al.*, 1993). This transient increase in IAM levels in young orange fruits corresponded with increased cytokinin levels and was correlated to a stage of rapid cell division (Kawaguchi *et al.*, 1993). IAM levels were highest in imbibed *Arabidopsis thaliana*

seeds and decreased within 24 h to much lower levels (Pollmann *et al.*, 2002). Similarly, IAM was detected in relatively low concentrations in both seaweeds analysed in the present study except for one *U. fasciata* sample collected in September where the IAM concentration was approximately three times higher than IAA. The reason for this transient increase in IAM levels needs to be further investigated. Further studies to elucidate the biosynthetic pathway(s) of IAA in seaweeds are required but the present results suggest that IAM is the likely intermediate. The results also suggest that little or no conjugation occurs and so imply that IAA levels are regulated by the rate of biosynthesis. The level of IAM estimated in seaweeds was significantly higher than that found in *A. thaliana* (between 1 and 20 pmol g^{-1} FW), as described by Pollmann *et al.* (2002).

In vascular plants, ABA increases under adverse environmental conditions (Taylor *et al.*, 2000). Similarly, when the microalgae *Dunaliella parva* and *Draparnaldia mutabilis* were grown in conditions of salt stress and increased pH, endogenous ABA levels increased (Hirsch *et al.*, 1989; Tietz *et al.*, 1989). In the current study, ABA levels were generally higher in *U. fasciata* compared with *D. humifusa* (Fig. 4). This may be due to *U. fasciata* being collected from a rock pool situated in the upper intertidal zone where it would be exposed to more extreme environmental changes compared to *D. humifusa* that was collected from a gully in the mid-intertidal zone. More species need to be analysed before such generalisations can be made about the potential role of ABA as a 'stress hormone' in seaweeds.

There is also evidence suggesting that ABA acts as a growth inhibitor in seaweeds as it does in vascular plants. When *Laminaria hyperborea* sporophytes were grown in a tank system under various environmental conditions and its endogenous ABA quantified by GC-MS, there was a strong negative correlation between growth rate and endogenous ABA concentrations (Schaffelke, 1995*a*). ABA concentrations increased during the resting phase and levels decreasing just prior to new blade generation (Schaffelke, 1995*a*, *b*). In the current study, ABA was detected in all *D. humifusa* samples and most *U. fasciata* samples. Its role in the growth and development of these seaweeds needs to be further investigated. However, in vascular plants, ABA levels are strongly dependent on the duration of the water stress, for example in *Arabidopsis thaliana* (Gómez-Cadenas *et al.*, 2002; López-Carbonell & Jáuregui, 2005) and tobacco (Hradecká *et al.*, 2007). ABA catabolism has been examined in *Brassica napus* siliques (Zhou *et al.*, 2003), lettuce seeds (Chiwocha *et al.*, 2003), Western white pine seeds (Feurtado *et al.*, 2004,

2007) and in Douglas fir seeds (von Aderkas *et al.*, 2005). Well-watered plants contained relatively constant, low levels of endogenous ABA (5–50 pmol g^{-1} FW); while water-stressed plants had 10–50-fold higher ABA amounts with concentrations peaking 24 hours after water stress.

This study, over a 1 year period, provides a clearer picture of the endogenous cytokinins, auxins and ABA present in two seaweed species growing under a range of environmental conditions. The cytokinin and auxin composition for both species was remarkably similar despite their different evolutionary lineages. Based on the cytokinins detected in both the seaweed species, we propose that the ribotide iPRMP is the first intermediate formed during *de novo* cytokinin biosynthesis. The ribotides are subsequently converted to free-base and riboside forms. However, glycosylation does not appear to be a mechanism extensively used in the regulation of active cytokinin concentrations in seaweeds. An alternative pathway involving tRNA degradation to produce cZ derivatives is also a possibility that requires further investigation. Furthermore, aromatic cytokinins were also detected in both seaweed species and their physiological function also warrants further investigated. Only free IAA and one conjugate, IAM were detected in the two seaweed species, indicating that IAM is the likely intermediate in IAA biosynthesis and like other non-vascular plants, very little conjugation occurs. ABA was also detected in most of the samples. Its role as a growth inhibitor and stress hormone in seaweeds are as yet little understood and also need further investigation.

References

ARMSTRONG, D.J. (1994). Cytokinin oxidase and the regulation of cytokinin degradation. In *Cytokinins: Chemistry, Activity, and Function* (MOK, D.W.S. & MOK, M.C, editors), 139–154. CRC Press, Boca Raton, USA.

ARTHUR, G.D., STIRK, W.A., NOVÁK, O., HEKERA, P. & VAN STADEN, J. (2007). Occurrence of nutrients and plant hormones (cytokinins and IAA) in the water fern *Salvinia molesta* during growth and composting. *Environ. Exp. Bot.*, **61**: 137–144.

ÅSTOT, C., DOLEŽAL, K., NORDSTRÖM, A., WANG, Q., KUNKEL, T., MORITZ, T., CHAU, N. & SANDBERG, G. (2000). An alternative cytokinin biosynthesis pathway. *Proc. Natl. Acad. Sci. USA*, **97**: 14778–14783.

AUER, C.A. (1997). Cytokinin conjugation: recent advances and patterns in plant evolution. *Plant Growth Regul.*, **23**: 17–32.

BOYER, G.L. & DOUGHERTY, S.S. (1988). Identification of abscisic acid in the seaweed *Ascophyllum nodosum*. *Phytochem.*, **27**: 1521–1522.

CHIWOCHA, S.D.S., ABRAMS, S.R., AMBROSE, S.J., CUTLER, A.J., LOEWEN, M., ROSS, A.R.S. & KERMODE, A.R. (2003). A method for profiling classes of plant hormones and their metabolites using liquid chromatography-electrospray ionization tandem mass spectrometry: an analysis of hormone regulation of thermodormancy of lettuce (*Lactuca sativa* seeds). *Plant J.*, **35**: 405–417.

DE CLERCK, O., BOLTON, J.J., ANDERSON, R.J. & COPPEJANS, E. (2005). *Guide to the Seaweeds of KwaZulu-Natal*. National Botanic Garden of Belgium, Meise, Belgium.

DE NYS, R., JAMESON, P.E., CHIN, N., BROWN, M.T. & SANDERSON, K.J. (1990). The cytokinins as endogenous growth regulators in *Macrocystis pyrifera* (L.) C. Ag. (Phaeophyceae). *Bot. Mar.*, **33**: 467–475.

DOLEŽAL, K., POPA, I., HAUSEROVÁ, E., SPÍCHAL, L., CHAKRABARTY, K., NOVÁK, O., KRYSTOF, V., VOLLER, J., HOLUB, J. & STRNAD, M. (2007). Preparation, biological activity and endogenous occurrence of N(6)-benzyladenosines. *Bioorg. Med. Chem.*, **15**: 3737–3747.

DOLEŽAL, K., POPA, I., KRYSTOF, V., SPÍCHAL, L., FOJTÍKOVÁ, M., HOLUB, J., LENOBEL, R., SCHMÜLLING, T. & STRNAD, M. (2006). Preparation and biological activity of 6-benzylaminopurine derivatives in plants and human cancer cells. *Bioorg. Med. Chem.*, **14**: 875–884.

DUAN, D., LIU, X., PAN, F., LIU, H., CHEN, N. & FEI, X. (1995). Extraction and identification of cytokinin from *Laminaria japonica* Aresch. *Bot. Mar.*, **38**: 409–412.

FAISS, M., ZALUBILOVÁ, J., STRNAD, M. & SCHMÜLLING, T. (1997). Conditional expression of the *ipt* gene indicates a function for cytokinins in paracrine signaling in whole tobacco plants. *Plant J.*, **12**: 401–415.

FEATONBY-SMITH, B.C. & VAN STADEN, J. (1984). Identification and seasonal variation of endogenous cytokinins in *Ecklonia maxima* (Osbeck) Papenf. *Bot. Mar.*, **27**: 527–531.

FEURTADO, J., AMBROSE, S., CUTLER, A., ROSS, A., ABRAMS, S. & KERMODE, A. (2004). Dormancy termination of Western White Pine (*Pinus monticola* Dougl. Ex D. Don) seeds is associated with changes in abscisic acid metabolism. *Planta*, **218**: 630–639.

FEURTADO, J.A., YANG, J., AMBROSE, S.J., CUTLER, A.J., ABRAMS, S.R. & KERMODE, A.R. (2007). Disrupting abscisic acid homeostasis in Western White Pine (*Pinus monticola* Dougl. Ex D. Don) seeds induces dormancy termination and changes in abscisic acid catabolites. *J. Plant Growth Regul.*, **26**: 46–54.

FRANCIS, D. & INZÉ, D. (2001). The plant cell cycle. In *The Plant Cell Cycle and its Interfaces* (FRANCIS, D., editors), 1–18. Sheffield Academic Press, Sheffield, UK.

GÓMEZ-CADENAS, A., POZO, O.J., GARCÍA-AUGUSTÍN, P. & SANCHO, J.V. (2002). Direct analysis of abscisic acid in crude plant extracts by liquid chromatography-electrospray/tandem mass spectrometry. *Phytochem. Anal.*, **13**: 228–234.

HIRSCH, R., HARTUNG, W. & GIMMLER, H. (1989). Abscisic acid content of algae under stress. *Bot. Acta*, **102**: 326–334.

HRADECKÁ, V., NOVÁK, O., HAVLÍCEK, L. & STRNAD, M. (2007). Immunoaffinity chromatography of abscisic acid combined with electrospray liquid chromatography-mass spectrometry. *J. Chromatogr. B*, **847**: 162–73.

JACOBS, W.P., FALKENSTEIN, K. & HAMILTON, R.H. (1985). Nature and amount of auxin in algae: IAA from extracts of *Caulerpa paspaloides* (Siphonales). *Plant Physiol.*, **78**: 844–848.

KASAHARA, H., TAKEI, K., UEDA, N., HISHIYAMA, S., YAMAYA, T., KAMIYA, Y., YAMAGUCHI, S. & SAKAKIBARA, H. (2004). Distinct isoprenoid origins of *cis*- and *trans*-zeatin biosynthesis in *Arabidopsis*. *J. Biol. Chem.*, **279**: 14049–14054.

KAWAGUCHI, M., FUJIOKA, S., SAKURAI, A., YAMAKI, Y.T. & SYONO, K. (1993). Presence of a pathway for the biosynthesis of auxin via indole-3-acetamide in Trifoliata Orange. *Plant Cell Physiol.*, **34**: 121–128.

LAMBRECHT, M., OKON, Y., BROEK, A.V. & VANDERLEYDEN, J. (2000). Indole-3-acetic acid: a reciprocal signaling molecule in bacteria-plant interactions. *Trends Microbiol.*, **8**: 298–300.

LÓPEZ-CARBONELL, M. & JÁUREGUI, O. (2005). A rapid method for analysis of abscisic acid (ABA) in crude extracts of water stressed *Arabidopsis thaliana* plants by liquid chromatography – mass spectrometry in tandem mode. *Plant Physiol. Biochem.*, **43**: 407–411.

MOONEY, P.A. & VAN STADEN, J. (1984). Seasonal changes in the levels of endogenous cytokinins in *Sargassum heterophyllum* (Phaeophyceae). *Bot. Mar.*, **27**: 437–442.

NOVÁK, O., TARKOWSKI, P., TARKOWSKÁ, D., DOLEŽAL, K., LENOBEL, R. & STRNAD, M. (2003). Quantitative analysis of cytokinins in plants by liquid chromatography-single-quadrupole mass-spectrometry. *Anal. Chim. Acta*, **480**: 207–218.

ÖRDÖG, V., STIRK, W.A., VAN STADEN, J., NOVÁK, O. & STRNAD, M. (2004). Endogenous cytokinins in three genera of microalgae from the Chlorophyta. *J. Phycol.*, **40**: 88–95.

POLLMANN, S., MÜLLER, A., PIOTROWSKI, M. & WEILER, E.W. (2002). Occurrence and formation of indole-3-acetamide in *Arabidopsis thaliana*. *Planta*, **216**: 155–161.

ROLCÍK, J., LENOBEL, R., SIGLEROVÁ, V. & STRNAD, M. (2002). Isolation of melatonin by immunoaffinity chromatography. *J. Chromatogr. B*, **775**: 9–15.

SAKAKIBARA, H. (2006). Cytokinins: Activity, biosynthesis, and translocation. *Ann. Rev. Plant Biol.*, **57**: 431–449.

SAKAKIBARA, H. & TAKEI, K. (2002). Identification of cytokinin biosynthesis genes in Arabidopsis: A breakthrough for understanding the metabolic pathway and the regulation in higher plants. *J. Plant Growth Regul.*, **21**: 17–23.

SAOTOME, M., SHIRAHATA, K., NISHIMURA, R., YAHABA, M., KAWAGUCHI, M., SYONO, K., KITSUWA, T., ISHII, Y. & NAKAMURA, T. (1993). The identification of indole-3-acetic acid and indole-3-acetamide in the hypocotyls of Japanese Cherry. *Plant Cell Physiol.*, **34**: 157–159.

SCHAFFELKE, B. (1995a). Abscisic acid in sporophytes of three *Laminaria* species (Phaeophyta). *J. Plant Physiol.*, **146**: 453–458.

SCHAFFELKE, B. (1995b). Storage carbohydrates and abscisic acid contents in *Laminaria hyperborean* are entrained by experimental daylengths. *Eur. J. Phycol.*, **30**: 313–317.

SPÍCHAL, L., RAKOVA, N.Y., RIEFLER, M., MIZUNO, T., ROMANOV, G.A., STRNAD, M. & SCHMÜLLING, T. (2004). Two cytokinin receptors of *Arabidopsis thaliana*, CRE1/AHK4 and AHK3 differ in their ligand specificity in a bacterial assay. *Plant Cell Physiol.*, **45**: 1299–1305.

STIRK, W.A., GOLD, J.D., NOVÁK, O., STRNAD, M. & VAN STADEN, J. (2005). Changes in endogenous cytokinins during germination and seedling establishment of *Tagetes minuta* L. *Plant Growth Reg.*, **47**: 1–7.

STIRK, W.A., NOVÁK, O., STRNAD, M. & VAN STADEN, J. (2003). Cytokinins in macroalgae. *Plant Growth Regul.*, **41**: 13–24.

STIRK, W.A., NOVÁK, O., VÁCLAVÍKOVÁ, K., TARKOWSKI, P., STRNAD, M. & VAN STADEN, J. (2008). Spatial and temporal changes in endogenous cytokinins in developing pea roots. *Planta*, **227**: 1279–1289.

STRNAD, M. (1997). The aromatic cytokinins. *Physiol. Plant.*, **101**: 674–688.

SZTEIN, A.E., COHEN, J.D., GARCÍA DE LA FUENTE, I. & COOKE, T.J. (1999). Auxin metabolism in mosses and liverworts. *Am. J. Bot.*, **86**: 1544–1555.

SZTEIN, A.E., COHEN, J.D., SLOVIN, P. & COOKE, T.J. (1995). Auxin metabolism in representative land plants. *Am. J. Bot.*, **82**: 1514–1521.

TAYLOR, I.B., BURBRIDGE, A. & THOMPSON, A.J. (2000). Control of abscisic acid synthesis. *J. Exp. Bot.*, **51**: 1563–1574.

TAYLOR, N.J., STIRK, W.A. & VAN STADEN, J. (2003). The elusive cytokinin biosynthetic pathway. *South Afr. J. Bot.*, **69**: 269–281.

TIETZ, A., RUTTKOWSKI, R., KÖHLER, R. & KASPRIK, W. (1989). Further investigations on the occurrence and the effects of abscisic acid in algae. *Biochem. Physiol. Pflanz.*, **184**: 259–266.

VON ADERKAS, P., ROUAULT, G., WAGNER, R., CHIWOCHA, S. & ROQUES, A. (2005). Multinucleate storage cells in Douglas-fir (*Pseudotsuga menziesii* (Mirbel) Franco) and the effect of seed parasitism by the chalcid *Megastigmus spermotrophus* Wachtl. *Heredity*, **94**: 616–622.

WEILER, E.W. (1982). An enzyme-immunoassay for *cis*-(+)-abscisic acid. *Physiol. Plant*, **54**: 510–514.

WOODWARD, A.W. & BARTEL, B. (2005). Auxin: regulation, action and interaction. *Ann. Bot.*, **95**: 707–735.

YONEKURA-SAKAIBARA, K., KOJIMA, M., YAMAYA, T. & SAKAKIBARA, H. (2004). Molecular characterisation of cytokinin-responsive histidine kinases in maize. Differential ligand preferences and response to cytokinin. *Plant Physiol.*, **134**: 1654–1661.

ZHANG, W., CHAPMAN, D.J., PHINNEY, B.O. & SPRAY, C.R. (1991). Identification of cytokinins in *Sargassum muticum* (Phaeophyta) and *Porphyra perforata* (Rhodophyta). *J. Phycol.*, **27**: 87–91.

ZHOU, R., SQUIRES, T.M., AMBROSE, S.J., ABRAMS, S.R., ROSS, A.R.S. & CUTLER, A.J. (2003). Rapid extraction of abscisic acid and its metabolites for liquid chromatography-tandem mass spectrometry. *J. Chromatogr. A*, **1010**: 75–85.

Zhang J, Nodzyński T, **Pěnčík A**, Rolčík J, Friml J (2010) PIN phosphorylation is sufficient to mediate PIN polarity and direct auxin transport. Proc Natl Acad Sci U S A, 107, 918-922.

PIN phosphorylation is sufficient to mediate PIN polarity and direct auxin transport

Jing Zhang[a], Tomasz Nodzyński[a], Aleš Pěnčík[b], Jakub Rolčík[b], and Jiří Friml[a,1]

[a]Department of Plant Systems Biology, Flanders Institute for Biotechnology (VIB) and Department of Plant Biotechnology and Genetics, Ghent University, B-9052 Gent, Belgium; and [b]Laboratory of Growth Regulators, Faculty of Science, Palacký University and Institute of Experimental Botany, Academy of Sciences of the Czech Republic, CZ-78371 Olomouc, Czech Republic

The plant hormone auxin plays a crucial role in regulating plant development and plant architecture. The directional auxin distribution within tissues depends on PIN transporters that are polarly localized on the plasma membrane. The PIN polarity and the resulting auxin flow directionality are mediated by the antagonistic actions of PINOID kinase and protein phosphatase 2A. However, the contribution of the PIN phosphorylation to the polar PIN sorting is still unclear. Here, we identified an evolutionarily conserved phosphorylation site within the central hydrophilic loop of PIN proteins that is important for the apical and basal polar PIN localizations. Inactivation of the phosphorylation site in PIN1(Ala) resulted in a predominantly basal targeting and increased the auxin flow to the root tip. In contrast, the outcome of the phosphomimic PIN1(Asp) manipulation was a constitutive, PINOID-independent apical targeting of PIN1 and an increased auxin flow in the opposite direction. Furthermore, the PIN1(Asp) functionally replaced PIN2 in its endogenous expression domain, revealing that the phosphorylation-dependent polarity regulation contributes to functional diversification within the PIN family. Our data suggest that PINOID-independent PIN phosphorylation at one single site is adequate to change the PIN polarity and, consequently, to redirect auxin fluxes between cells and provide the conceptual possibility and means to manipulate auxin-dependent plant development and architecture.

cell polarity | auxin distribution | plant architecture

The plant hormone auxin acts, on account of its differential distribution (gradients) within tissues, as a major determinant of plant architecture (1–3). Auxin is distributed throughout the plant by a network of carrier proteins (4–8), and the directionality of the auxin flow is determined by asymmetrically localized plasma membrane PIN transporters (9). The differentially expressed and polarly localized PIN proteins constitute the backbone of a transport network for directional auxin distribution in different parts of the plant (10). The local biosynthesis (11–13) together with the PIN-dependent transport (14) largely account for the formation of local auxin maxima and minima that regulate various developmental processes, including embryonic axis establishment, tropic growth, root meristem patterning, lateral organ and fruit formation, and vascular tissue differentiation and regeneration (15, 16). The polar PIN localization determines direction of the auxin flow; thus, any signal that acts upstream to control the cellular PIN localization and activity can be translated into changes in the auxin distribution that modulate multiple aspects of the plant development. Phosphorylation has been shown to be important for auxin transport and distribution (17–20). So far, the only known regulators that specifically regulate the PIN polar targeting are the serine/threonine protein kinase PINOID (PID) (18–20) and the protein phosphatase 2A (PP2A) (21, 22) that mediate antagonistically the phosphorylation of PIN proteins (22). Loss-of-function *pid* mutant leads to a preferentially basal (lower cell side) PIN localization (23), whereas *pid* gain-of-function and *pp2a* loss-of-function mutants favor an apical (upper cell side) PIN localization (22, 23). These results suggest that phosphorylated and dephosphorylated PIN proteins might be recruited into the apical and basal polar targeting

pathways, respectively. Thus, PIN phosphorylation would determine the directional aspects of auxin transport. To test this model, we analyzed the impact of the PIN phosphorylation at a specific site on the PIN polar targeting, auxin distribution, and auxin-mediated development.

Results

PIN1 Phosphorylation at Ser337/Thr340 Is Required for Auxin-Related Development. A putative phosphorylation site of PIN1 had been isolated by mass spectrometry at Ser337 and/or Thr340 in the central hydrophilic loop of the PIN1 coding sequence (22). These Ser and Thr of the phosphorylation site are conserved in all plasma membrane-localized PIN proteins in *Arabidopsis thaliana* (Fig. 1*A*) and other species (Fig. S1) when compared to the endoplasmic reticulum-localized subfamily of PIN proteins (24). To test the involvement of the phosphorylation site in the polar PIN targeting in vivo, site-directed mutagenesis of the conserved residues within the PIN1 sequence was carried out (Fig. 1*A*). Ser and Thr were both converted into Ala, which is a nonphosphorylatable residue, and to Asp, which mimics phosphorylation. The *PIN1* genes, fused to the green fluorescent protein (GFP) (*PIN1::PIN1-GFP*) and the hemagglutinin (HA) (*PIN2::PIN1-HA*), were mutagenized and the constructs were transformed into the wild type and the *pin1* and *pin2* mutants, respectively. *PIN1-GFP(Ala)* and *PIN1-GFP(Asp)* partially rescued a shoot phenotype of the *pin1* mutant, but the rescued lines displayed various developmental defects in adult plants. The independent transgenic lines *PIN1-GFP(Ala)* (5/7) as well as *PIN1-GFP(Asp)* (7/9) caused defective phyllotaxis and floral morphology, discernible by fused flowers with two pistils, outgrowth of two siliques from the same position and nondeveloped pistils (Fig. 1*B*). The same range of the phenotypes (Fig. 1*B*) with comparable frequencies [*PIN1-GFP(Ala)* (6/8) and *PIN1-GFP (Asp)* (6/7)] was observed when *PIN1-GFP(Ala)* and *PIN1-GFP (Asp)* were transformed into the wild type, demonstrating the dominant effect of the mutations. In contrast, whereas *PIN1-GFP(Asp)* rescued to a large extent the shoot development, it completely failed to complement embryonic and cotyledon phenotypes of *pin1*; the transformants still showed a defective embryo development, reflected by monocots, tricots, or fused cotyledons at the seedling stage (Fig. 1*C*). To investigate why the *PIN1-GFP(Asp)* could not rescue the embryonic phenotype, we examined the subcellular localization of PIN1-GFP(Asp) during embryogenesis. Consistently, defects in the polar PIN1 localization were observed in triangular-stage embryos ($n = 62$),
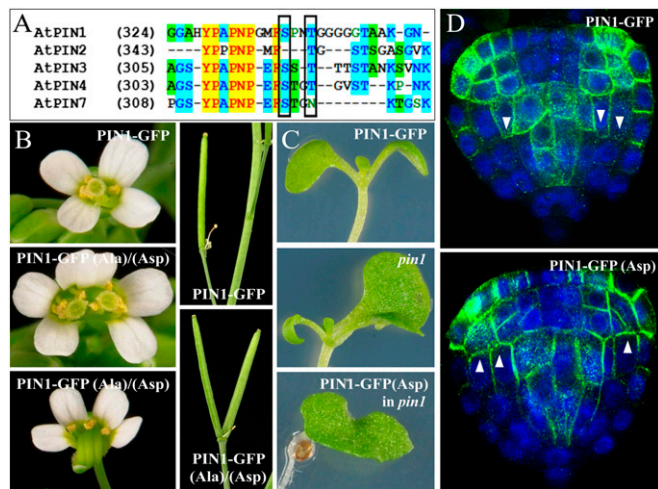

Fig. 1. Developmental consequences of the mutations in Ser337/Thr340 of PIN1-GFP. (*A*) Amino acid sequence alignment of PIN1 and other PIN family members in the putative phosphorylation site-spanning region. Framed Ser and Thr were mutagenized to Ala or Asp. (*B*) Morphological defects of flowers and silliques in adult plants of *PIN1-GFP(Ala)* and *PIN1-GFP(Asp)* in *pin1* or wild type. (*C*) Defects on cotyledon formation: *PIN1-GFP(Asp)* fails to complement the *pin1* mutant at the cotyledon stage. (*D*) Immunolocalization of GFP-tagged PIN1 in triangular-stage embryos of *pin1*: PIN1-GFP(Asp) localizes more apically in the inner cells as compared to the basally localized PIN1-GFP facing the root pole. Arrowheads mark polarity of the PIN localization.

Fig. 2. Effects of Ser337/Thr340 mutations in *PIN1-HA* on root gravitropism and polarity. (*A*) Quantitative evaluation of root gravitropism: the *pin2* agravitropic phenotype is slightly enhanced by *PIN1-HA(Ala)*, but partially rescued by *PIN1-HA(Asp)*. Data are means ± SEM, *P < 0.05 (*t* test). (*B*) Auxin relocation during root gravitropic response: *PIN1-HA(Asp)*, but not *PIN1-HA* or *PIN1-HA(Ala)*, when introduced into the *pin2* mutants, mediated the auxin translocation to the lower side of the root after gravistimulation as visualized by *DR5rev::GFP*. (*C*) Immunolocalization of PIN1-HA in the *pin2* root epidermal cells: the basal localizations of PIN1-HA and PIN1-HA(Ala) contrast with the predominantly apical localization of PIN1-HA(Asp). Arrowheads mark polarity of the PIN localization.

predominantly manifested by the loss of the basal polar localization facing the root pole in the inner embryo cells and its replacement by an apolar or preferentially apical localization (Fig. 1*D*). These results reveal that the PIN1 phosphorylation at the site involving Ser337/Thr340 is important for the PIN1 function, particularly during flower and embryo development. Moreover, the flower defects in the wild-type plants highlight the dominant effect of these mutations.

Phosphomimic PIN1-HA(Asp) Can Functionally Replace PIN2. We tested the effects of PIN1-HA(Ala) and PIN1-HA(Asp) in the PIN2 expression domain (*PIN2::PIN1-HA* constructs) in the *pin2* mutant background. PIN2 is a key regulator of root gravitropism; it localizes to the apical side of epidermis cells and, after gravistimulation, it mediates the auxin flow along the lower side of the root from the tip toward the elongation zone where the auxin response is activated and inhibits elongation (25–27). The expression of *PIN1-HA* in *pin2* mutants was not sufficient to restore either the gravitropic response or the asymmetric auxin accumulation as monitored by the GFP-fused artificial auxin-responsive reporter *DR5rev::GFP* (9) (Fig. 2 *A* and *B*). *PIN1-HA(Ala)* slightly enhanced the agravitropic phenotype of the *pin2* mutant (*n* = 45) and did not rescue the activation of the *DR5*-visualized auxin response at the lower side of roots (*n* = 25) (Fig. 2 *A* and *B*). In contrast, *PIN1-HA(Asp)* rescued to a large extent the agravitropic phenotype of the *pin2* mutant (*n* = 39) and also restored the *DR5*-visualized auxin response along the lower side of the root (*n* = 30) during gravitropic responses (Fig. 2 *A* and *B*). These results reveal that mutation of the phosphorylation site in PIN1 is sufficient to acquire a PIN2-like function in root epidermal cells and to efficiently mediate the auxin flow for the root gravitropic response.

PIN Phosphorylation at Ser337/Thr340 Mediates PIN Polarity and Auxin Distribution. All observations in the *PIN1::PIN1-GFP* and *PIN2::PIN1-HA* transgenic lines suggest that the Ala and Asp mutation-induced phenotypes might result from the modulated polar targeting of mutated PIN1 variants. Therefore, we investigated the subcellular polar targeting of PIN1-HA(Ala) and PIN1-

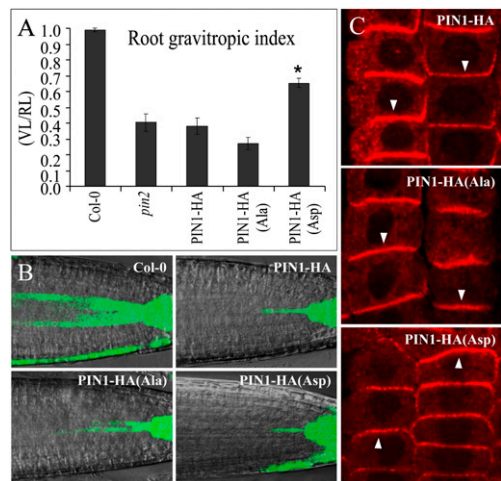HA(Asp) proteins in epidermal cells. Ectopically expressed PIN1-HA in the epidermis localizes predominantly to the basal side of cells, whereas the endogenous PIN2 localizes to the apical side (9) (Fig. 2*C*). PIN1-HA(Ala) localized at the basal side of epidermal cells, but, importantly, PIN1-HA(Asp) predominantly to the opposite apical side, similar to the endogenous PIN2 (Fig. 2*C*). Accordingly, only PIN1-HA(Asp) was able to functionally replace PIN2 in the *pin2* mutant.

Similarly to PIN1-HA, the mutations in Ser337/Thr340 influenced also the PIN1-GFP targeting. In roots of the wild type, PIN1 localizes to the basal side of stele cells (28)(Fig. 3*A*). In comparison with PIN1-GFP, the polar localization of PIN1-GFP (Asp) was dramatically disturbed (*n* = 83 roots). Generally, the basal polarity of PIN1 was much less pronounced and resulted in a largely nonpolar (68%) or preferentially apical distribution (7%) (Fig. 3*A*). In contrast, PIN1-GFP(Ala) had a largely strict basal localization (*n* = 56; Fig. 3*A*). Importantly, these polarity changes correlated well with the incidence of the auxin response in the root tip as visualized indirectly by the auxin response reporter *DR5::GUS*. *PIN1-GFP(Ala)* lines revealed an increased *DR5* activity in the root tip, contrasting with the dramatically decreased *DR5* signal in the roots of *PIN1-GFP(Asp)* (Fig. 3*B*). The changes in *DR5* activity were confirmed by direct auxin measurements in the 1-mm seedling root tips. Consistently with the *DR5* observations, *PIN1-GFP(Ala)* and *PIN1-GFP(Asp)* showed a higher and lower auxin content than that of *PIN1-GFP*, respectively (Fig. 3*C*). These results demonstrate that preferentially the basally localized PIN1(Ala) promotes, whereas more apically localized PIN1(Asp) diminishes the auxin accumulation at the root tips. These quantitative changes in *DR5* activity and auxin content show that the PIN phosphorylation-mediated PIN polarity changes have a direct impact on the auxin distribution.

PIN1 Phosphorylation at Ser337/Thr340 Is Related to the PID Action in Polar Targeting. The observed changes of PIN1 polarity, auxin distribution, and resulting phenotypes revealed that phosphorylation of the Ser337/Thr340 site is sufficient to redirect the PIN
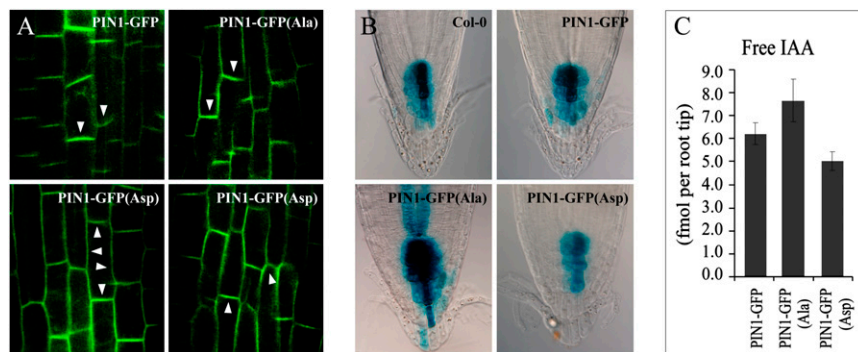
Fig. 3. Effects of Ser337/Thr340 mutations in *PIN1-GFP* on polarity and auxin distribution. (*A*) Live images of GFP-tagged PIN1 in the stele of wild-type roots: normal, predominant basal localization of PIN1-GFP(Ala) as compared to either nonpolar localization or basal-to-apical shift of PIN-GFP(Asp). Arrowheads mark polarity of the PIN localization. (*B*) Auxin distribution in the root tip as inferred from the *DR5::GUS* expression: the *DR5* signal is increased in *PIN1-GFP(Ala)* roots, but reduced in *PIN1-GFP(Asp)* when compared to the wild type. (*C*) Measurement of the endogenous auxin content in the 1-mm root tips: *PIN1-GFP(Ala)* has higher whereas *PIN1-GFP (Asp)* lower auxin levels as compared with the *PIN1-GFP* control.

polarity as well as directionality of the auxin flow, similarly as shown for manipulations of the PID kinase activity (18, 23). Therefore, we addressed the question of whether this particular phosphorylation site is related to the PID kinase action in the PIN polarity determination. *pid* gain of function (*35S::PID*) leads to a basal-to-apical PIN polarity shift, which causes auxin depletion from the root meristem, ultimately leading to its collapse (23). Several independent transgenic lines of *PIN1-HA (Ala)* and *PIN1-HA(Asp)* showed the consistent changes in the root collapse frequency. We observed that *PIN1-HA(Ala)* significantly delayed the *35S::PID*-mediated root collapse (*n* = 96) when compared to that of the wild-type *PIN1-HA* (*n* = 85) (Fig. 4*A*). In contrast, the collapse of the root meristem in *PIN1-HA (Asp)* (*n* = 97) and *PIN1-HA* seedlings did not differ significantly (Fig. 4*A*), which might be due to the already near maximum effect of *35S::PID* on PIN apicalization and root collapse.

Next, we tested the *pid* loss-of-function line. We introduced *PIN1-GFP(Ala)* and *PIN1-GFP(Asp)* transgenes into the *pid*^{+/−} *wag1 wag2* allele. WAG1 and WAG2 are the closest homologs of PID in the family of the AGC serine/threonine protein kinases of *Arabidopsis* and the triple mutant *pid wag1 wag2* displays a completely disrupted cotyledon formation (29, 30). We analyzed the F₂-segregating progeny and quantified the seedlings with defective cotyledon patterning. The frequency of the seedlings that failed to make any cotyledon was increased by *PIN1-GFP(Ala)* and reduced by *PIN1-GFP(Asp)* transgenes. We observed 16% (*n* = 816) and 4% (*n* = 454) aberrant seedlings without cotyledons in *PIN1-GFP (Ala)* and *PIN1-GFP(Asp)*, respectively, when compared to 8% (*n* = 788) in the F₂ progeny of control crosses with the wild-type *PIN1-GFP* (Fig. 4*B*). Furthermore, the *pid wag1 wag2* mutations did not affect the PIN1-HA(Ala) and PIN1-HA(Asp) localizations at the basal and apical sides of the epidermal cells, respectively (Fig. 4*C*). Altogether, these data show that PIN1(Ala) have antagonistic and PIN1(Asp) mutations agonistic effects with the PID action, consistently with the PID regulating the PIN polarity targeting this and/or other phosphorylation sites. Importantly, the apical localization of PIN1(Asp) does not require the function of PID and related kinases, suggesting that other potential phosphorylation sites targeted by PID or other kinases cannot override the effect of the phosphomimic mutation at the Ser337/Thr340 site. These results reveal that the Ser337/Thr340 phosphorylation site is involved in the similar mechanism of PIN polarity regulation as PID action; nonetheless these results cannot discriminate whether Ser337/Thr340 is a target of PID.

PID Might Not Directly Target Ser337/Thr340. Next, we tested whether the Ser337/Thr340 site of the PIN proteins can be directly phosphorylated by PID. The HIS-tagged wild-type hydrophilic loop of PIN1 (HIS-PIN1HL, amino acids 288–452; Fig. S2 *A and B*), GST-tagged PID (GST-PID), and a 30-amino-acid stretch encompassing the Ser337/Thr340 site (GST-PIN1P-site, amino acids 321–350; Fig. S2 *A and B*) as well as its Ala-substituted version were

heterologously expressed in *Escherichia coli* and coincubated in an in vitro phosphorylation reaction. After electrophoretic separation of the proteins, PID autophosphorylation was detected as well as phosphorylation of HIS-PIN1HL and the standard Ser/Thr kinase substrate myelin basic protein (MBP) (Fig. 4*D* and Fig. S3). In contrast, we failed to observe any PID-dependent phosphorylation of both the wild-type and mutated versions of the GST-PIN1P-site (Fig. 4*D* and Fig. S3). These results show that the PID kinase phosphorylates the large hydrophilic loop of PIN1 in vitro, but is probably not able to phosphorylate the Ser337/Thr340 site in the same assay.
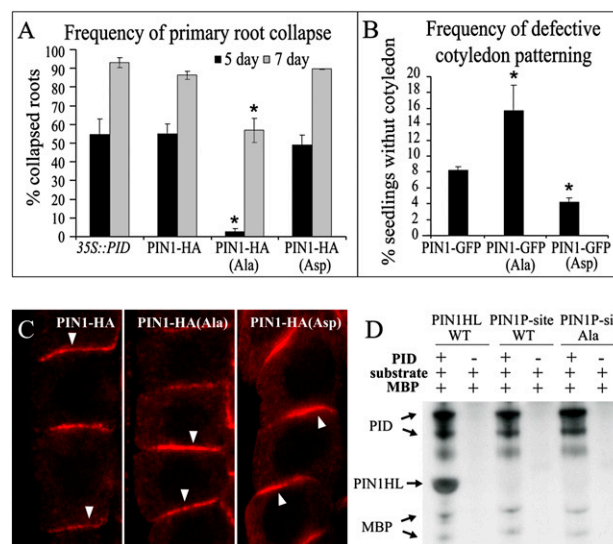

Fig. 4. Effects of Ser337/Thr340 mutations similar to PID action. (*A*) Quantification of frequencies of primary root collapse in 5-day-old and 7-day-old seedlings in *35S::PID*: the collapse of root meristems mediated by *35S::PID* is significantly delayed by *PIN1-HA(Ala)*. Data are means ± SEM, *$P < 0.05$ (Fisher exact test). (*B*) Quantification of frequencies of defective cotyledon patterning in *pid wag1 wag2* triple mutant: the failure to make cotyledons in the progeny of *pid*^{+/−} *wag1 wag2* is increased by the *PIN1-GFP(Ala)* but decreased by *PIN1-GFP(Asp)*. Data are means ± SEM, *$P < 0.05$ (Fisher exact test). (*C*) Immunolocalization of PIN1-HA in the root epidermal cells of the *pid wag1 wag2* mutant: PIN1-HA and PIN1-HA(Ala) show a normal basal localization, whereas PIN1-HA(Asp) displays a basal-to-apical polarity shift, also in the absence of the PID function. Arrowheads mark polarity of the PIN localization. (*D*) Autoradiograph of an in vitro phosphorylation assay: GST-PID autophosphorylates and efficiently phosphorylates the large wild-type hydrophilic loop of PIN1 (HIS-PIN1HL) and myelin basic protein (MBP); both the wild-type and the Ala mutant version of the short peptide (GST-PIN1P-site) are not phosphorylated by PID. + and − indicate incubated with or without the PID kinase, substrate, and MBP, respectively. Arrows mark positions of the different proteins.

Taken together, the results obtained in in vivo genetic and cell biological studies and in vitro phosphorylation assays are consistent with a scenario in which the Ser337/Thr340 phosphorylation site could be a target for the other potential kinases that act together with PID in regulating the PIN phosphorylation and the apical/basal PIN polar targeting.

Discussion

Our work demonstrates that phosphorylation of the PIN proteins regulates their polar targeting and the directionality of the auxin flow, which mediates various developmental processes. We identified a phosphorylation site that is required and sufficient to promote the PIN polar targeting, similarly to the activity of the PID kinase. Our in vitro phosphorylation results do not support that this site is a target of PID, although we cannot exclude that the short PIN1P-site peptide might not form the appropriate tertiary structure or not provide enough binding energy as offered by the large protein substrate essential for PID phosphorylation. Alternatively, it is possible that residues important for recognition of the substrate are more distant from the targeted phosphorylation site (31). On the other hand, protein kinases have also been shown to recognize and phosphorylate minimal peptide segments encompassing a very few residues (32, 33). Altogether, we believe that this site might be a phosphorylation target of other kinases, presumably MAP kinases, because the site shares sequence similarities to a consensus MAP kinase target characterized by a Pro following the Ser or Thr in the phosphorylation site (34, 35). Furthermore, Ser337 of PIN1 has been found to be phosphorylated in *Arabidopsis* cells treated with flg22, which induces the activation of multiple MAPKs (36). Our data are also consistent with a view of multiple phosphorylation sites, of which some are targets of PID (37), that all mediate decisions about the PIN polar targeting.

Manipulation of Ser337 and Thr340 is sufficient to change the PIN polarity and to redirect the auxin flow. This observation provides a conceptual explanation for how various signaling pathways that control the expression (16) or activity of upstream kinases can, via the PIN phosphorylation, regulate the auxin distribution and, thus, influence different developmental processes. Identification of the upstream components in the phosphorylation cascade will be the challenge for the coming years and will fill the mechanistic gap on the integration of various external and internal signals into rearrangements in the auxin distribution. Moreover, similar manipulations of this evolutionarily conserved site in other PIN proteins, in other species (Fig. S1), and in a cell-type-specific fashion will enable a targeted engineering of auxin fluxes to achieve the desired changes in plant architecture and development.

Materials and Methods

Materials. The following mutants, transgenic plants, and constructs have been described previously: *pin1* (*pin1-1*) (38), *pin2* (*eir1-1*) (25), *pid*^{+/−} *wag1 wag2* (kind gift of Remko Offringa, Leiden University, The Netherlands), *PIN1::PIN1-GFP* (39), *PIN2::PIN1-HA* (9), *DR5rev::GFP* (40), *DR5::GUS* (41), *35S::PID* (19), *pHIS-PIN1HL* (amino acids 288–452) (42), and *pGST-PID* (43). Myelin basic protein (MBP) was purchased from Sigma.

The constructs *pPIN1::PIN1-GFP(Ala)*, *pPIN1::PIN1-GFP(Asp)*, *pPIN2::PIN1-HA(Ala)*, and *pPIN2::PIN1-HA(Asp)* were generated from the original *pPIN1::PIN1-GFP* (39) and *pPIN2::PIN1:HA* (9) by converting the two residues Ser337 (TCG) and Thr340(ACT) on the PIN1 fragment to Ala(GCG) and Ala(GCT) or Asp(GAC) and Asp(GAT), respectively, through the PCR-based site-directed mutagenesis kit (Stratagene Quickchange XL). The mutated strands were synthesized with the following primer combinations: 5′-CCCAGGGGATGTT-TGCGCCCAACGCTGGCGGTGGTGGAG-3′ and 5′-CTCCACCACCGCCAGCGTTG-GGCGCAAACATCCCTGGG-3′ for the Ala mutation and 5′-CCCAGGGGATGTT-TGACCCCAACGATGGCGGTGGTGGAGGC-3′ and 5′-GCCTCCACCACCGCCATC-GTTGGGGTCAAACATCCCTGGG-3′ for the Asp mutation. The resulting constructs were transformed into the wild-type and the *pin1*, *pin2*, and *35S::PID* lines. *DR5rev::GFP*, *DR5::GUS* markers, and *pid*^{+/−} *wag1 wag2* mutations were introduced into the phosphorylation transgenic mutant lines by crosses. For the in vitro phosphorylation assay, the sequences of wild-type *PIN1P-site* and mutant *PIN1P-site(Ala)* encompassing 30 amino acids surrounding the Ser337 were generated by PCR amplification with the primer pairs containing *attB* recombination sites (underlined): 5′-GGGGACAAGTT-TGTACAAAAAAGCAGGCTGCGGTGGCGGTGGAGGAGCGCAT-3′ and 5′-GGG-GACCACTTTGTACAAGAAAGCTGGGTGTCATCCTTTCGCCGCCGCGCCTCCACC-3′ from the *pPIN1::PIN1-GFP* and *pPIN1::PIN1-GFP(Ala)* constructs, respectively.

E. coli BL21 Star (DE3) cells were used for heterologous expression of wild-type HIS-PIN1HL and Rosetta cells for the other recombinant proteins.

Growth Conditions and Phenotypic Analyses. *A. thaliana* (L.) Heynh. plants were grown on soil or half-strength Murashige and Skoog medium with sucrose as described (28) under a 16-h light/8-h dark cycle at 21°C or 18°C. All phenotypic comparisons were done at least in duplicate, with three to nine independent lines of a minimum of 25 seedlings each time. For evaluation of root gravitropism in 6-day-old seedlings, we used the quantification tool Image J (rsbweb.nih.gov/ij/download.html) and calculated the vertical growth index (VGI = vertical length [VL]/root length [RL]) (44). For the timing of the *35S::PID*-mediated collapse of the primary root meristem, we assayed 5-day-old and 7-day-old seedlings with a Leica binocular. The root collapse becomes visually apparent a few days after germination and can be recognized by the thin and pointed appearance of the root tip (19). Results are presented as means with standard error bars and all claimed comparisons are based on statistical evaluations with t test or Fisher exact test.

In Situ Expression and Localization Analyses. Histochemical stainings for GUS activity and whole-mount immunolocalizations in 5-day-old seedlings were carried out as described (39, 45, 46). Each experiment was done on three to nine independent lines with three repetitions (homozygous lines, $n > 15$; segregating lines, $n > 300$ individuals). Antibodies were diluted as follows: 1:1,000 for rabbit anti-PIN1 (42); 1:500 for mouse anti-HA (Babco); 1:500 for mouse anti-GFP (Roche); and 1:600 for CY3- (Sigma) and Alex- (Invitrogen) conjugated anti-rabbit and anti-mouse secondary antibodies, respectively. For the HA-tagged PIN proteins, colocalization of anti-PIN1 and anti-HA were always carried out to confirm the identity of the proteins. For in vivo GFP inspection, 6-day-old seedlings were mounted in 5% glycerol without fixation for live-cell imaging. Regarding the auxin translocation assay, confocal imaging was done in 6-day-old seedlings, immediately after 3 h of a 90° gravistimulation in the dark. All of the fluorescence signals were evaluated on a Zeiss LSM 510 or Leica TCS SP2 confocal laser scanning microscope. Always the same microscope settings were used for each independent experiment, and pixel intensities were taken into account when comparing the images between control and mutants. Images were finally processed with Adobe Photoshop 7.0 and Adobe Illustrator 8.0.

Auxin Measurements. One-millimeter-long root tips were transferred immediately after harvest to tubes containing 1 mL of methanol kept at 0°C. To each tube, ^{2}H$_5$-IAA was added at the concentration of 10 fmol per root tip. The samples were put into a freezer (−20°C) and centrifuged at $36,000 \times g$ after 24 h. Supernatants were transferred into glass tubes, evaporated to dryness, and methylated with ethereal diazomethanol. Further processing by immunopurification was performed as described (47) and final analysis was done with a UHPLC coupled to a Waters Xevo TQ MS detector.

In Vitro Phosphorylation Assays. Approximately 3 μg of purified protein expressed in *E. coli* (PID and substrates) was added to the kinase reaction mix, containing 1× kinase buffer [25 mM Tris-HCl (pH 7.5), 1 mM DTT, 5 mM MgCl$_2$, 2 mM CaCl$_2$] and 1× ATP solution (100 μM MgCl$_2$, 100 μM ATP-Na$_2$, 2 μCi ^{32}P-γ-ATP). Reactions were incubated at 30°C for 45 min and stopped by addition of 5 μl of 5× protein loading buffer [310 mM Tris-HCl (pH 6.8), 10% SDS, 50% glycerol, 750 mM β-mercaptoethanol, 0.125% bromophenol blue] and boiling for 5 min. Reactions were subsequently separated over 12% acrylamide gels, which were washed three times for 30 min with kinase gel wash buffer (5% trichoroacetic acid, 1% Na$_2$H$_2$P$_2$O$_7$), coomassie stained, destained, and dried. Autoradiography was done for 48 h with Hyperfilm MP films and a Hypercassette (GE Healthcare Life Sciences).

PLANT BIOLOGY

1. Kepinski S, Leyser O (2005) Plant development: Auxin in loops. *Curr Biol* 15: R208–R210.
2. Mockaitis K, Estelle M (2008) Auxin receptors and plant development: A new signaling paradigm. *Annu Rev Cell Dev Biol* 24:55–80.
3. Vanneste S, Friml J (2009) Auxin: A trigger for change in plant development. *Cell* 136:1005–1016.
4. Bennett MJ, et al. (1996) *Arabidopsis AUX1* gene: A permease-like regulator of root gravitropism. *Science* 273:948–950.
5. Blakeslee JJ, et al. (2007) Interactions among PIN-FORMED and P-glycoprotein auxin transporters in *Arabidopsis*. *Plant Cell* 19:131–147.
6. Geisler M, et al. (2005) Cellular efflux of auxin catalyzed by the Arabidopsis MDR/PGP transporter AtPGP1. *Plant J* 44:179–194.
7. Petrášek J, et al. (2006) PIN proteins perform a rate-limiting function in cellular auxin efflux. *Science* 312:914–918.
8. Yang Y, Hammes UZ, Taylor CG, Schachtman DP, Nielsen E (2006) High-affinity auxin transport by the AUX1 influx carrier protein. *Curr Biol* 16:1123–1127.
9. Wiśniewska J, et al. (2006) Polar PIN localization directs auxin flow in plants. *Science* 312:883.
10. Petrásek J, Friml J (2009) Auxin transport routes in plant development. *Development* 136:2675–2688.
11. Stepanova AN, et al. (2008) *TAA1*-mediated auxin biosynthesis is essential for hormone crosstalk and plant development. *Cell* 133:177–191.
12. Tao Y, et al. (2008) Rapid synthesis of auxin via a new tryptophan-dependent pathway is required for shade avoidance in plants. *Cell* 133:164–176.
13. Zhao Y (2008) The role of local biosynthesis of auxin and cytokinin in plant development. *Curr Opin Plant Biol* 11:16–22.
14. Vieten A, Sauer M, Brewer PB, Friml J (2007) Molecular and cellular aspects of auxin-transport-mediated development. *Trends Plant Sci* 12:160–168.
15. Tanaka H, Dhonukshe P, Brewer PB, Friml J (2006) Spatiotemporal asymmetric auxin distribution: A means to coordinate plant development. *Cell Mol Life Sci* 63:2738–2754.
16. Sorefan K, et al. (2009) A regulated auxin minimum is required for seed dispersal in *Arabidopsis*. *Nature* 459:583–586.
17. Zourelidou M, et al. (2009) The polarly localized D6 PROTEIN KINASE is required for efficient auxin transport in *Arabidopsis thaliana*. *Development* 136:627–636.
18. Christensen SK, Dagenais N, Chory J, Weigel D (2000) Regulation of auxin response by the protein kinase PINOID. *Cell* 100:469–478.
19. Benjamins R, Quint A, Weijers D, Hooykaas P, Offringa R (2001) The PINOID protein kinase regulates organ development in *Arabidopsis* by enhancing polar auxin transport. *Development* 128:4057–4067.
20. Sukumar P, Edwards KS, Rahman A, DeLong A, Muday GK (2009) PINOID kinase regulates root gravitropism through modulation of PIN2-dependent basipetal auxin transport in Arabidopsis. *Plant Physiol* 150:722–735.
21. Zhou HW, Nussbaumer C, Chao Y, DeLong A (2004) Disparate roles for the regulatory A subunit isoforms in Arabidopsis protein phosphatase 2A. *Plant Cell* 16:709–722.
22. Michniewicz M, et al. (2007) Antagonistic regulation of PIN phosphorylation by PP2A and PINOID directs auxin flux. *Cell* 130:1044–1056.
23. Friml J, et al. (2004) A PINOID-dependent binary switch in apical-basal PIN polar targeting directs auxin efflux. *Science* 306:862–865.
24. Mravec J, et al. (2009) Subcellular homeostasis of phytohormone auxin is mediated by the ER-localized PIN5 transporter. *Nature* 459:1136–1140.
25. Luschnig C, Gaxiola RA, Grisafi P, Fink GR (1998) EIR1, a root-specific protein involved in auxin transport, is required for gravitropism in *Arabidopsis thaliana*. *Genes Dev* 12:2175–2187.
26. Swarup R, et al. (2005) Root gravitropism requires lateral root cap and epidermal cells for transport and responset to a mobile auxin signal. *Nat Cell Biol* 7:1057–1065.
27. Abas L, et al. (2006) Intracellular trafficking and proteolysis of the *Arabidopsis* auxin-efflux facilitator PIN2 are involved in root gravitropism. *Nat Cell Biol* 8:249–256.
28. Friml J, et al. (2002) AtPIN4 mediates sink-driven auxin gradients and root patterning in *Arabidopsis*. *Cell* 108:661–673.
29. Cheng Y, Qin G, Dai X, Zhao Y (2008) NPY genes and AGC kinases define two key steps in auxin-mediated organogenesis in *Arabidopsis*. *Proc Natl Acad Sci USA* 105:21017–21022.
30. Robert HS, Offringa R (2008) Regulation of auxin transport polarity by AGC kinases. *Curr Opin Plant Biol* 11:495–502.
31. Kallunki T, Deng T, Hibi M, Karin M (1996) c-Jun can recruit JNK to phosphorylate dimerization partners via specific docking interactions. *Cell* 87:929–939.
32. Sondhi D, Xu W, Songyang Z, Eck MJ, Cole PA (1998) Peptide and protein phosphorylation by protein tyrosine kinase Csk: Insights into specificity and mechanism. *Biochemistry* 37:165–172.
33. Hawkins J, Zheng S, Frantz B, LoGrasso P (2000) p38 map kinase substrate specificity differs greatly for protein and peptide substrates. *Arch Biochem Biophys* 382:310–313.
34. Pearson G, et al. (2001) Mitogen-activated protein (MAP) kinase pathways: Regulation and physiological functions. *Endocr Rev* 22:153–183.
35. Liu Y, Zhang S (2004) Phosphorylation of 1-aminocyclopropane-1-carboxylic acid synthase by MPK6, a stress-responsive mitogen-activated protein kinase, induces ethylene biosynthesis in Arabidopsis. *Plant Cell* 16:3386–3399.
36. Benschop JJ, et al. (2007) Quantitative phosphoproteomics of early elicitor signaling in Arabidopsis. *Mol Cell Proteomics* 6:1198–1214.
37. Huang F, Zago MK, van Marion A, Galván-Ampudia CS, Offringa R (2009) Phosphorylation of conserved PIN motifs by PINOID controls *Arabidopsis* PIN1 polar targeting. *Plant Cell*, in press.
38. Okada K, Ueda J, Komaki MK, Bell CJ, Shimura Y (1991) Requirement of the auxin polar transport system in early stages of Arabidopsis floral bud formation. *Plant Cell* 3:677–684.
39. Benková E, et al. (2003) Local, efflux-dependent auxin gradients as a common module for plant organ formation. *Cell* 115:591–602.
40. Friml J, et al. (2003) Efflux-dependent auxin gradients establish the apical-basal axis of *Arabidopsis*. *Nature* 426:147–153.
41. Ulmasov T, Murfett J, Hagen G, Guilfoyle TJ (1997) Aux/IAA proteins repress expression of reporter genes containing natural and highly active synthetic auxin response elements. *Plant Cell* 9:1963–1971.
42. Paciorek T, et al. (2005) Auxin inhibits endocytosis and promotes its own efflux from cells. *Nature* 435:1251–1256.
43. Benjamins R, Ampudia CS, Hooykaas PJ, Offringa R (2003) PINOID-mediated signaling involves calcium-binding proteins. *Plant Physiol* 132:1623–1630.
44. Grabov A, et al. (2005) Morphometric analysis of root shape. *New Phytol* 165:641–651.
45. Friml J, Benková E, Mayer U, Palme K, Muster G (2003) Automated whole mount localisation techniques for plant seedlings. *Plant J* 34:115–124.
46. Sauer M, Paciorek T, Benková E, Friml J (2006) Immunocytochemical techniques for whole mount *in situ* protein localization in plants. *Nat Protoc* 1:98–103.
47. Pěnčík A, et al. (2009) Isolation of novel indole-3-acetic acid conjugates by immunoaffinity extraction. *Talanta* 80:651–655.